CONSTRUCTION MATERIALS CONSULTANTS, INC.

Cracking Of Precast Concrete Wall Panels – A Petrographic Investigation

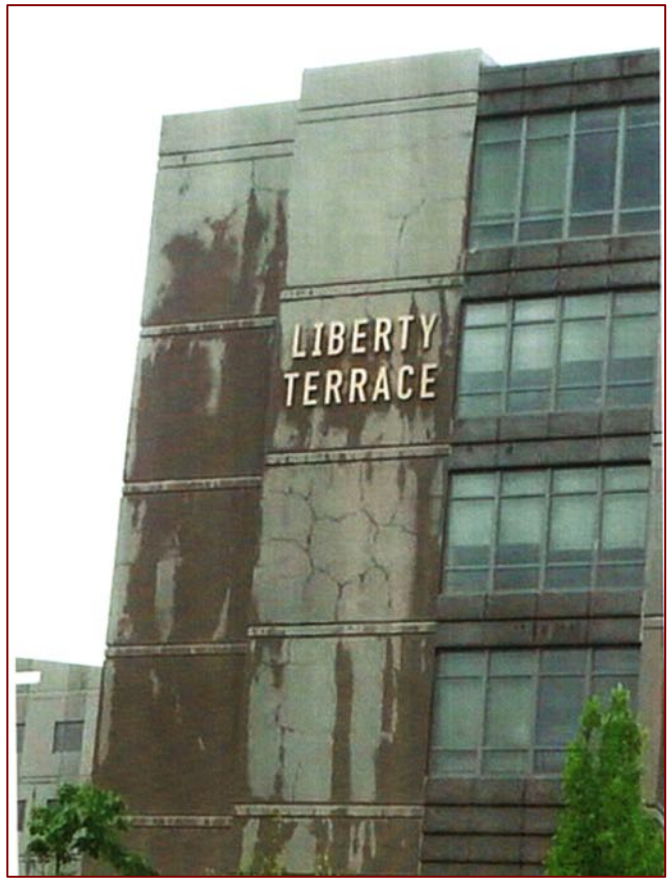

Liberty Terrace Apartments
University At Albany
East University Drive
Albany, NY 12203

February 03, 2022
CMC 0122101

TABLE OF CONTENTS*

* Precast wall panels, cracking from unsound greywacke-siltstone-shale gravels.

EXECUTIVE SUMMARY

Extensive cracking of precast concrete wall panels in the Liberty Terrace Apartments of University at Albany has prompted this investigation. As a result, two concrete cores were drilled through full thickness of panel, one (No. 1) from over visible cracks, and another (No. 2) from a visibly sound location of panel and provided for detailed petrographic examinations according to the procedures of ASTM C 865 to diagnose possible causes for cracking.

The panels in question were reportedly constructed approximately 10 years ago. Visible cracks were repaired, and exterior faces of panels were coated with 2 coats of a silane sealer. Apparently, sealer has its lost effectiveness, and a lot more cracking has developed. The wall panels were casted at plant, where current exterior surface was downside in the form. Measurement of crack widths in the field showed a width of 0.025 to 0.030 inch. The overall system is a sandwich panel consisting of a 3 in. nominal exterior face, a 4 in. rigid insulation typically extending to panel edges, and a 5 inch. load-bearing inner wythe that supports precast hollow-core plank. Composite ties connect the two wythes through the insulation layer. The exterior of the panel has a series of feature lines (chamfers). To provide adequate concrete cover at them, the mesh is located approximately 1.5 to 1.75 inches below the exterior surface of the panel.

Reported mix design of the precast concrete contains a complex system of chemical admixtures and pigments beside the normal coarse and fine aggregates, Portland cement, and water components of concrete, which are as follows (in a cubic yard): (a) 630 pounds of ASTM C 150 Type III Portland cement, which is finely ground compared to normal Type I/II Portland cement; (b) 70 pounds of highly reactive pozzolan metakaolin, which is difficult to determine during petrographic examinations for its almost immediate and early-stage reactivity with calcium hydroxide component of Portland cement hydration to generate calcium silicate hydrate product of pozzolanic reactions; (c) 1675 pounds of 1-B round stone - pea gravel; (d) 1196 pounds of Type A sand as the fine aggregate; (e) various pigments, e.g., red (SK2097), black iron oxide (SX5599), and yellow (SY2387) pigments at 6.4, 19.2, and 6.4 ounces, respectively; (f) 273 pounds of water; (g) MB-AE 90 air-entraining admixture to generate 6% air; and (h) various 'as-needed' chemical admixtures, e.g., Glenium 7500 (2 to 16 fl oz/100 lb. of cement), Pozzolith 100-XR admixture for increase strength, improve freeze-thaw durability, reduce water content for a given workability, and retard setting characteristics (1 to 3 fl oz/100 lb. of cement), Pozzolith NC 534 non-chloride accelerating admixture (10 to 45 fl oz./100 lb. of cement), and Sikamix W-10 water repelling and efflorescence controlling admixture (21 fl oz/1.00 cu. yd.). Reported design slump is 3 in. before adding the water-reducing agent; design water-cement ratio is 0.39; unit weight is 143. 56 lbs; and 28-day design compressive strength is 6000 psi.

Both cores are $2^{3}/_{4}$ in. (70 mm) in diameters, and $3^{1}/_{4}$ in. (82 mm) and $2^{7}/_{8}$ in. (74 mm) in nominal lengths for Nos. 1 and 2, respectively. Core 1 was reportedly extracted at the intersection of a crack repaired in 2011, and a new crack that has significantly widened during 10 years of exposure. Core 2 was extracted at a location that was not cracked but had a small popout repaired as part of the original installation. As a result, Core 1 showed a Y-shaped intersecting cracks on the exposed face that are part of a closed polygonal-shaped cracks on the wall panel. Extension of the cracks to the formed bottom end of Core 1 through the entire thickness indicated full-thickness extension of cracks in the wall panel. The side cylindrical surface of Core 1 showed full-depth extension of parallel cracks from the Y-shaped intersection at the surface. The cracks have circumscribed the No. 4 mesh situated at depths of 1.5 to 2.25 in. from the exposed faces of cores. All the mesh found on side cylindrical surfaces or became exposed on lapped cross sections are not corroded.

The apparently sound exposed surface of Core 2, however, showed a central repair patch as mentioned, which was applied to cover an underlying surface popout of near-surface shale and greywacke particles in gravel coarse aggregate, which indicated a prior unsoundness of these particles to cause fracturing and popouts in the presence of moisture during service. The smooth, formed bottom (inside panel face) end of Core 2 showed no visible cracking.

Based on detailed petrographic examinations, concretes in both are found to be compositionally similar. Coarse aggregates are compositionally similar sedimentary pea gravels, having nominal maximum sizes of $^{3}/_{8}$ in. (9.5 mm) and containing: (a) major amounts of greywacke, which are sandstones having detrital quartz and feldspar in a dominantly argillaceous (wacke) matrix, (b) subordinate amounts of reddish-brown ferruginous and argillaceous siltstone and shale where iron oxide-based ferruginous impurities have imparted the characteristic reddish-brown colors of these particles to be readily identified, (c) subordinate amounts of non-ferruginous but argillaceous shale and siltstone particles where lack of iron oxide impurity has prevented development of reddish brown color tone except having the same fine clay-silt grain sizes and quartz-feldspar-fine-grained carbonate-clay mineralogies of ferruginous shale-siltstone particles, and (d) minor amounts of quartzite, which are either orthoquartzite or metaquartzite, latter having strained quartz particles. All particles are subrounded to well-rounded, mostly equidimensional, variably hard and porous, well-graded, and well-distributed.

A PennDOT petrographic testing report of the pea gravel aggregate to be used mentions the gravel to be "composed of fine to coarse grained framework supported, GREYWACKE SANDSTONE (95.5%), which is occasionally moderately weathered and slightly micaceous; and rarely with shaly intraclasts and partings and slightly pyritiferous; silty with very fine grain, SILTSTONE (2.3%), which is massive to thinly laminated; sometimes slightly pyritiferous; SHALE (2.2%), which is thinly laminated; sometimes slightly micaceous; occasionally moderately weathered; and rarely with sandy zones; microcrystalline, CHERT (TRACE) which is massive and moderately weathered."

Contrary to the PennDOT testing report of the pea gravel, despite having major amount of greywacke, and subordinate amounts of siltstone, and shale in pea gravel as the testing report has mentioned, however, the amount of greywacke in the two cores examined are well below 95.5% whereas that of argillaceous siltstone and shale components combined are well-above 5.5%. Quantitative determination of these rock types in gravels is not possible from ASTM C 856 without doing a point count analyses, e.g., by ASTM C 457, based on visual examinations of lapped cross sections and thin sections of two cores, greywacke content is estimated to be 65 to 70% by volume, whereas argillaceous, ferruginous, and non-ferruginous shale and siltstone components combined are estimated to be 25 to 30% by volume, and the rest, e.g., ortho and metaquartzite (no chert *per se* was detected in the cores) component is detected to be less than 5%, by volume. Besides, the matrix of the dominant greywacke sandstone rock types in pea gravel contains clay-rich argillaceous components (to be called 'wacke), which is susceptible to absorb moisture and expand during wetting and drying and/or freezing and thawing cycles.

Fine aggregates in both cores are compositionally similar natural siliceous-argillaceous-calcareous sands of nominal maximum sizes $^1/4$ in. (6 mm) consisting of: (a) major amount of finer fraction of lightly crushed sedimentary pea gravel particles; (b) major amounts of detrital quartz and feldspar grains; (c) subordinate amount of detrital feldspar, shale, siltstone; and (d) minor amounts of limestone and dolomite as the calcareous component. Fine aggregate particles are variably colored, subangular to subrounded to well-rounded, variably dense and hard, equidimensional to elongated, unaltered, uncoated, and uncracked. There is no evidence of alkali-aggregate reactions, or any other potentially deleterious reactions found. Unsoundness of argillaceous particles are mostly seen in the pea gravel and not in their finer sand-size fractions.

Paste is compositionally similar dense, and hard in the interior bodies except some patchy discoloration at the minimally carbonated expose surface ends. Freshly fractured surfaces have subtranslucent vitreous lusters and subconchoidal fractures. Residual and relict Portland cement particles are present and estimated to constitute 6 to 8 percent of the paste volumes. Besides residual Portland cement, no other pozzolanic or cementitious materials are found. The entire paste is intermixed with ultrafine iron oxide-based pigment to impart an overall pigmented brown color tone of concrete. Patchy carbonation is noted at exposed ends extended to depths of 5 mm. Extensive microcracking is noticed in the paste from unsound greywacke-siltstone-shale particles in pea gravel as well as near the exposed surface ends in both cores. Aggregate-paste bonds are moderately tight to weak in areas where cracks have circumscribed the aggregate particles.

There is no evidence of any chemical deterioration such as alkali-aggregate reaction, or, delayed ettringite formation from the thermal treatments during manufacturing process of precast panels, etc. found in the paste.

The textural and compositional features of pastes are indicative of Portland cement contents similar in both cores and estimated to be 7 to $7^1/_2$ bags per cubic yard, and water-cement ratios in the bodies similar in both cores and estimated to be 0.40 to 0.45.

Concretes in both cores are air-entrained having numerous fine, discrete, spherical and near-spherical voids of sizes 1 mm or less, which are characteristic of entrained air and a few coarse, near-spherical and irregularly-shaped voids greater than 1 mm in size, which are characteristic of entrapped air. Air contents are estimated to be 6 to 7 percent in both cores.

Petrographic evidence showed gross unsoundness of many greywacke, ferruginous-argillaceous shale-siltstone, and non-ferruginous shale-siltstone particles in pea gravel coarse aggregate as: (i) internal cracking, (ii) internal cracks extended into paste, (iii) gravel transected by major visible cracks as well as minor invisible microcracks, (iv) peripheral cracks, and (v) porous zones of paste along the peripheries. All these textural and microstructural evidence indicate physical unsoundness of these clay-rich argillaceous sedimentary gravels in the presence of moisture during service. All these sedimentary gravel particles have one common compositional feature, which is their clay-rich composition, which makes them susceptible to absorb moisture during service and expand.

Beside cracking, another surface manifestation of unsoundness is popout of many of these particles when present near the exposed face of the panels and exposed to moisture during service. As in the case of Core 2 where despite having no visible cracks in the core, a near-surface shale and adjacent greywacke particle in coarse aggregate showed unsoundness as fracturing and popout that had required a repair patch to place over the popout location.

Reported failure of sealer and widening of cracks in the wall panel are consistent with gross unsoundness of these clay-rich (argillaceous) gravel particles in concrete that have absorbed moisture during service and expanded, followed by repeated volume instabilities during wetting and freezing, and freezing and thawing cycles to cause internal cracking of those particles, eventually leading to development of new cracks in the panel as well as widening of existing cracks.

Due to the complex composition of concrete as found in the reported mix design, many of which are difficult, if not impossible to determine during petrographic examinations, e.g., various chemical admixtures listed in the design, from water-reducing (Glenium 7500), to set-retarding (Pozzolith 100-XR), air-entraining (MB-AE 90), non-chloride set accelerating (Pozzolith NC 534), water repelling and efflorescence controlling (Sikamix W-10), as well as various pigments (red SK2097, black iron oxide SX5599, and yellow SY2387) their overall combined effects on the properties and performance of concrete during service after the precast manufacturing process is difficult to ascertain from the present investigation. Depending on what chemical admixtures were actually added in the mix at the precast plant for the concrete represented in the two cores examined here, their effects on the overall drying shrinkage of concrete during service is important to consider. Perhaps, restrained shrinkage of the panels has introduced some of the observed cracks along which moisture has penetrated deeper inside to attack the absorptive greywacke-siltstone-shale gravel particles to cause further cracking. Additionally, use of finely ground (compared to normal Type I/II) high early-strength Type III Portland cement during heat-treatment in precast plant may develop some thermal cracks during or after the manufacturing process from its inherent high heat of hydration (than normal Type I/II cement), which may introduce some cracking. These possibilities are impossible to investigate from petrographic examinations but are worthy to consider to get a comprehensive understanding of all possible causes of cracking, above and beyond the ones formed from the use of unsound pea gravel aggregate, which is adequately demonstrated from the present petrographic examinations.

Due to the overwhelming abundance of clay-rich particles in pea gravels and even in their finer size fractions in sands, and their widespread distribution throughout the entire thickness of the panels, exposure to moisture during service poses threat for continued unsoundness of these particles along with continued development of new cracks, popout of near-surface particles, and widening of pre-existing cracks due to overall volume expansion of concrete when these particles absorb moisture during service.

Good air entrainment, use of finely ground high-early strength Portland cement plus iron oxide-based pigment as cementitious and pigment components, respectively in the paste, and overall dense, low *w/c* (0.40-0.45), and well-consolidated nature of concrete, let alone with an impressive list of advertised chemical admixtures in the mix, apparently, did not provide the necessary resistance of the panels to combat against potential moisture absorption of the dominant argillaceous gravel coarse aggerate particles that are scattered all throughout the thickness of the panels. Despite the lack of visible cracks at the location of Core 2, however, concrete in Core 2 also showed microcracking and unsoundness of aggregates, which have not yet developed to full scale to cause cracking of exterior face.

Unfortunately, since the past repair attempts with silane sealer did not prevent cracking, or widening of existing cracks, replacement of the panels appears to the best option to prevent future cracking. Aggregates to be used in a replaced panel must avoid any clay-rich or other potentially deleterious components since due to their dominance at 60 to 70 percent level by volume, aggregates play a dominant role in future durability and serviceability of concrete. The present case testifies the importance of use of sound aggregates in creating a durable and serviceable precast panel, especially when exposed to an outdoor moist environment of cyclic freezing and thawing.

INTRODUCTION

Two concrete cores (Nos. 1 and 2) were provided from a precast concrete wall panel of Liberty Terrace Apartments of University at Albany. The panel has exhibited closed polygonal-shaped cracks on the surface.

BACKGROUND INFORMATION AND FIELD PHOTOGRAPHS

The panels in question were reportedly constructed approximately 10 years ago. Visible cracks were repaired, and exterior of panels were coated with 2 coats of a silane sealer. Apparently, sealer has its lost effectiveness, and a lot more cracking has become visible. The wall panels were plant cast, current exterior surface was downside in the form.

Figure 1 shows closed polygonal-shaped cracks on the exterior face of the wall panel around Liberty Terrace sign of the panel. Figure 2 shows close-up of cracks and measurement of crack widths in the field, which show a width of 0.025 to 0.030 inch.

The overall system is a sandwich panel consisting of a 3 in. nominal exterior face, a 4 in. rigid insulation typically extending to panel edges, and a 5 inch. load-bearing inner wythe that supports precast hollow-core plank. Composite ties connect the two wythes through the insulation layer. The exterior of the panel has a series of feature lines (chamfers). To provide concrete cover at them the mesh is approximately 1.5 to 1.75 inches below the exterior surface of the panel.

Reported mix design of the precast concrete contains a complex system of chemical admixtures beside the normal coarse and fine aggregates, Portland cement, and water components of concrete, which are as follows (in a cubic yard):

a. 630 pounds of ASTM C 150 Type III Portland cement, which is finely ground compared to normal Type I/II Portland cement;
b. 70 pounds of highly reactive pozzolan metakaolin, which is difficult to determine during petrographic examinations for its almost immediate and early-stage reactivity with calcium hydroxide component of Portland cement hydration to generate calcium silicate hydrate product of pozzolanic reactions;
c. 1675 pounds of 1-B round stone - pea gravel,
d. 1196 pounds of Type A sand as the fine aggregate,
e. Various pigments, e.g., red (SK2097), black iron oxide (SX5599), and yellow (SY2387) pigments at 6.4, 19.2, and 6.4 ounces, respectively,
f. 273 pounds of water,
g. MB-AE 90 air-entraining admixture to generate 6% air,
h. Various 'as-needed' chemical admixtures, e.g., Glenium 7500 (2 to 16 fl oz/100 lb. of cement), Pozzolith 100-XR admixture for increase strength, improve freeze-thaw durability, reduce water content for a given

workability, and retard setting characteristics (1 to 3 fl oz/100 lb. of cement), Pozzolith NC 534 non-chloride accelerating admixture (10 to 45 fl oz./100 lb. of cement), and Sikamix W-10 water repelling and efflorescence controlling admixture (21 fl oz/1.00 cu. yd.).

i. Design slump is 3 in. before adding the water-reducing agent. Design water-cement ratio is 0.39. Unit weight is 143. 56 lbs. Design 28-day compressive strength is 6000 psi.

Petrographic description of the pea gravel in the aggregate testing report of PennDOT mentions the gravel added to be

"…*composed of fine to coarse grained framework supported, GREYWACKE SANDSTONE (95.5%), which is occasionally moderately weathered and slightly micaceous; and rarely with shaly intraclasts and partings and slightly pyritiferous; silty with very fine grain, SILTSTONE (2.3%), which is massive to thinly laminated; sometimes slightly pyritiferous; SHALE (2.2%), which is thinly laminated; sometimes slightly micaceous; occasionally moderately weathered; and rarely with sandy zones; microcrystalline, CHERT (TRACE) which is massive and moderately weathered*."

Samples were collected from the exterior face layer of insulated load-bearing sandwich panels that exhibit widespread cracking. One core (No. 1), drilled through full depth of the panel show cracks on the exposed face that have extended through the entire depth of the core. The second core (No. 2) was collected from a visually sound area, which is free of any visible cracks.

PURPOSES

Based on field photos, and background information provided, the purposes of the present laboratory investigations are to determine:

(a) The overall condition and composition of concrete in the cores from detailed petrographic examinations, and

(b) Investigation of evidence of any potentially deleterious physical or chemical reactions or unsoundness of concrete ingredients from petrography, which may have contributed to the cracking.

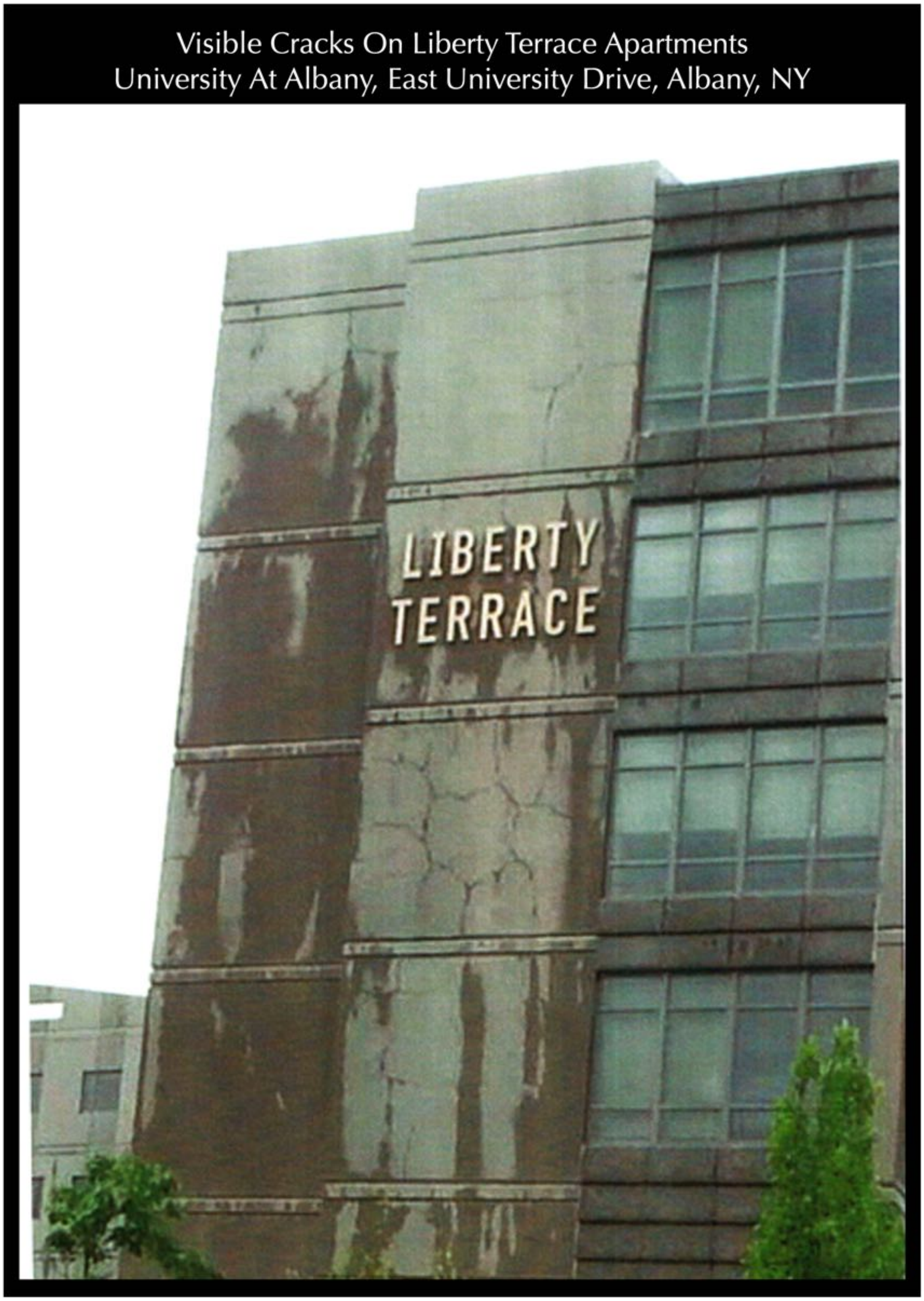

Figure 1: Field photo of precast concrete wall panel showing closed polygonal-shaped cracks on the exposed surface.

Figure 2: A close-up of the cracks on the precast wall panel in the top photo, and measurement of crack width at the bottom two photos showing widths of 0.025 to 0.030 inch.

METHODOLOGIES

PETROGRAPHIC EXAMINATIONS

The cores were examined using the methods and procedures of ASTM C 856 "Standard Practice for Petrographic Examination of Hardened Concrete." Details of concrete petrography, and sample preparation techniques for petrographic examinations of concrete are provided in Jana (2006).

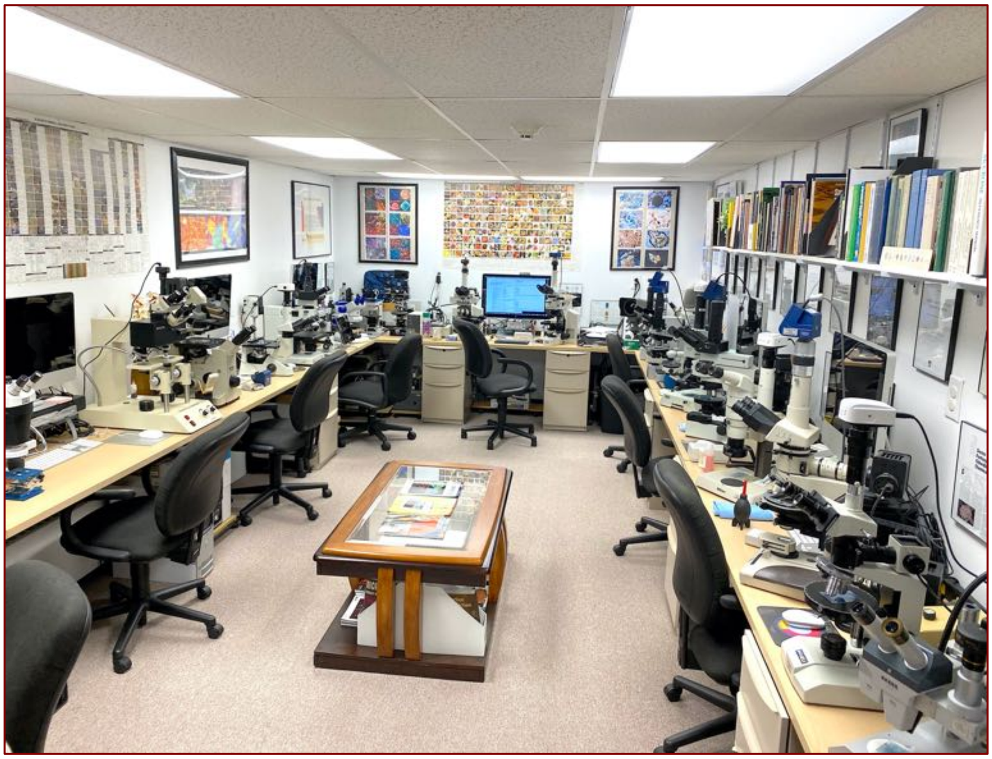

Figure 3: Some of the optical microscopes in the optical microscopy laboratory that were used for this investigation, e.g., from low-power stereo microscope, to high-power transmitted-light stereo-zoom microscope with plane and crossed-polarized light, to epi-fluorescent microscope for observations of florescent dye-mixed epoxy impregnated thin sections and petrographic microscopes for further observations of thin sections of concretes.

Briefly, the steps followed during petrographic examination of samples include:

i. Visual examinations of the cores, as received, including adequate documentation of dimensions, measurements, condition, physical properties, integrity, etc.;
ii. Low-power stereo microscopical examinations of as-received, saw-cut and freshly fractured sections, and lapped cross sections of samples for evaluation of texture, air-void systems, and compositions;
iii. Examinations of oil immersion mounts in a petrographic microscope for mineralogical compositions of specific areas of interests;
iv. Examinations of fluorescent dye-mixed (to highlight open spaces, cracks, air voids, etc.) low-viscosity epoxy-impregnated large area (50 mm × 75 mm) thin sections of concretes in a petrographic microscope for detailed compositional and microstructural analyses;
v. Photographing the samples, as received, and at various stages of preparation with a digital camera and a flatbed scanner; and,
vi. Photomicrographs of lapped sections and thin sections of concretes taken with stereomicroscope and petrographic microscope, respectively to provide detailed compositional and mineralogical information of concretes.

SAMPLES

Preliminary descriptions of two concrete cores, Nos. 1 and 2 are listed in the following Table 1 and in subsequent Figures 4 to 11.

Core ID	Diameter	Length	Exposed Surface	Bottom Surface	Cracking	Reinforcing Steel	Core Condition
1	$2\frac{3}{4}$ in. (70 mm)	$3\frac{1}{4}$ in. (82 mm)	Y-shaped intersecting cracks on exposed face	Formed with extension of surface cracks through depth	Through-depth cracks	No. 2 mesh at 1½, 1¾, 2, and 2¼ in. depths from the exterior face	Intact, Dry, Ring-sounded
2	$2\frac{3}{4}$ in. (70 mm)	$2\frac{7}{8}$ in. (74 mm)	Sound with a central repair patch over an underlying surface popout	Smooth, flat, formed with coarse voids	No visible cracks	No 2 at $1\frac{5}{8}$ in. depth from the exterior face	Intact, Dry, Ring-sounded

Table 1: Detailed preliminary descriptions and dimensions of two cores, as received.

- Core 1 was reportedly extracted at the intersection of a crack repaired in 2011, and a new crack that has significantly widened during 10 years of exposure.
- Core 2 was extracted at a location that was bot cracked but had a small bug hole or pop-out repaired as part of the original installation.
- Figure 4 shows Y-shaped intersecting cracks on the exposed face that are part of a closed polygonal-shaped cracks on the wall panel.
- Figure 5 shows extension of the cracks to the formed bottom end through the entire thickness of the core indicating full-thickness extension of cracks in the wall panel.
- Figures 6 and 7 show side cylindrical views of Core 1 where full-depth extension of cracks are seen. The cracks have circumscribed the No. 4 mesh situated at depths of 1.5 to 2.25 in. from the exposed faces of cores. All the mesh found on side cylindrical surfaces are not corroded.
- Figure 8 shows the sound exposed surface of Core 2, except, however, a central repair patch, which was applied to cover an underlying surface popout of near-surface shale and greywacke particles in gravel coarse aggregate indicating a prior unsoundness of these particles to cause fracturing and popouts in the presence of moisture during service.
- Figure 9 shows the smooth, formed bottom (inside panel face) end of Core 2 without any visible cracking.
- Figures 10 and 11 show side cylindrical views of Core 2 where concrete is sound, dense, and well-consolidated.
- The side, cylindrical surfaces of both cores show compositionally similar concrete consisting of pea gravel coarse aggregate particles that are well-graded and well-distributed.

Figure 4: Exposed surface of wall panel in Core 1 showing intersecting Y-shaped cracks that have extended through the entire thickness of the wall (depth of the core).

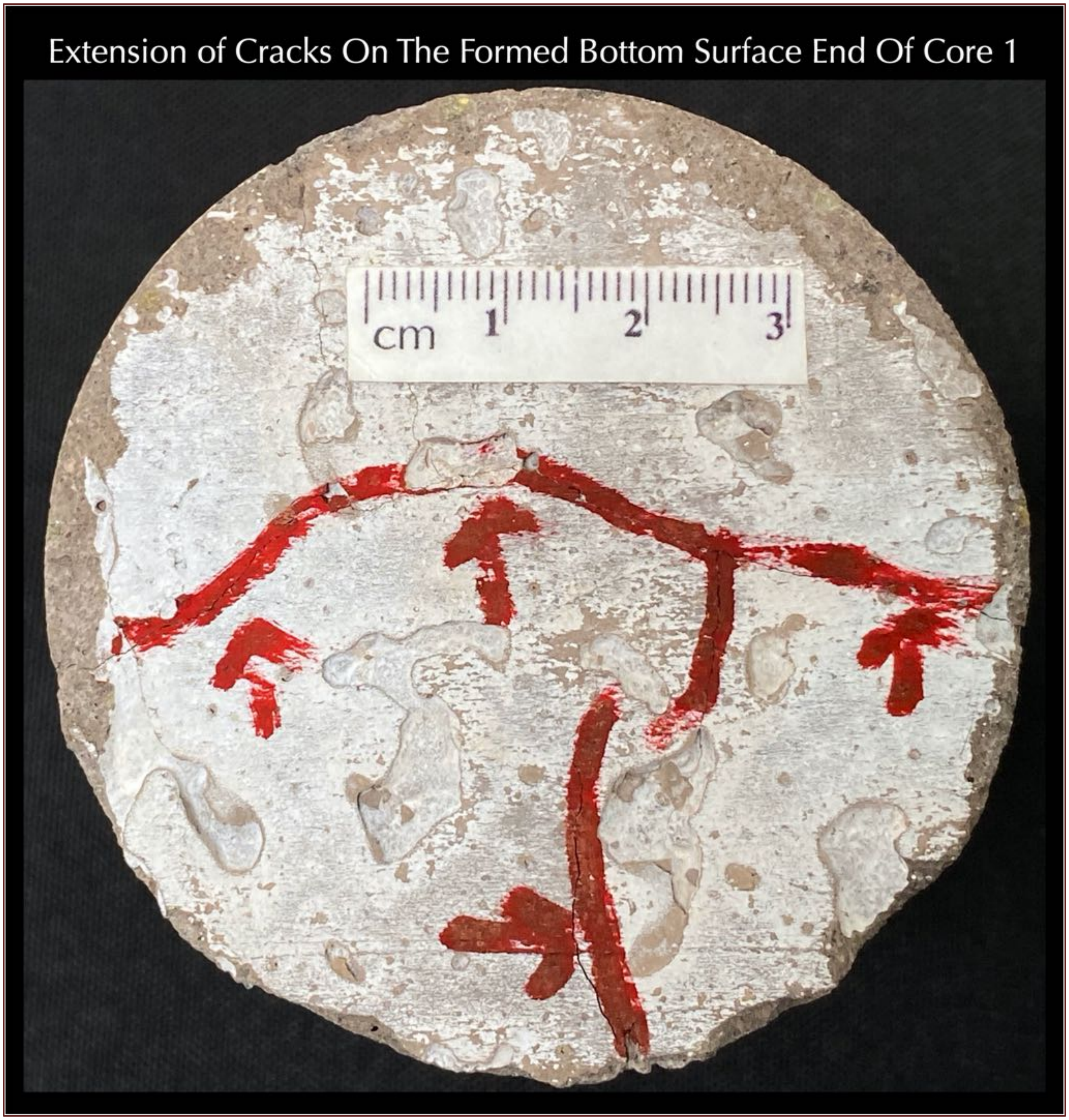

Figure 5: Formed bottom end of Core 1 representing the inside surface of wall panel showing full-depth extension of surface cracks through the entire thickness of the core, indicating surface cracks at the location of Core 1 has extended through the entire thickness of the precast wall.

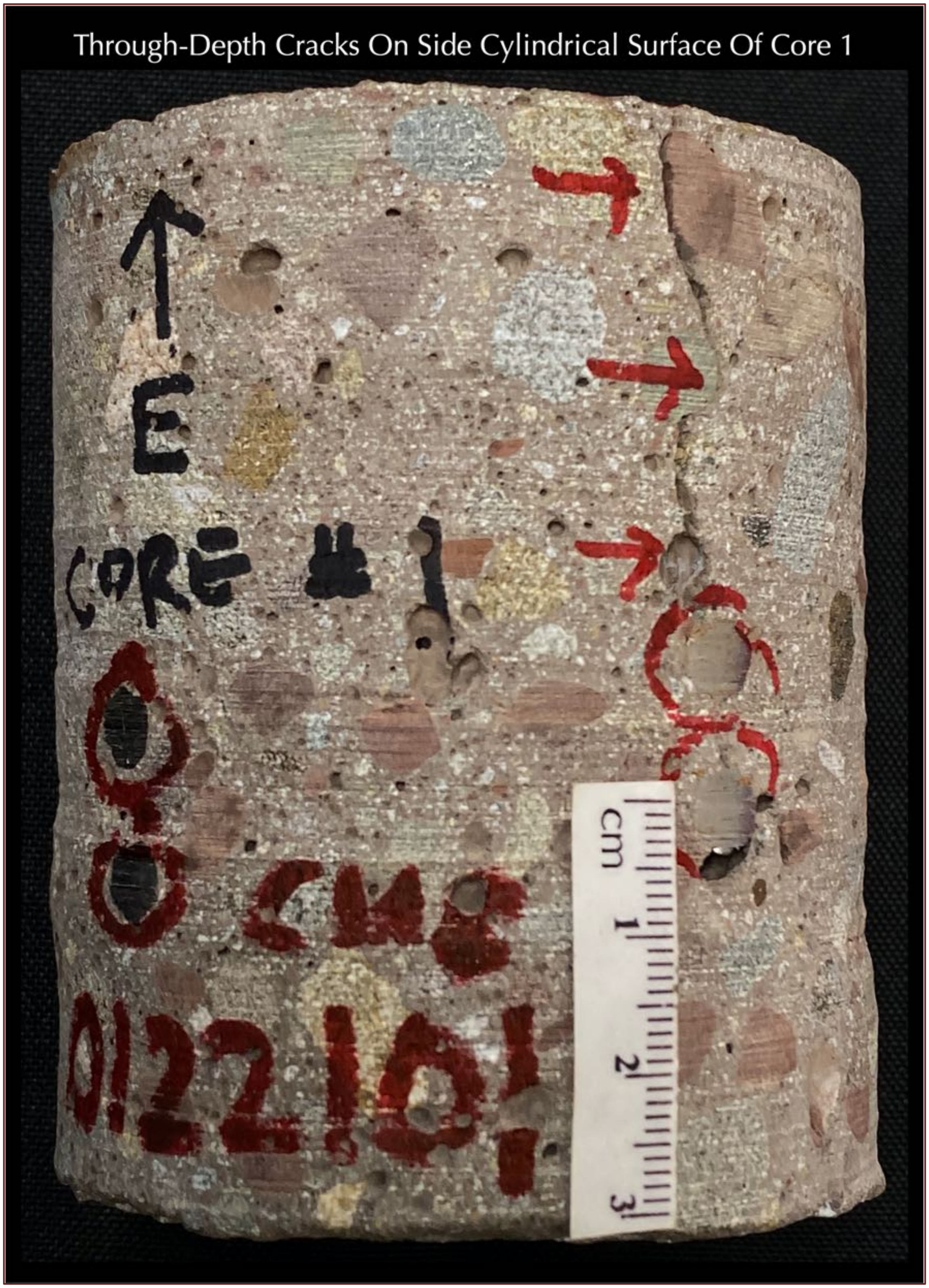

Figure 6: Side, cylindrical surface of Core 1 showing full-depth extension of cracks that have circumscribed two No. 2 reinforcing steel along its path. No. 2 steel bars are present at depths of 1½, 1¾, 2, and 2¼ in. from the top exposed end.

Figure 7: Side, cylindrical surface of Core 1 showing full-depth extension of two parallel trails of cracks that have circumscribed two No. 2 reinforcing steel along its path. No. 2 steel bars are present at depths of 1½, 1¾, 2, and 2¼ in. from the top exposed end.

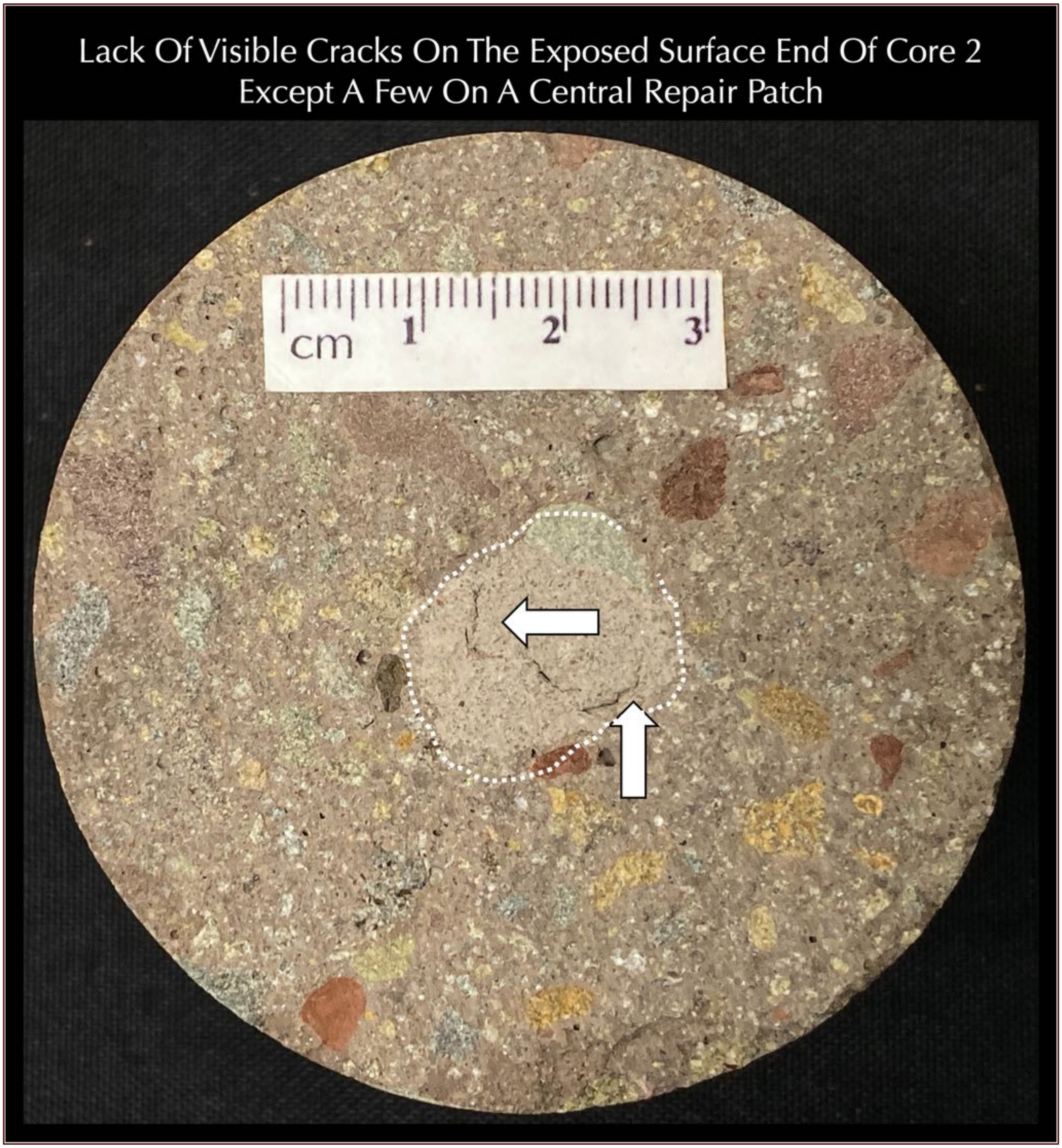

Figure 8: Top exposed end of wall panel in Core 2 showing lack of any visible surface cracks as seen in Core 1, except, perhaps, a few small microcracks marked by arrows formed on a central repair patch, which was applied to patch an underlying aggregate popout as seen during longitudinal sectioning of the core through the patch (see Figure 15).

Figure 9: Smooth, flat formed inside surface of wall panel having some coarse voids representing a sound condition of panel at this location as far as lack of any visible cracking is concerned.

Figure 10: Side, cylindrical surface of Core 2 showing lack of any visible cracks as seen in Core 1. No. 2 steel bars are present at a depth of $1^5/_8$ in. from the top exposed end.

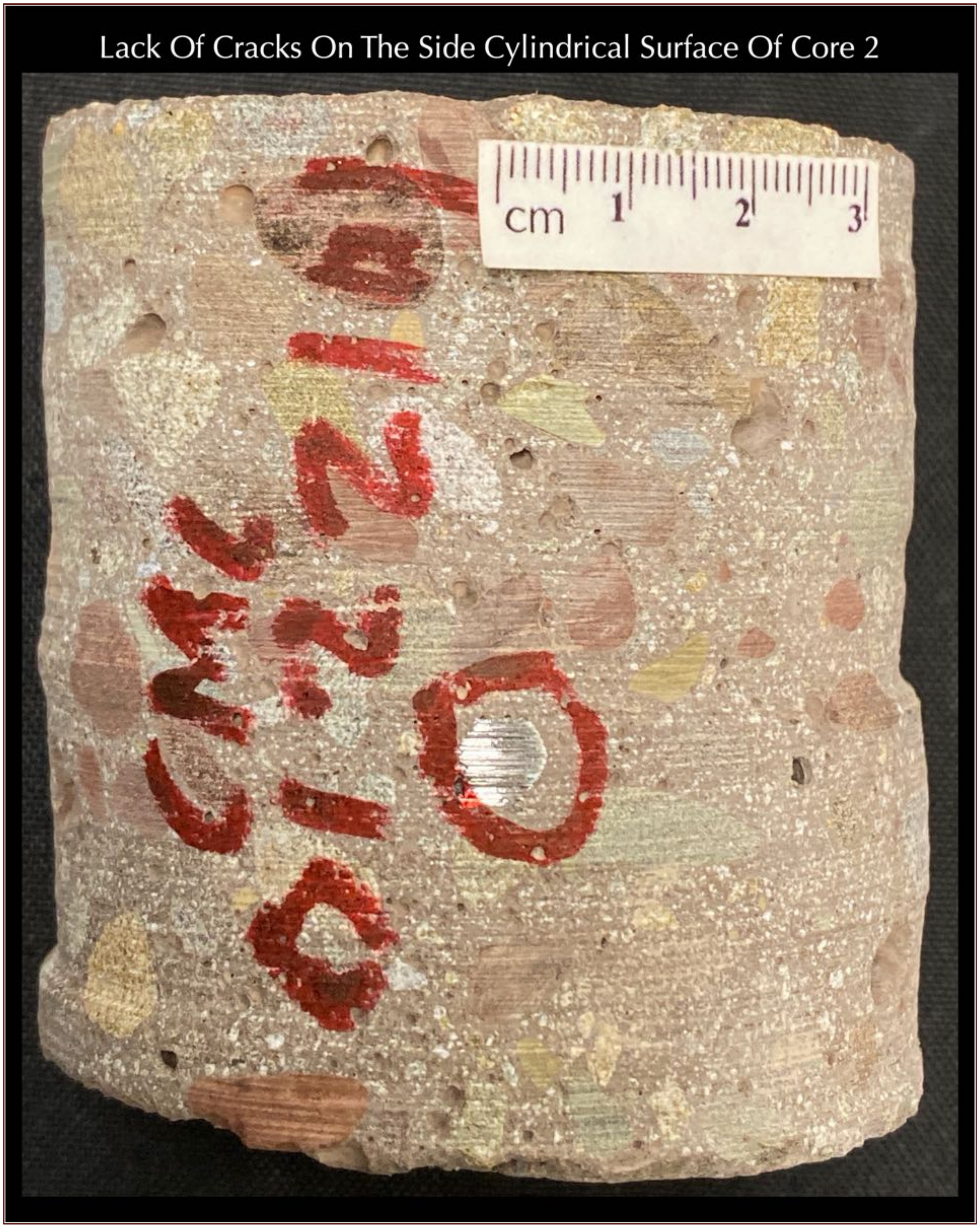

Figure 11: Side, cylindrical surface of Core 2 showing lack of any visible cracks as seen in Core 1. No. 2 steel bars are present at a depth of $1\frac{5}{8}$ in. from the top exposed end.

PETROGRAPHIC EXAMINATIONS

LAPPED CROSS SECTIONS

Figure 12: Lapped cross section of Core 1 showing:

a. Sedimentary pea gravel coarse aggregate particles having nominal maximum size of $^{3}/_{8}$ in. (9.5 mm) containing subrounded to well-rounded, equidimensional, well-graded, and well-distributed particles of light speckled gray to brown particles of greywacke (a variety of sandstone having detrital quartz, feldspar, and interstitial argillaceous matrix), reddish-brown particles of ferruginous-argillaceous siltstone and shale, and some other minor components (quartzite);

b. Finer natural siliceous-argillaceous-calcareous sand fine aggregate containing many finer (lightly crushed) fractions of gravel coarse aggregate; and

c. Interstitial pigmented reddish-brown paste.

d. The main vertical crack is marked with arrows, which have extended through the entire depth and circumscribed No. 2 reinforcing steel along its path.

e. Steel is non-corroded.

f. Overall concrete away from crack is dense and well-consolidated.

Crack widths on lapped cross section are measured to be from 0.020 to 0.030 inch.

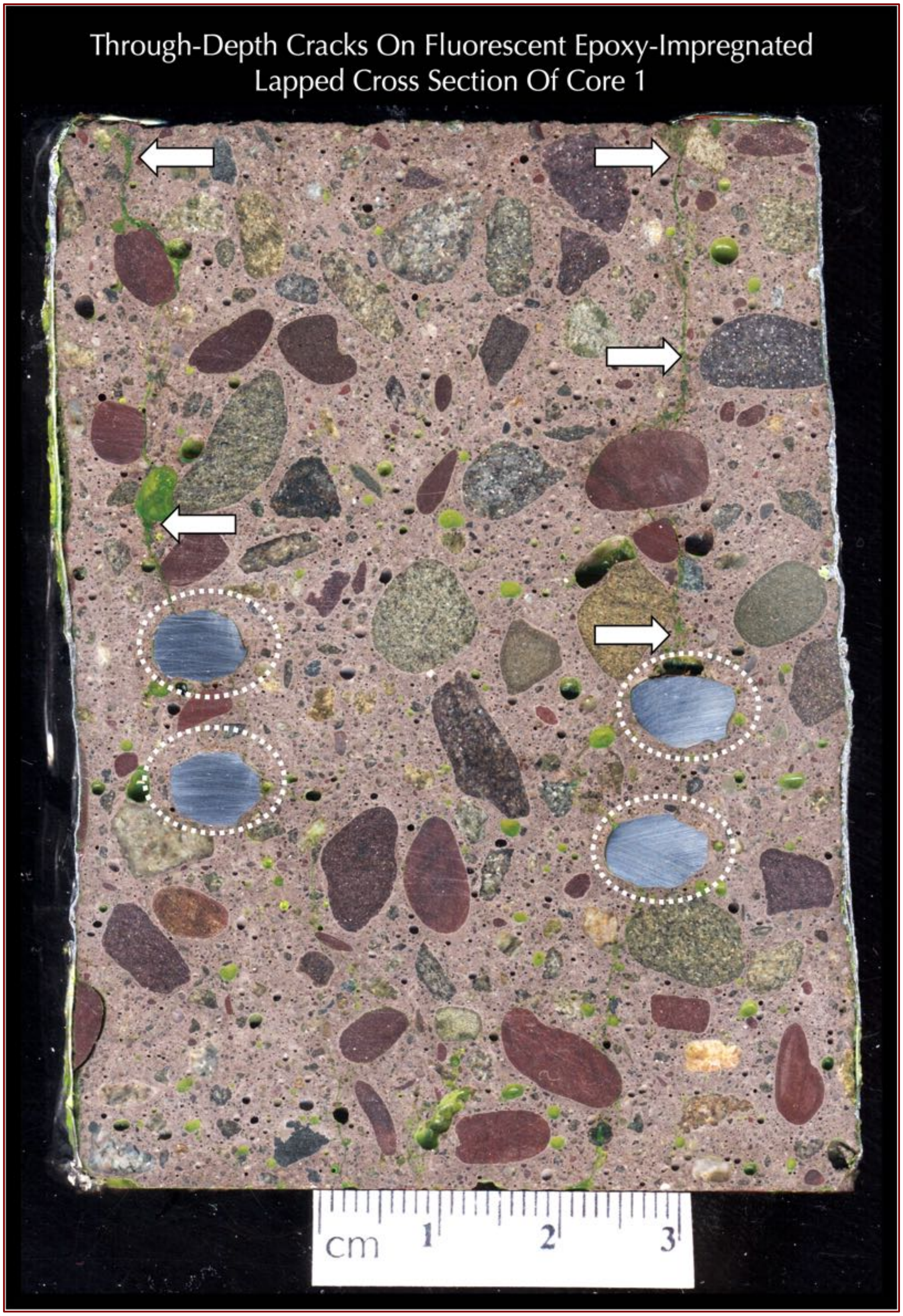

Figure 13: A second fluorescent epoxy-impregnated lapped cross section of Core 1 showing:

a. Sedimentary pea gravel coarse aggregate particles having nominal maximum size of $^{3}/_{8}$ in. (9.5 mm) containing subrounded to well-rounded, equidimensional, well-graded, and well-distributed particles of light speckled gray to brown particles of greywacke (a variety of sandstone having detrital quartz, feldspar, and interstitial argillaceous matrix), reddish-brown particles of ferruginous-argillaceous siltstone and shale, and some other minor components (quartzite);

b. Finer natural siliceous-argillaceous-calcareous sand fine aggregate containing many finer (lightly crushed) fractions of gravel coarse aggregate; and

c. Interstitial pigmented reddish-brown paste.

d. Two parallel vertical cracks (marked with arrows), which have extended through the entire depth and circumscribed No. 2 reinforcing steel along its path.

e. Steel is non-corroded.

Overall concrete away from crack is dense and well-consolidated.

Crack widths on lapped cross section are measured to be from 0.020 to 0.030 inch.

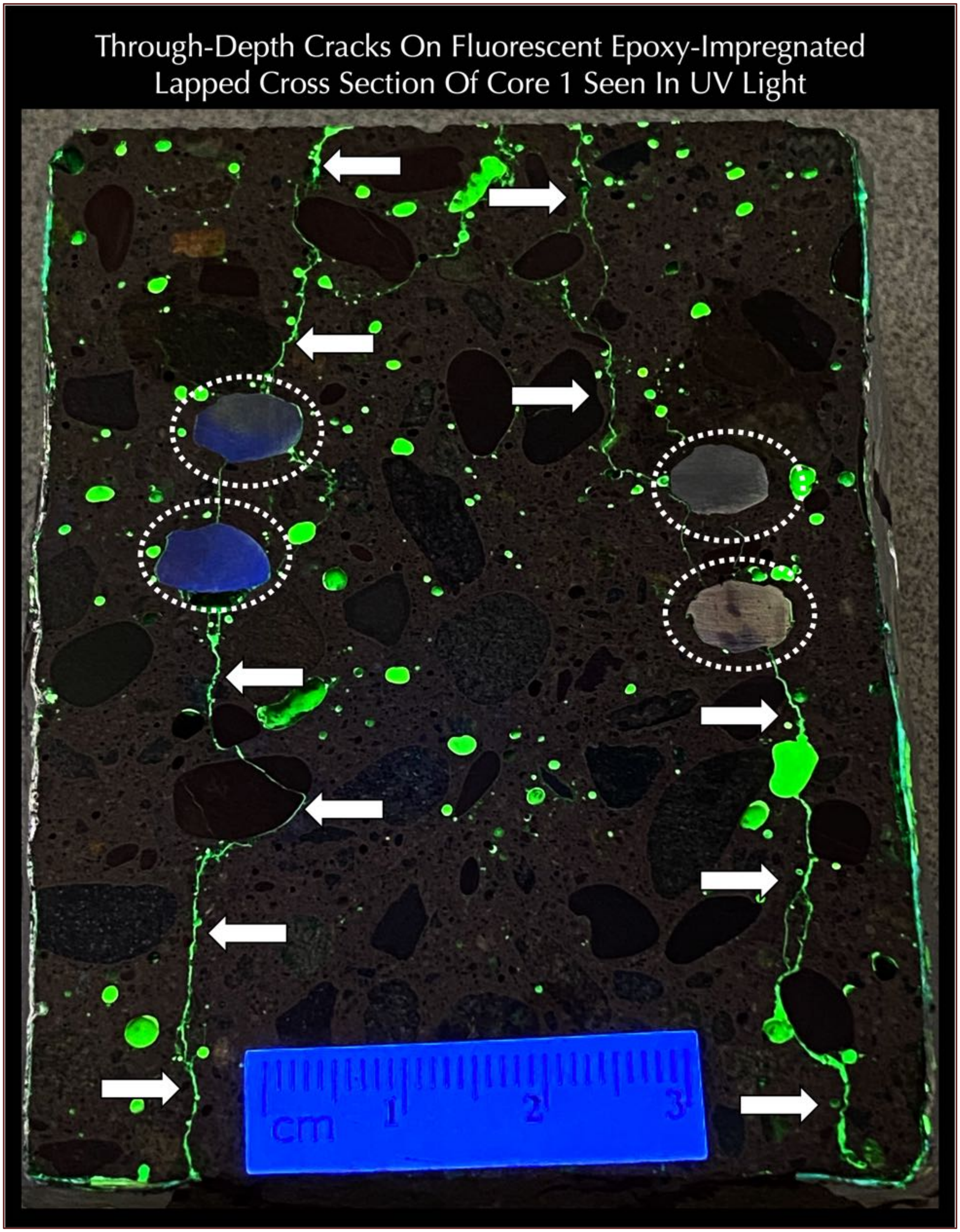

Figure 14: The same lapped section from Figure 13 shown in UV light to highlight air voids and two main vertical cracks impregnated with fluorescent epoxy.

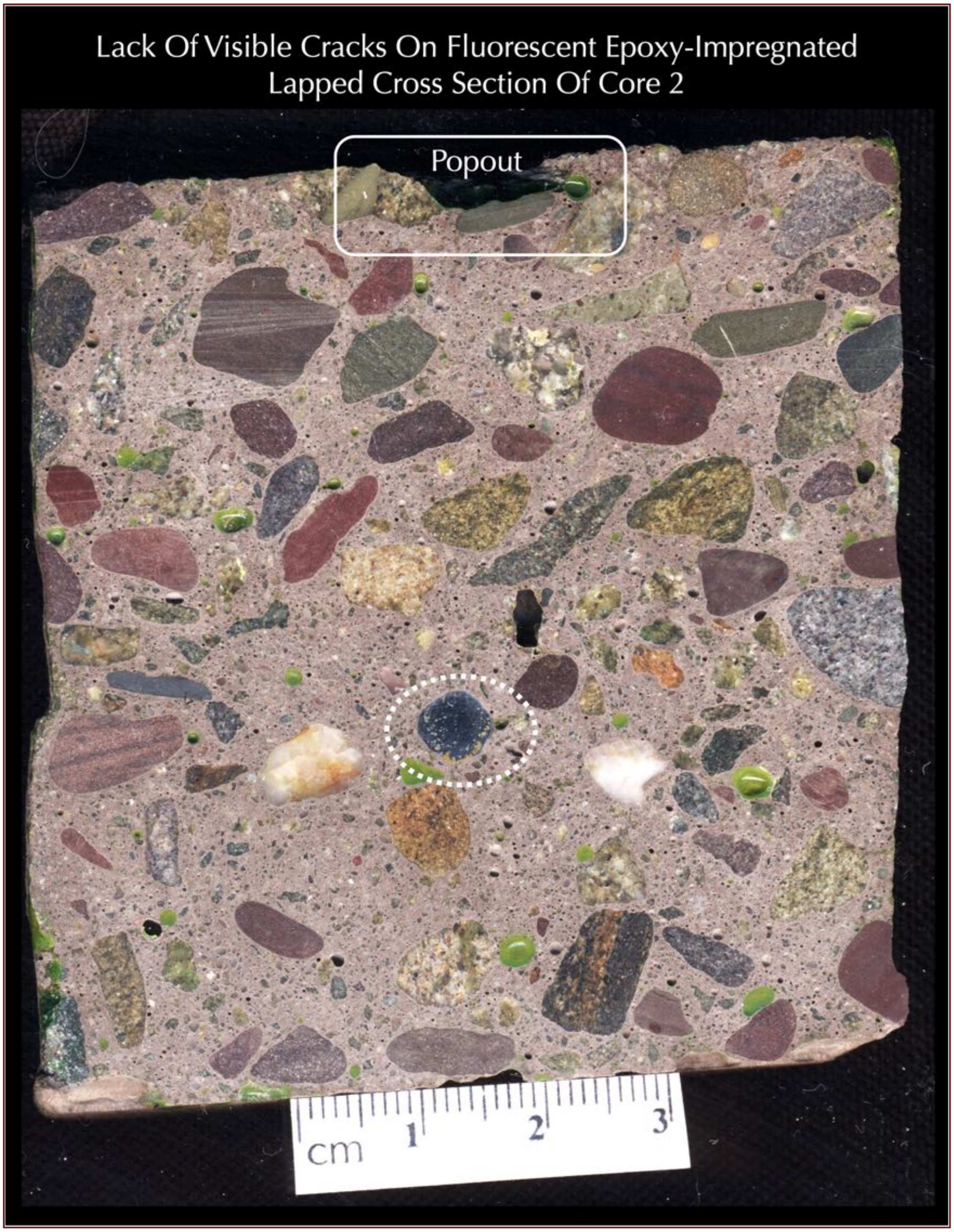

Figure 15: Fluorescent epoxy-impregnated lapped cross section of Core 2 showing: (a) same sedimentary pea gravel coarse aggregate particles seen in Core 1 having nominal maximum size of $^3/_8$ in. (9.5 mm) containing subrounded to well-rounded, equidimensional, well-graded, and well-distributed particles of light speckled gray to brown particles of greywacke (a variety of sandstone having detrital quartz, feldspar, and interstitial argillaceous matrix), reddish-brown particles of ferruginous-argillaceous siltstone and shale, and some other minor components (quartzite); (b) finer natural siliceous-argillaceous-calcareous sand fine aggregate containing many finer (lightly crushed) fractions of gravel coarse aggregate; and (c) interstitial pigmented reddish-brown paste. A shale and an adjacent greywacke particle in pea gravel coarse aggregate at the surface show fracturing and popout (boxed). A No. 2 reinforcing steel is marked at a depth of $1^5/_8$ in. from top exposed end.

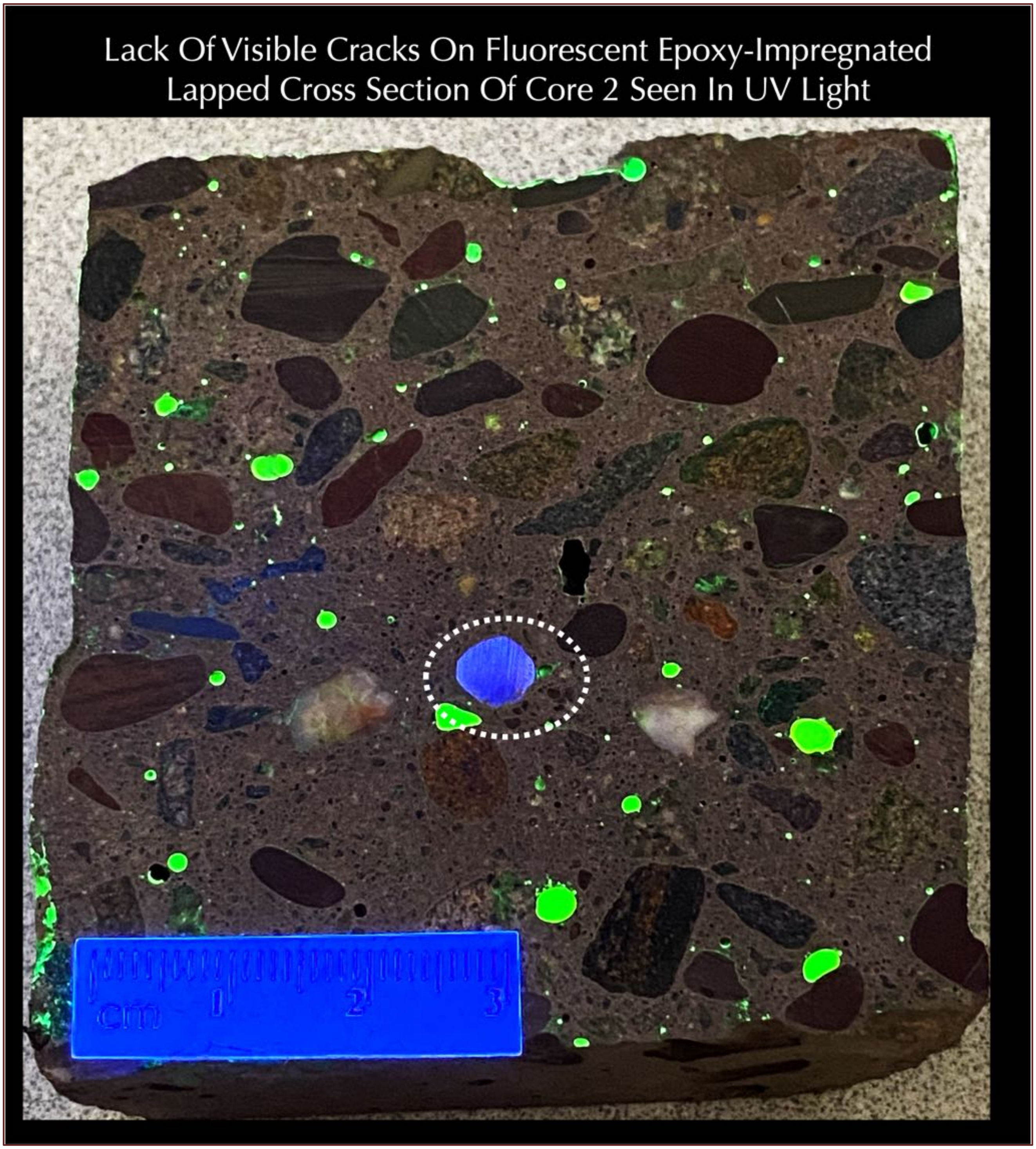

Figure 16: Same lapped section shown in Figure 15 but seen in UV light to highlight air voids and cracks that are impregnated with fluorescent epoxy.

SAW-CUT CROSS SECTIONS

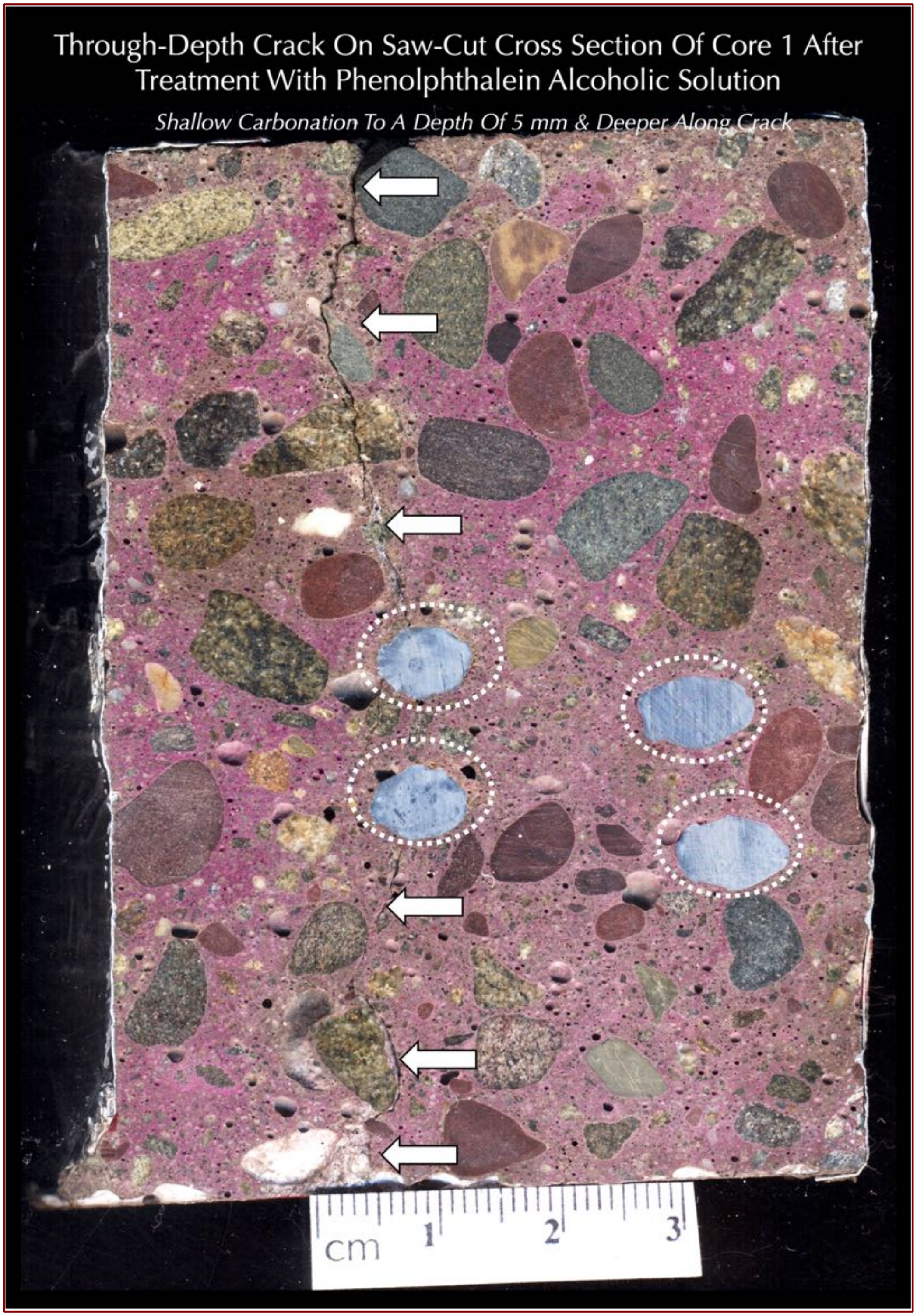

Figure 17: Saw-cut cross section of Core 1 after treatment with phenolphthalein alcoholic solution to show the negligible depth of carbonation, mostly depicting the non-carbonated interior concrete, which turned pink during alcohol treatment. Carbonation has extended to a deeper level along surface cracks.

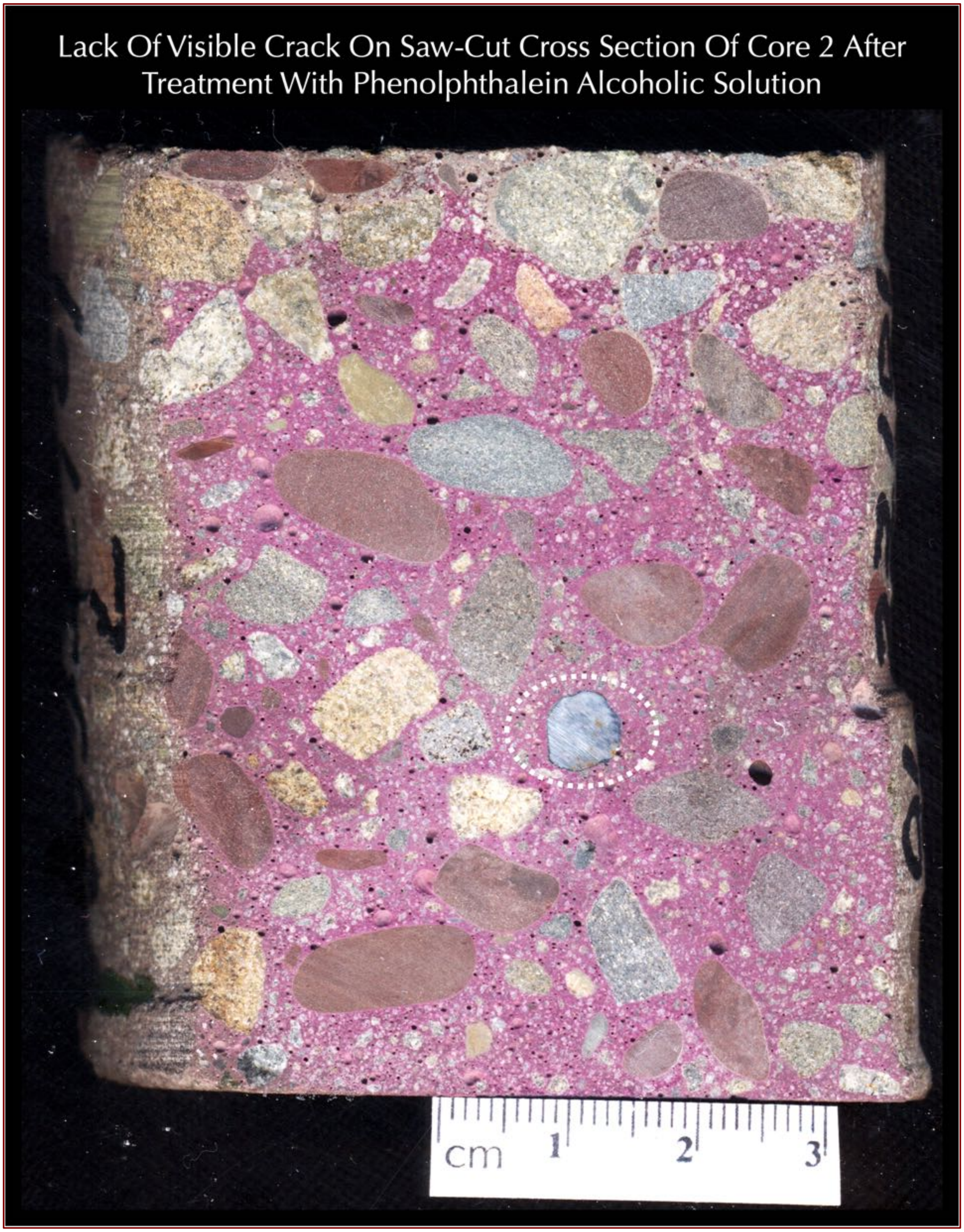

Figure 18: Saw-cut cross section of Core 2 after treatment with phenolphthalein alcoholic solution to show the negligible depth of carbonation, mostly depicting the non-carbonated interior concrete, which turned pink during alcohol treatment.

MICROGRAPHS OF LAPPED CROSS SECTION

Figure 19: Micrographs of lapped cross section of Core 1 from the surface region showing:

a. The main vertical crack that has transected a greywacke gravel coarse aggregate particle (red arrow in top photo) and circumscribed another larger gravel along its path; the crack path is marked by white arrows;

b. Air-entrained concrete consisting of numerous fine, discrete spherical and near-spherical entrained voids of sizes 1 mm or less; air content is estimated to be 6 to 7 percent; and,

c. Internal cracking in a greywacke gravel coarse aggregate particlen in the bottom photo (red arrow in bottom photo).

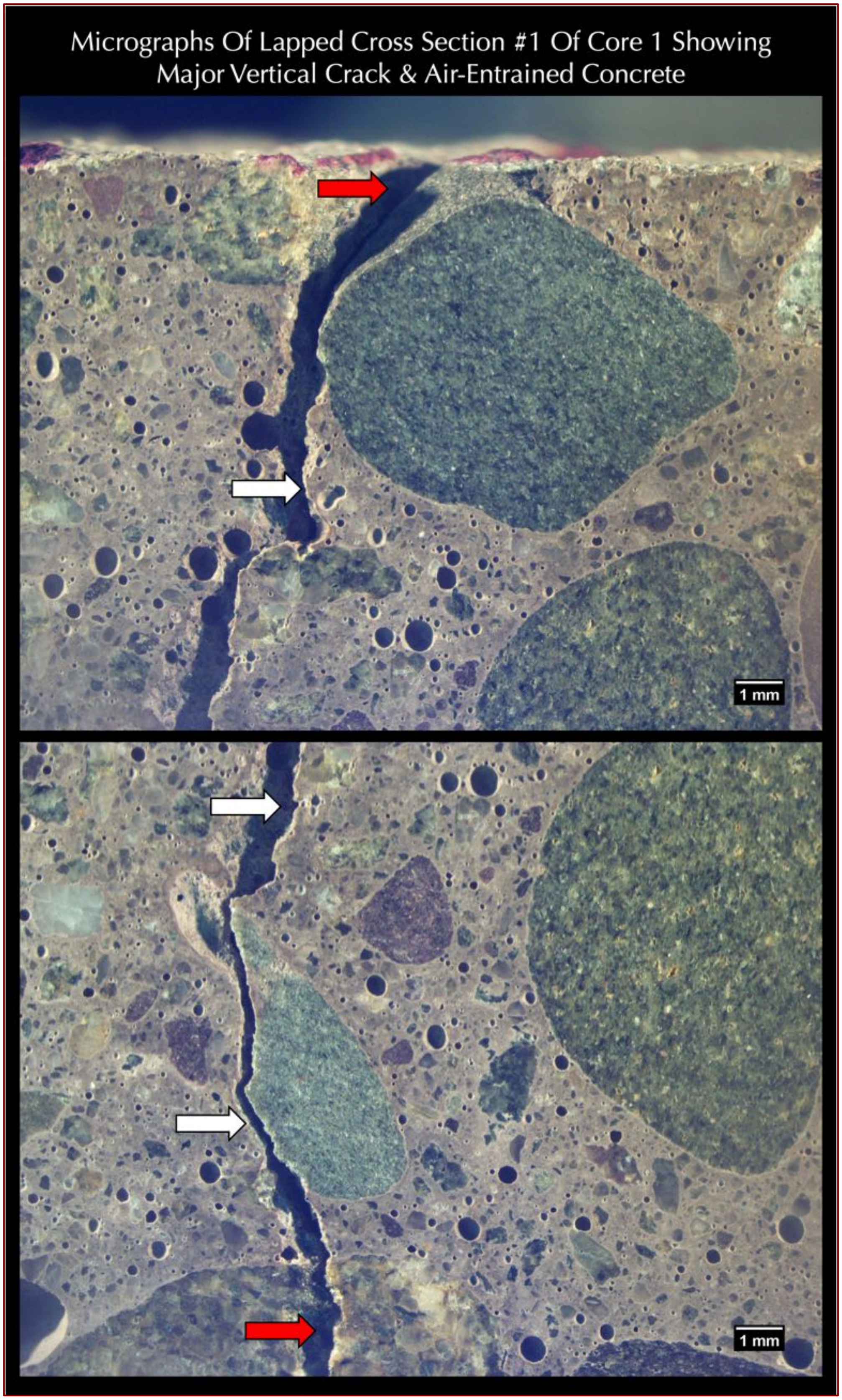

Figure 20: Micrographs of lapped cross section of Core 1 from the surface region showing:

a. The main vertical crack that has transected a greywacke gravel (red arrow in top photo) and circumscribed another larger gravel along its path; the crack path is marked by white arrows;

b. Air-entrained concrete consisting of numerous fine, discrete spherical and near-spherical entrained voids of sizes 1 mm or less; air content is estimated to be 6 to 7 percent; and,

c. Internal cracking in a greywacke gravel in the bottom photo (red arrow in bottom photo).

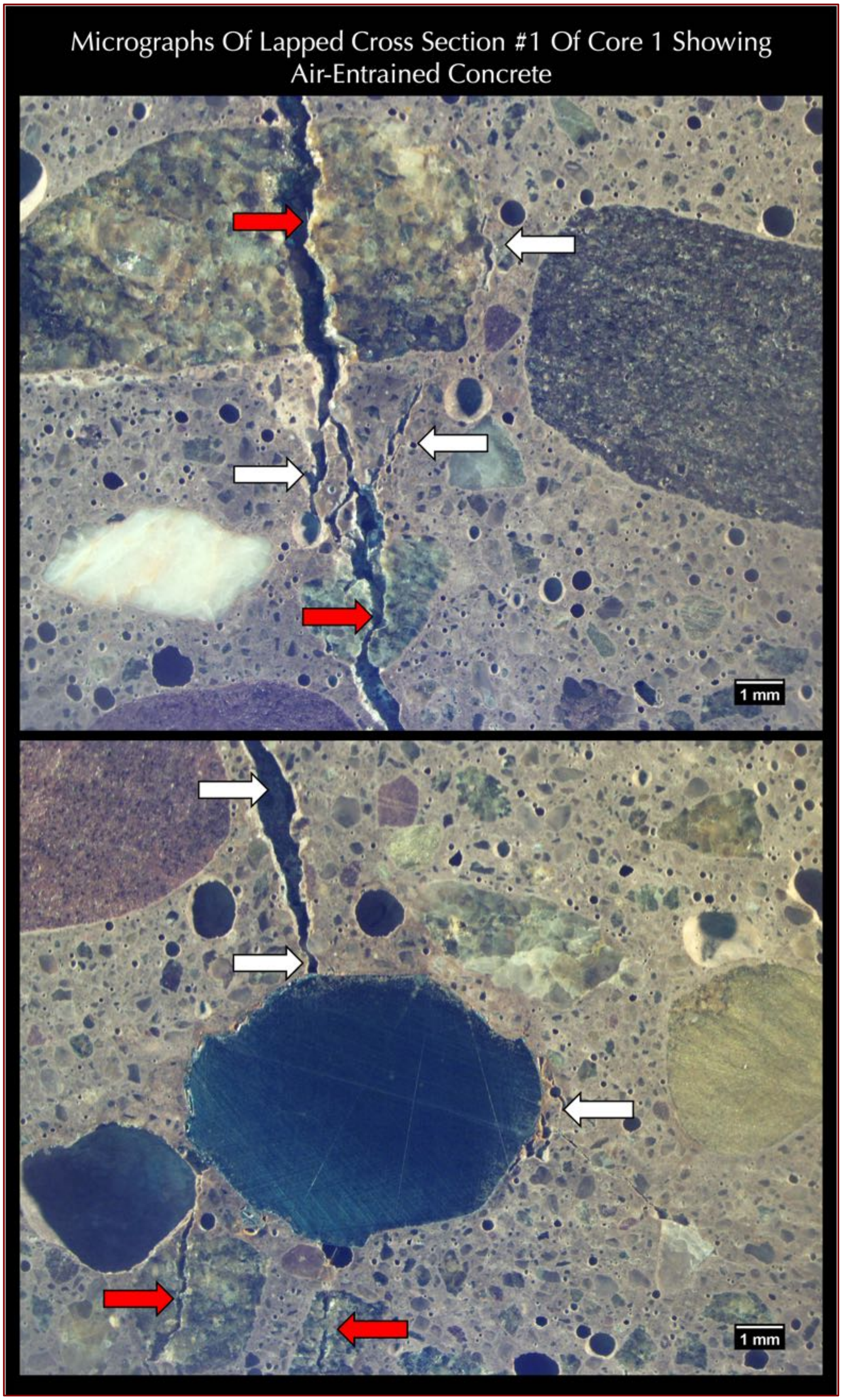

Figure 21: Micrographs of lapped cross section of Core 1 from the near-surface region showing:

a. The main vertical crack that has transected two greywacke gravel (red arrows in top photo) coarse aggregate particles along its path; the crack paths are marked by white arrows;

b. Air-entrained concrete consisting of numerous fine, discrete spherical and near-spherical entrained voids of sizes 1 mm or less; air content is estimated to be 6 to 7 percent; and,

c. Internal cracking in two greywacke gravel coarse aggregate particles in the bottom photo (red arrows in bottom photo).

d. A No. 2 mesh in the bottom photo, and the main crack that has gone around the steel.

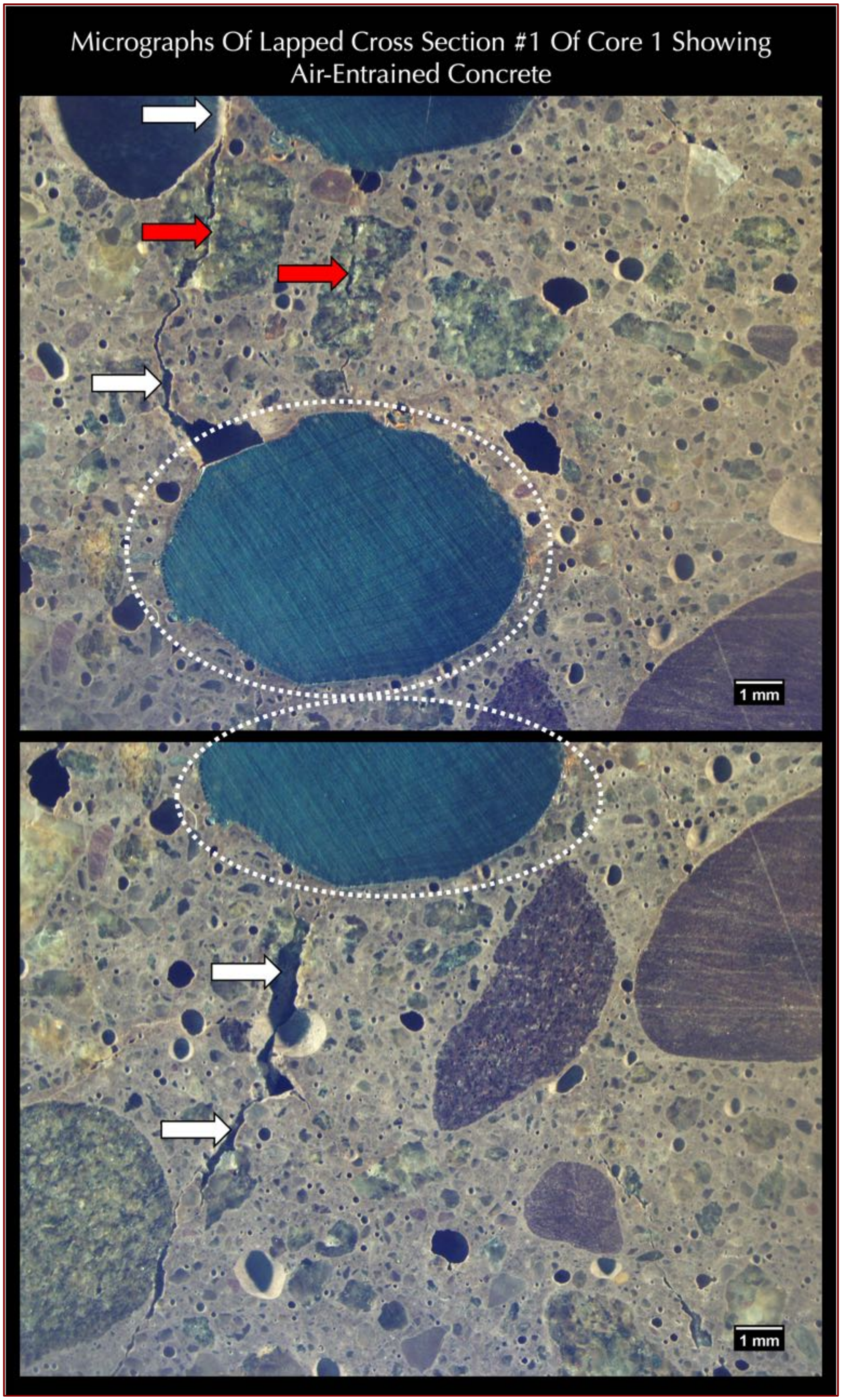

Figure 22: Micrographs of lapped cross section of Core 1 from the mid-depth location of core showing:

a. Extension of the main vertical crack that has transected a greywacke gravel (red arrows in top photo) coarse aggregate particle along its path; the crack paths are marked by white arrows;

b. Air-entrained concrete consisting of numerous fine, discrete spherical and near-spherical entrained voids of sizes 1 mm or less; air content is estimated to be 6 to 7 percent; and,

c. Internal cracking in a greywacke gravel coarse aggregate particle in the top photo (red arrow in the top photo) beside the main crack.

d. A No. 2 mesh in the top and bottom photos, and the main crack that has gone around the steel.

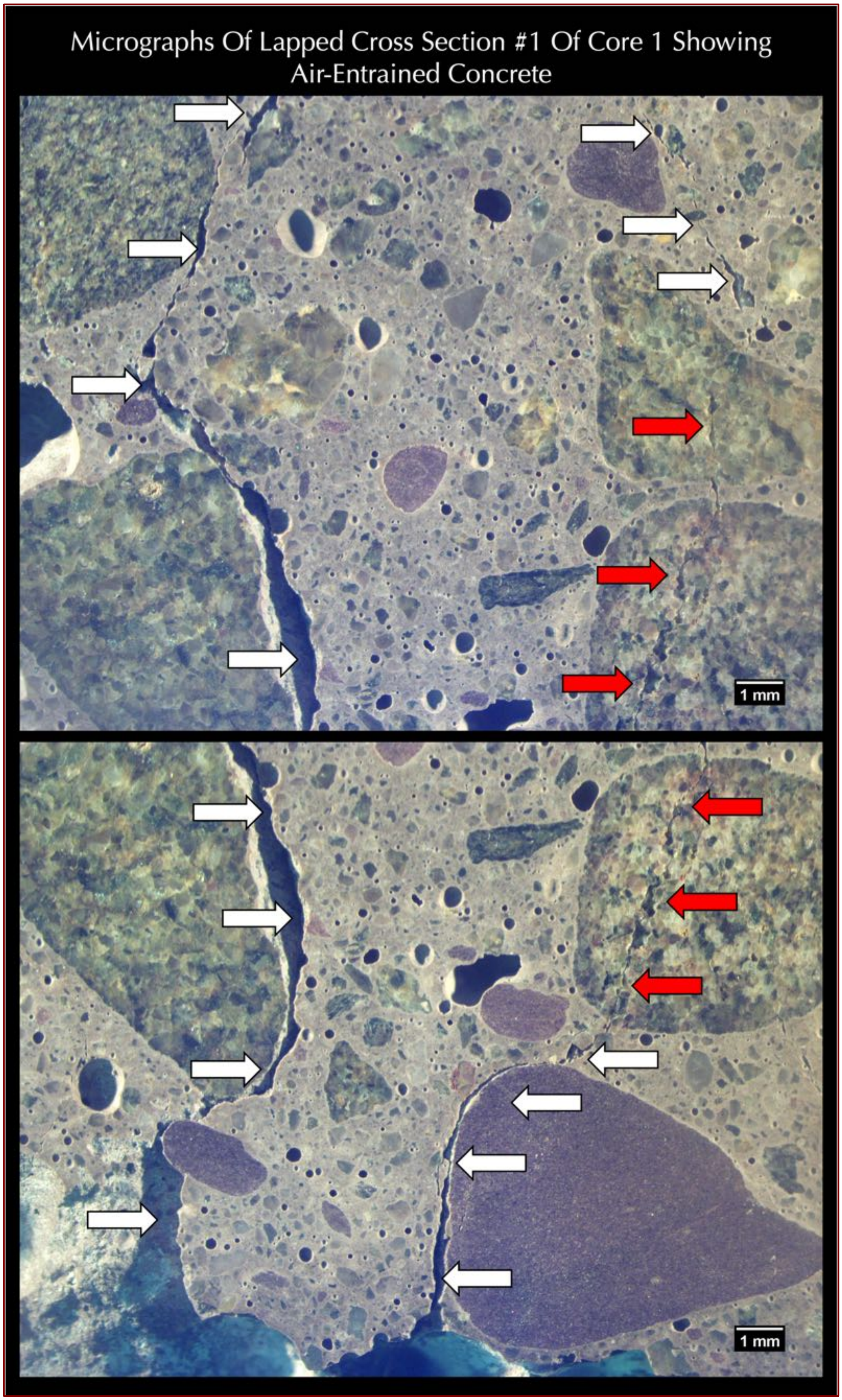

Figure 23: Micrographs of lapped cross section of Core 1 from the mid-depth and bottom location of core showing:

a. Extension of the main vertical crack that has circumscribed greywacke gravel (white arrows in the top photo) coarse aggregate particles along its path;

b. Air-entrained concrete consisting of numerous fine, discrete spherical and near-spherical entrained voids of sizes 1 mm or less; air content is estimated to be 6 to 7 percent; and,

c. Internal cracking in two greywacke gravel coarse aggregate particles in the top and bottom photos (red arrows in top and bottom photos) beside the main crack.

d. A reddish-brown ferruginous shale-siltstone gravel particle in the bottom photo, and extension of the crack from greywacke gravel that has circumscribed the ferruginous gravel particle (white arrows in the bottom photo).

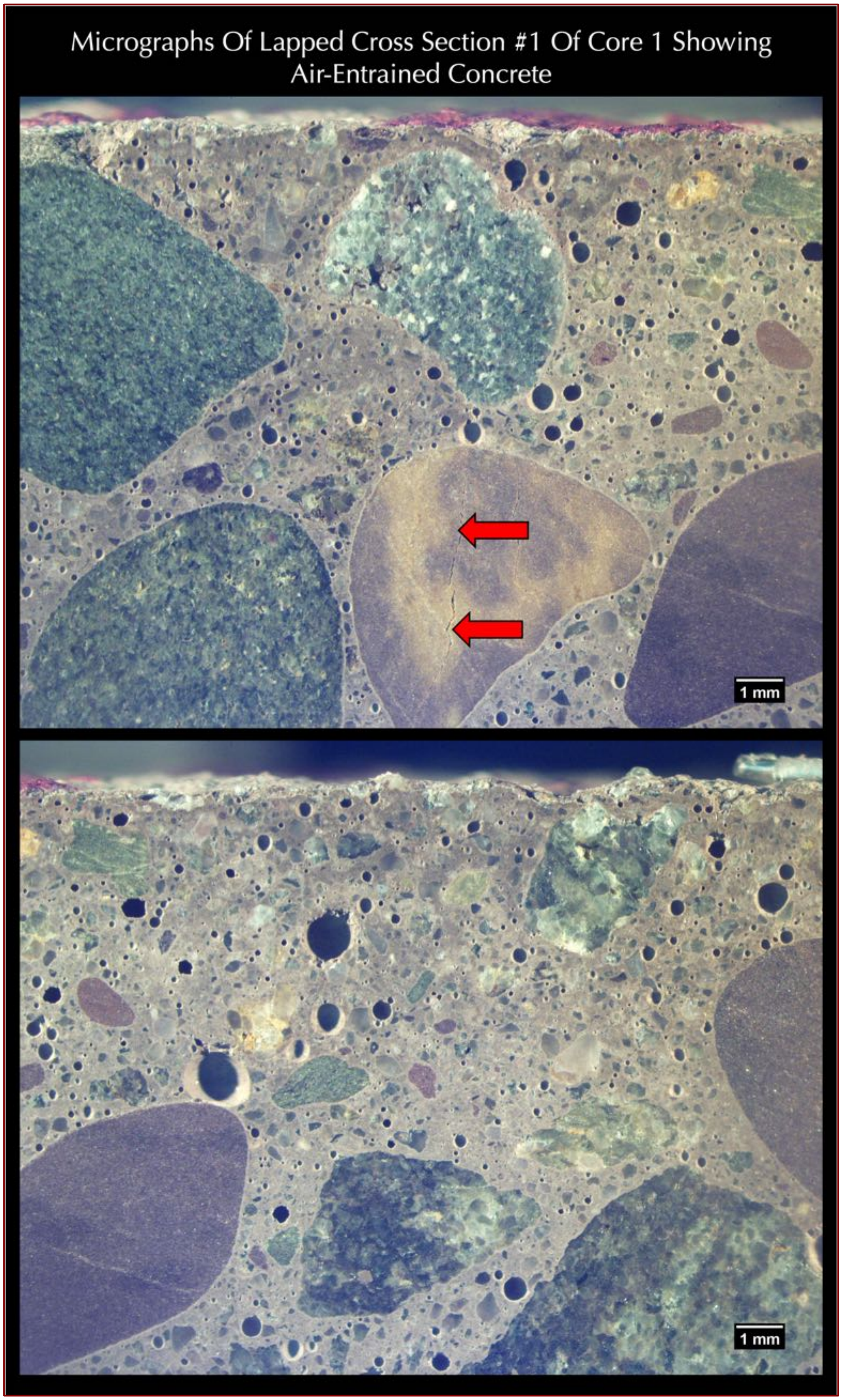

Figure 24: Micrographs of lapped cross section of Core 1 from the surface region of core showing:

a. Internal cracking in a shale gravel coarse aggregate particle in the top photo (marked by red arrows).

b. Air-entrained concrete consisting of numerous fine, discrete spherical and near-spherical entrained voids of sizes 1 mm or less. Air content is estimated to be 6 to 7 percent.

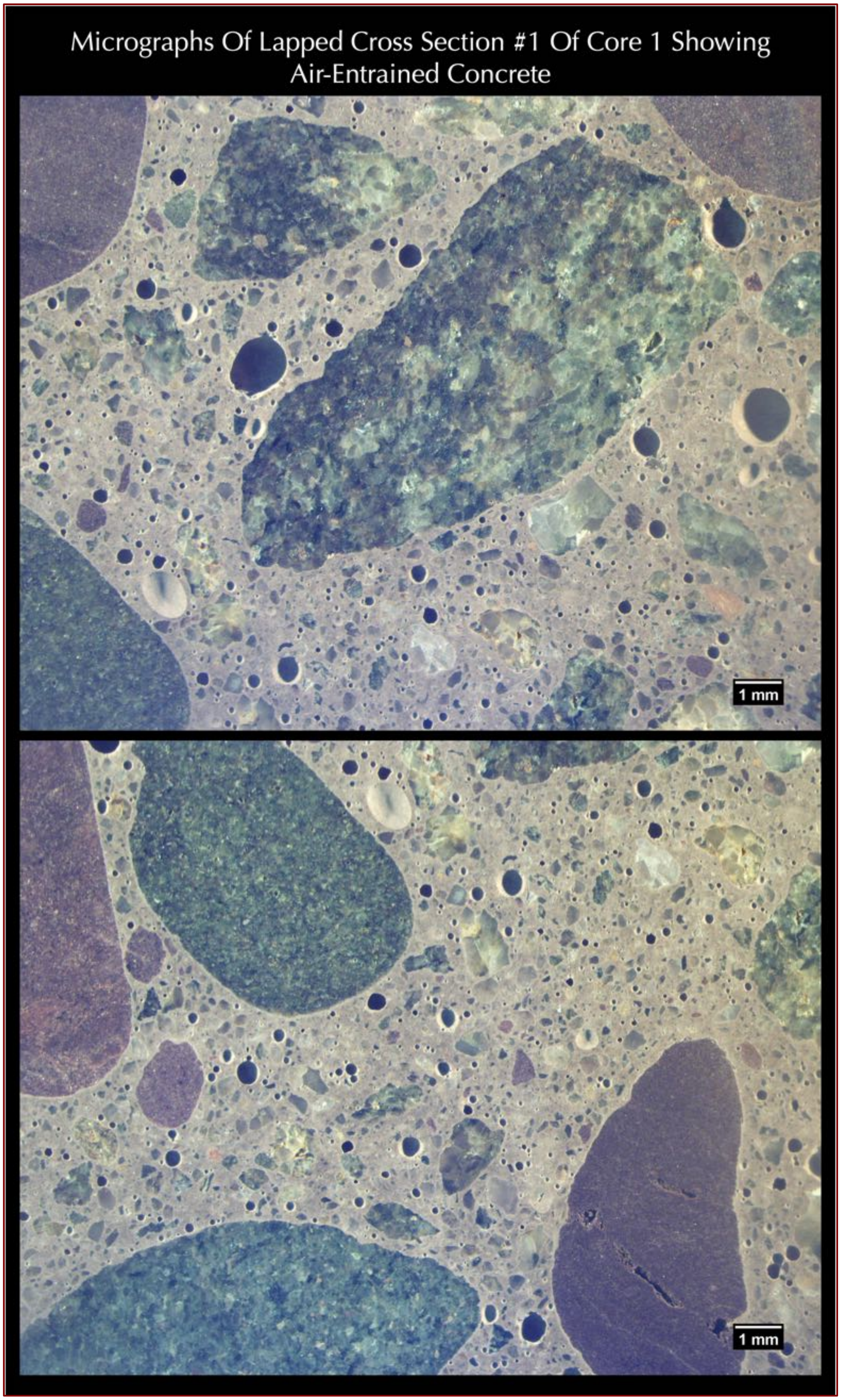

Figure 25: Micrographs of lapped cross section of Core 1 from the mid-depth and bottom half of core showing:

a. Air-entrained concrete consisting of numerous fine, discrete spherical and near-spherical entrained voids of sizes 1 mm or less. Air content is estimated to be 6 to 7 percent.

b. Internal cracking in a reddish-brown ferruginous shale-siltstone particle in gravel coarse aggregate in the bottom photo.

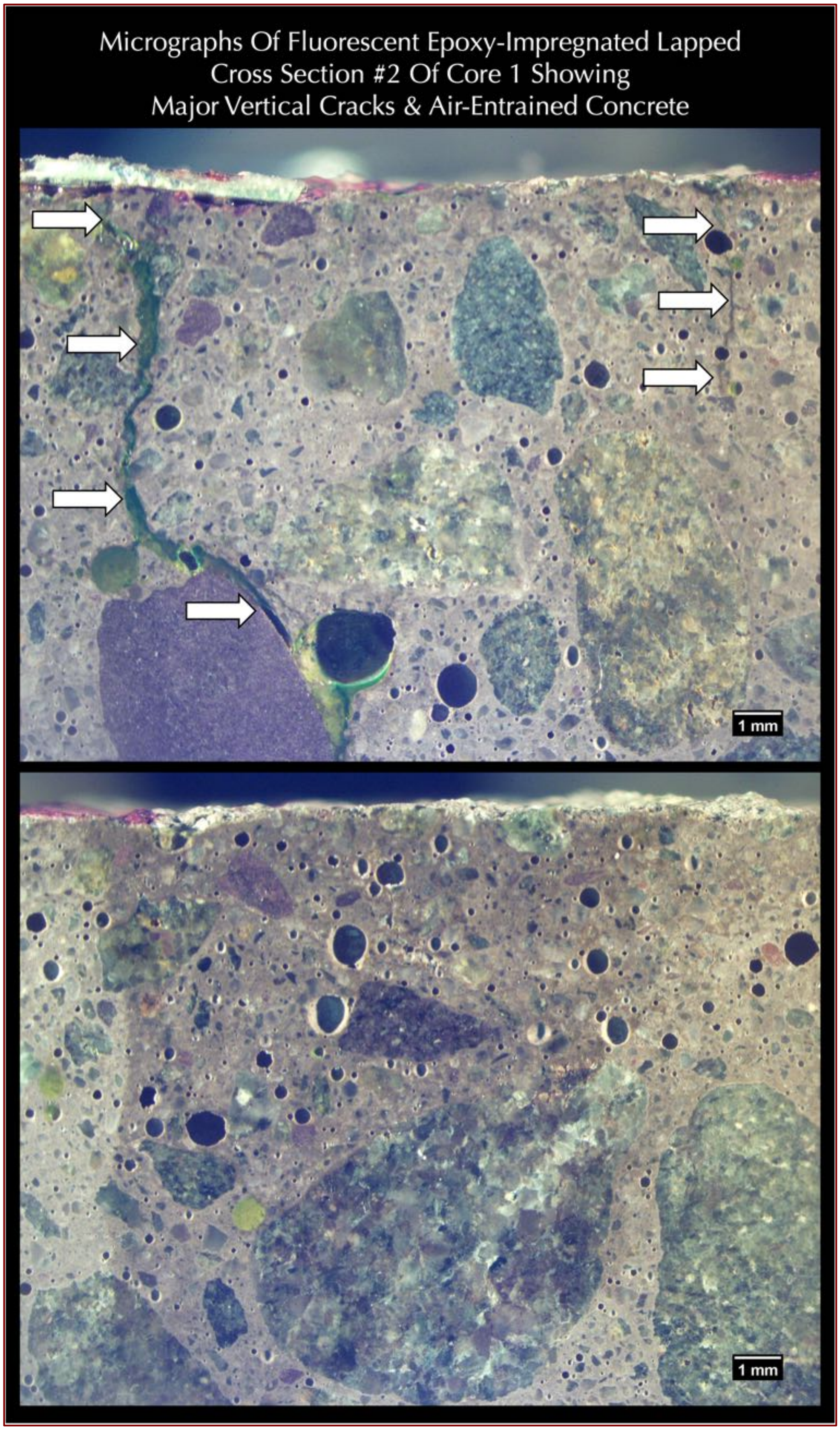

Figure 26: Micrographs of a second fluorescent epoxy-impregnated lapped cross section of Core 1 from the surface region showing:

a. Two main vertical cracks that have transected the coarse and fine aggregate particles along its path in the top photo (the crack paths are marked by white arrows; and,

b. Air-entrained concrete consisting of numerous fine, discrete spherical and near-spherical entrained voids of sizes 1 mm or less. Air content is estimated to be 6 to 7 percent.

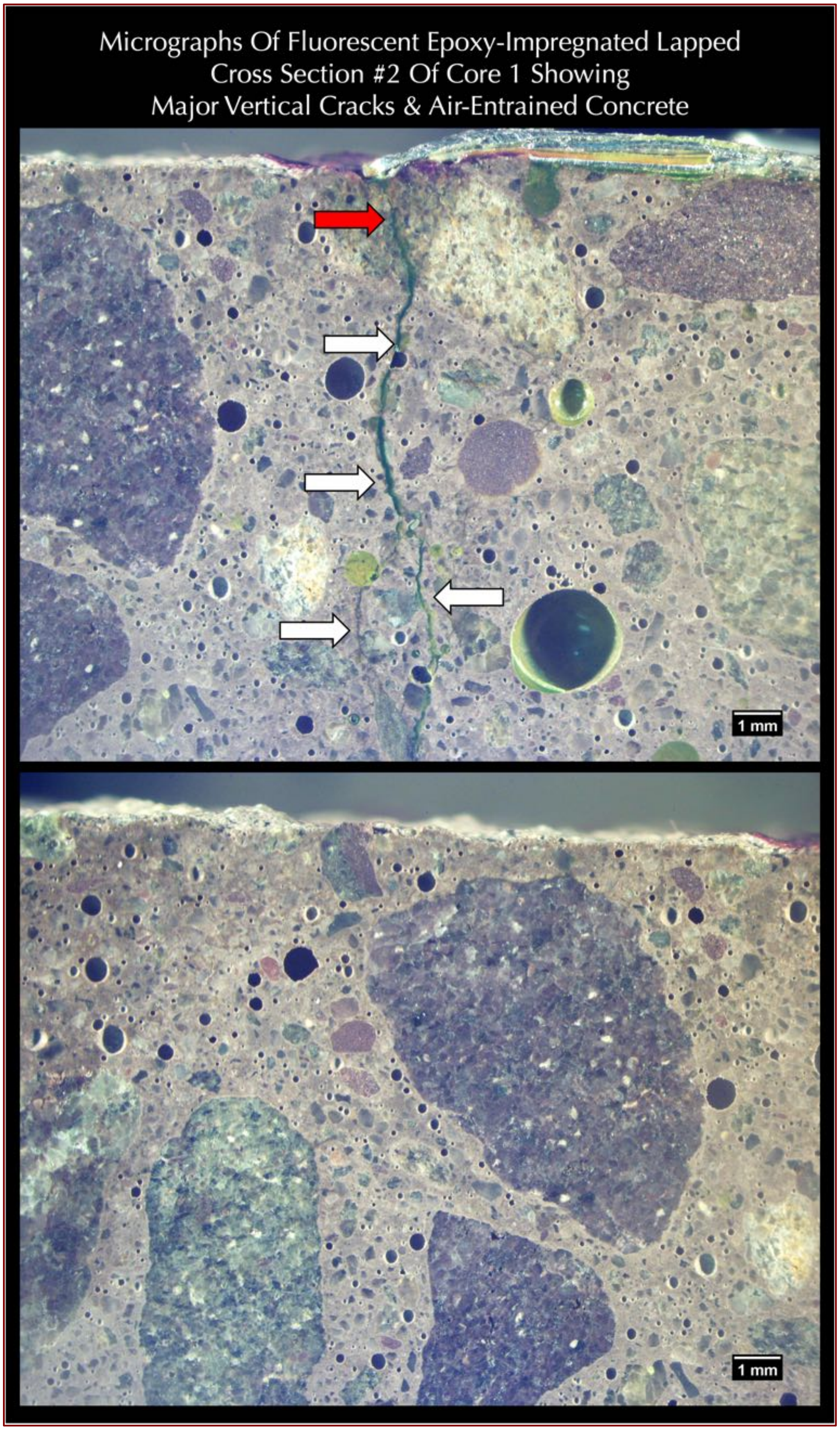

Figure 27: Micrographs of a second fluorescent epoxy-impregnated lapped cross section of Core 1 from the surface region showing:

a. The main vertical crack in the top photo that has transected a near-surface greywacke gravel coarse aggregate particle (red arrow in top photo); the crack path is marked by white arrows; and,

b. Air-entrained concrete consisting of numerous fine, discrete spherical and near-spherical entrained voids of sizes 1 mm or less. Air content is estimated to be 6 to 7 percent.

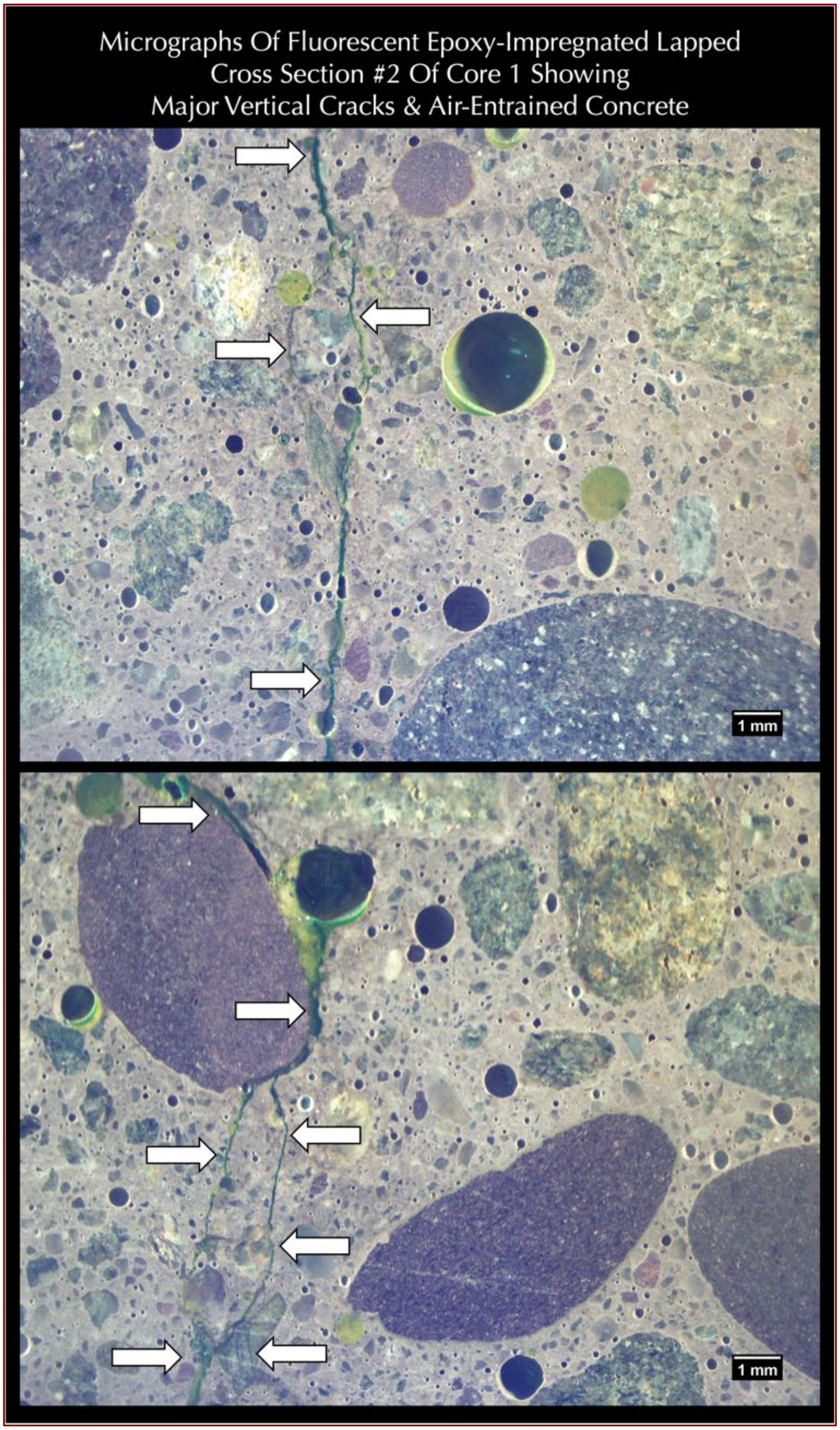

Figure 28: Micrographs of a second fluorescent epoxy-impregnated lapped cross section of Core 1 from the near-surface region showing:

a. Extension of the main vertical crack that has transected and circumscribed aggregate particles along its crack path (the crack path is marked by white arrows); and,

b. Air-entrained concrete consisting of numerous fine, discrete spherical and near-spherical entrained voids of sizes 1 mm or less. Air content is estimated to be 6 to 7 percent.

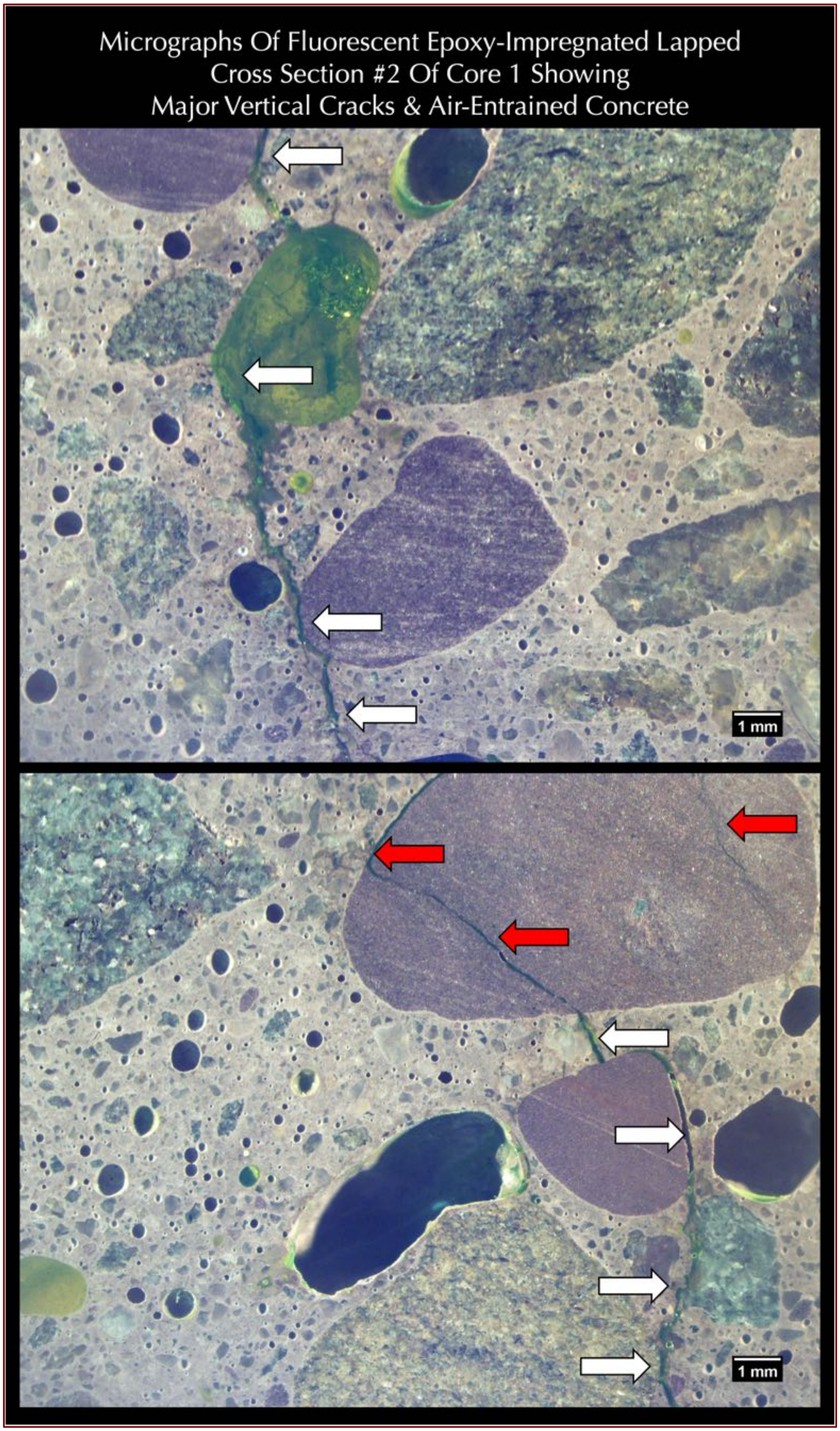

Figure 29: Micrographs of a second fluorescent epoxy-impregnated lapped cross section of Core 1 from the interior showing:

a. Extension of the main vertical crack that has transected and circumscribed aggregate particles along its crack path (the crack path is marked by white arrows);

b. Red arrows in the bottom photo shows extension of crack through a reddish brown ferruginous shale-siltstone partice in coarse aggregate as well as internal cracking in the particle; and,

c. Air-entrained concrete consisting of numerous fine, discrete spherical and near-spherical entrained voids of sizes 1 mm or less. Air content is estimated to be 6 to 7 percent.

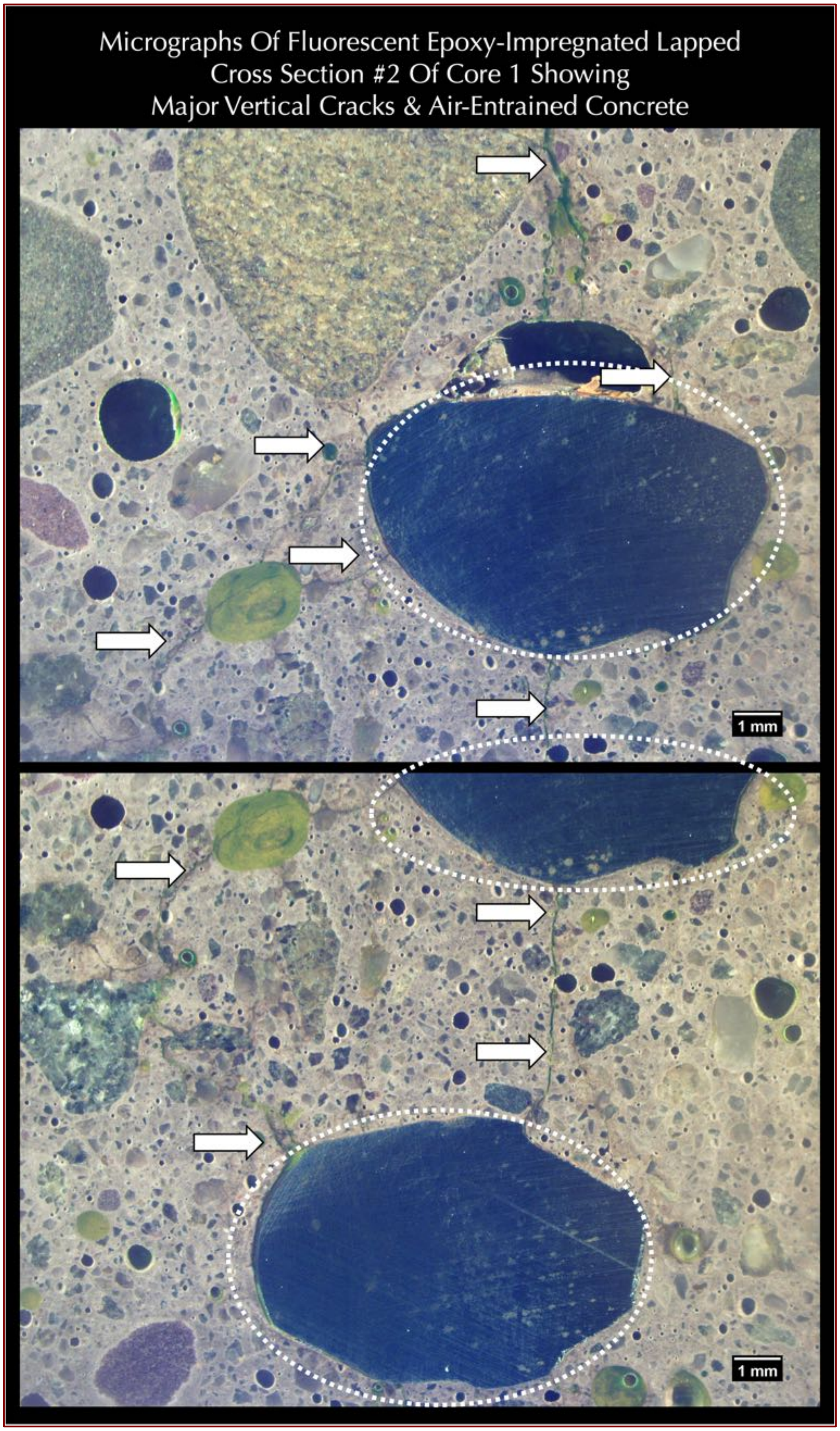

Figure 30: Micrographs of a second fluorescent epoxy-impregnated lapped cross section of Core 1 from the interior showing:

a. Extension of the main vertical crack that has gone around a No. 2 mesh (the crack path is marked by white arrows); and,

b. Air-entrained concrete consisting of numerous fine, discrete spherical and near-spherical entrained voids of sizes 1 mm or less. Air content is estimated to be 6 to 7 percent.

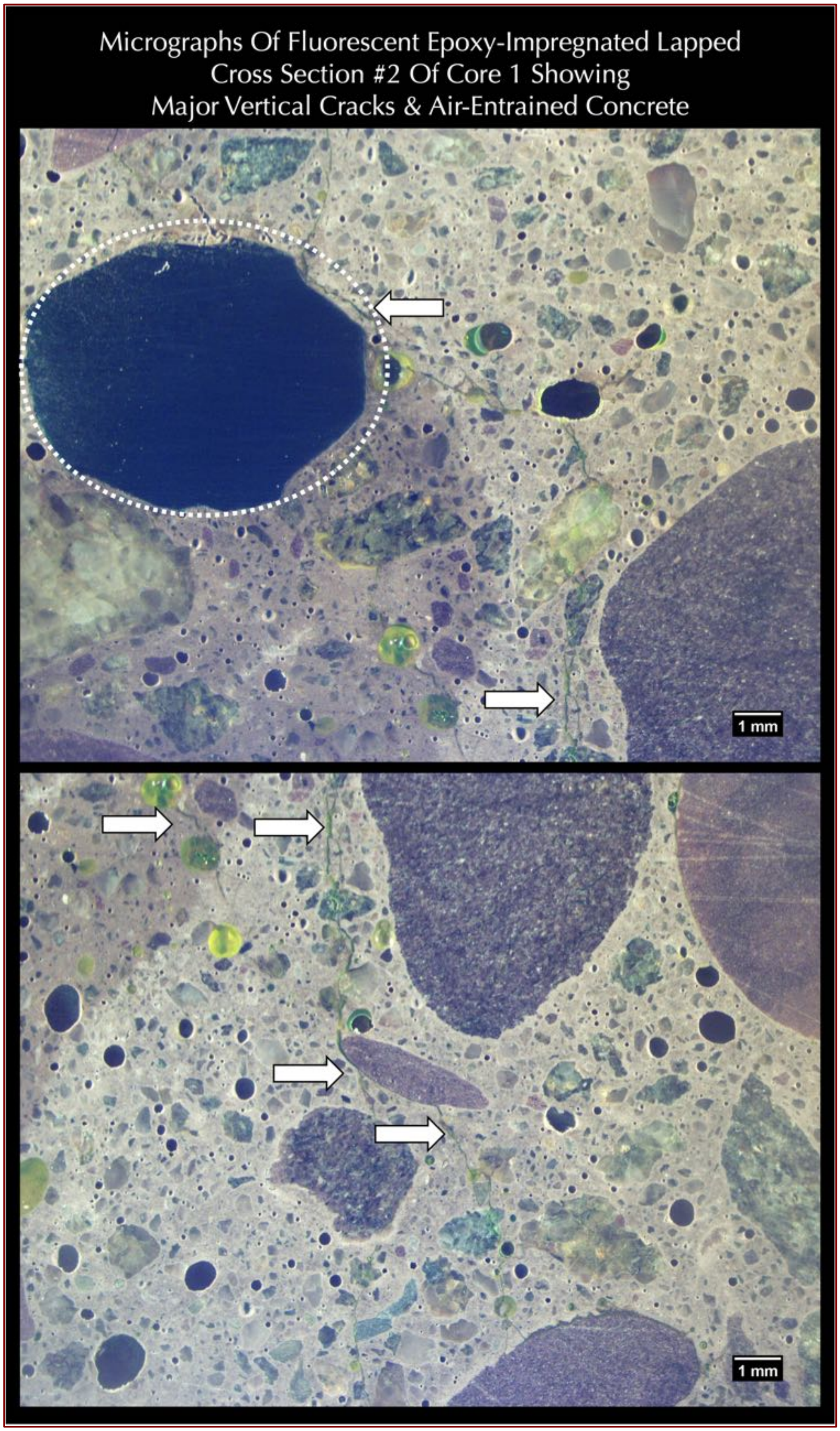

Figure 31: Micrographs of a second fluorescent epoxy-impregnated lapped cross section of Core 1 from the interior showing:

a. Extension of the main vertical crack that has gone around a No. 2 mesh (the crack path is marked by white arrows); and,

b. Air-entrained concrete consisting of numerous fine, discrete spherical and near-spherical entrained voids of sizes 1 mm or less. Air content is estimated to be 6 to 7 percent.

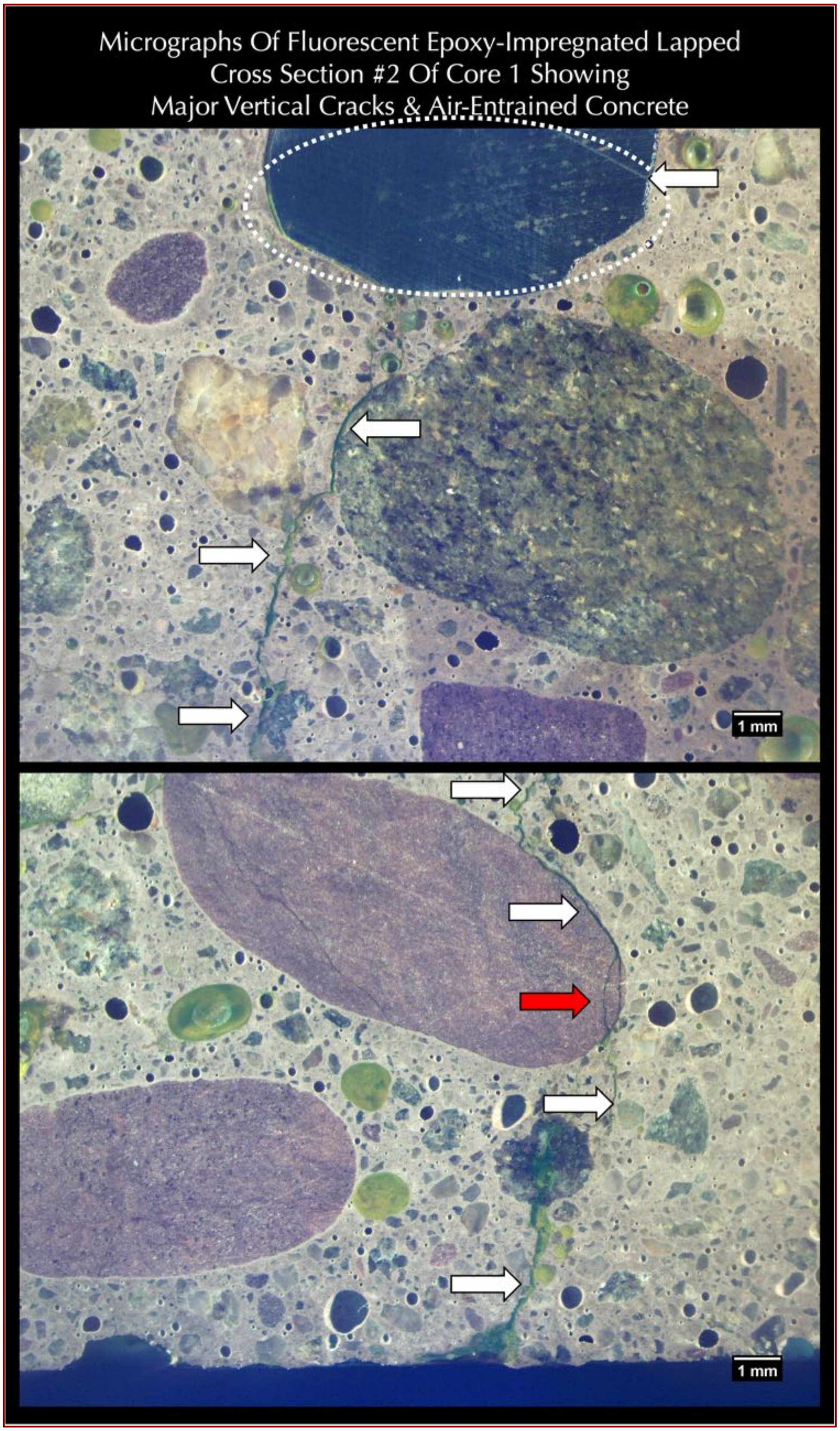

Figure 32: Micrographs of a second fluorescent epoxy-impregnated lapped cross section of Core 1 from the interior and bottom end showing:

a. Extension of the main vertical crack that has gone around a No. 2 mesh (the crack path is marked by white arrows);

b. Red arrow in the bottom photo shows extension of crack through a reddish brown ferruginous shale-siltstone partice in coarse aggregate; and,

c. Air-entrained concrete consisting of numerous fine, discrete spherical and near-spherical entrained voids of sizes 1 mm or less. Air content is estimated to be 6 to 7 percent.

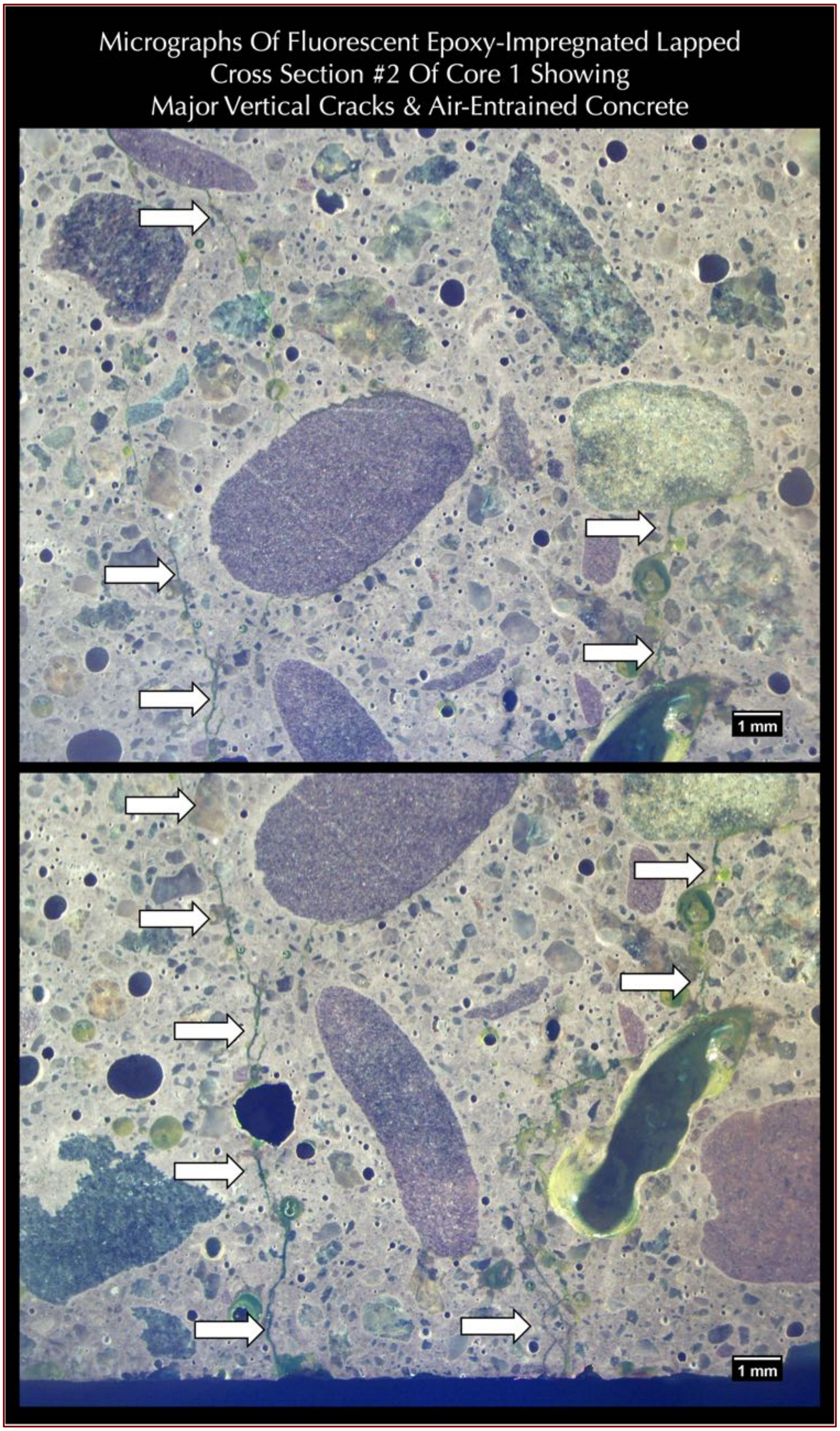

Figure 33: Micrographs of a second fluorescent epoxy-impregnated lapped cross section of Core 1 from the interior and bottom end showing:

a. Extension of the main vertical crack that has gone around aggregate particles along its path (the crack path is marked by white arrows);

b. Arrows at right side of the main crack shows secondary cracks formed from internal cracking of greywacke particles in gravel coarse aggregate; and,

c. Air-entrained concrete consisting of numerous fine, discrete spherical and near-spherical entrained voids of sizes 1 mm or less. Air content is estimated to be 6 to 7 percent.

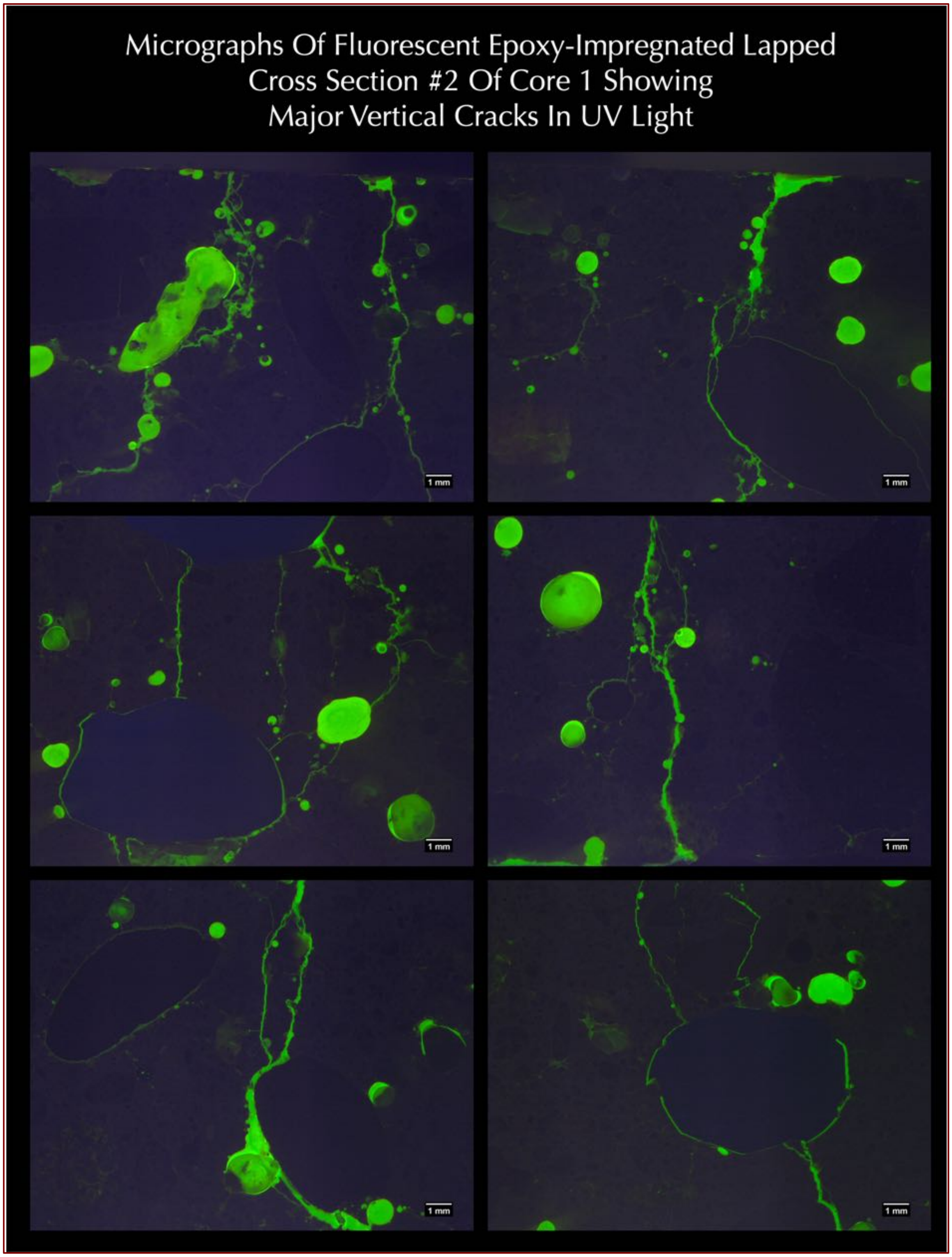

Figure 34: Fluorescent epoxy-impregnated lapped cross section of Core 1 seen in UV light to highlight the crack paths and a few coarse air voids.

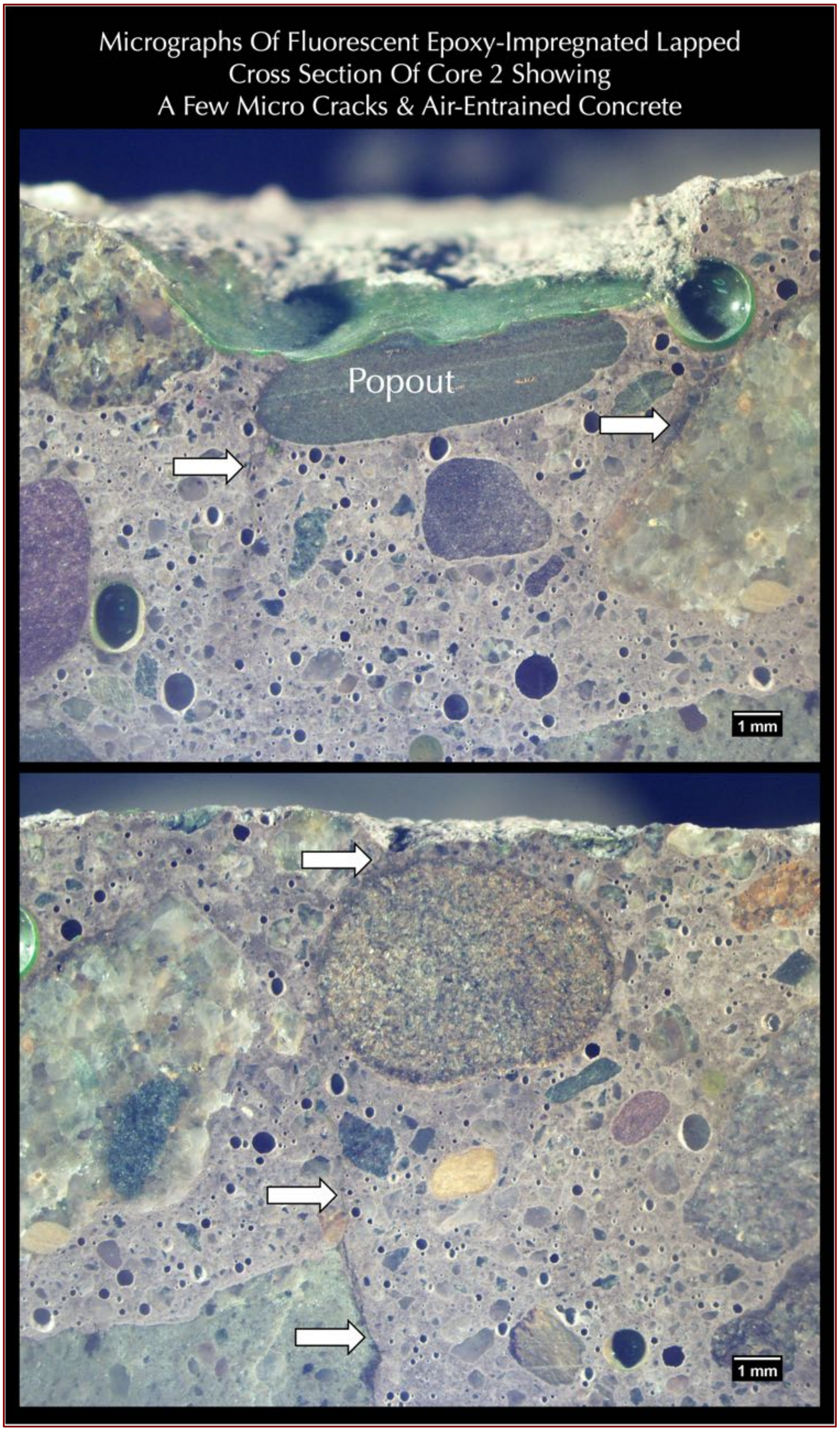

Figure 35: Micrographs of fluorescent epoxy-impregnated lapped cross section of Core 2 from the surface region showing:

a. Fracturing and popout of a shale and adjacent greywacke particle in gravel coarse aggregate at the surface and associated cracking from the fractured particles (marked by white arrows in the top photo);

b. A second microcrack from the surface in the bottom photo, which has circumscribed aggregate particles along its path (the crack path is marked by white arrows); and,

c. Air-entrained concrete consisting of numerous fine, discrete spherical and near-spherical entrained voids of sizes 1 mm or less. Air content is estimated to be 6 to 7 percent.

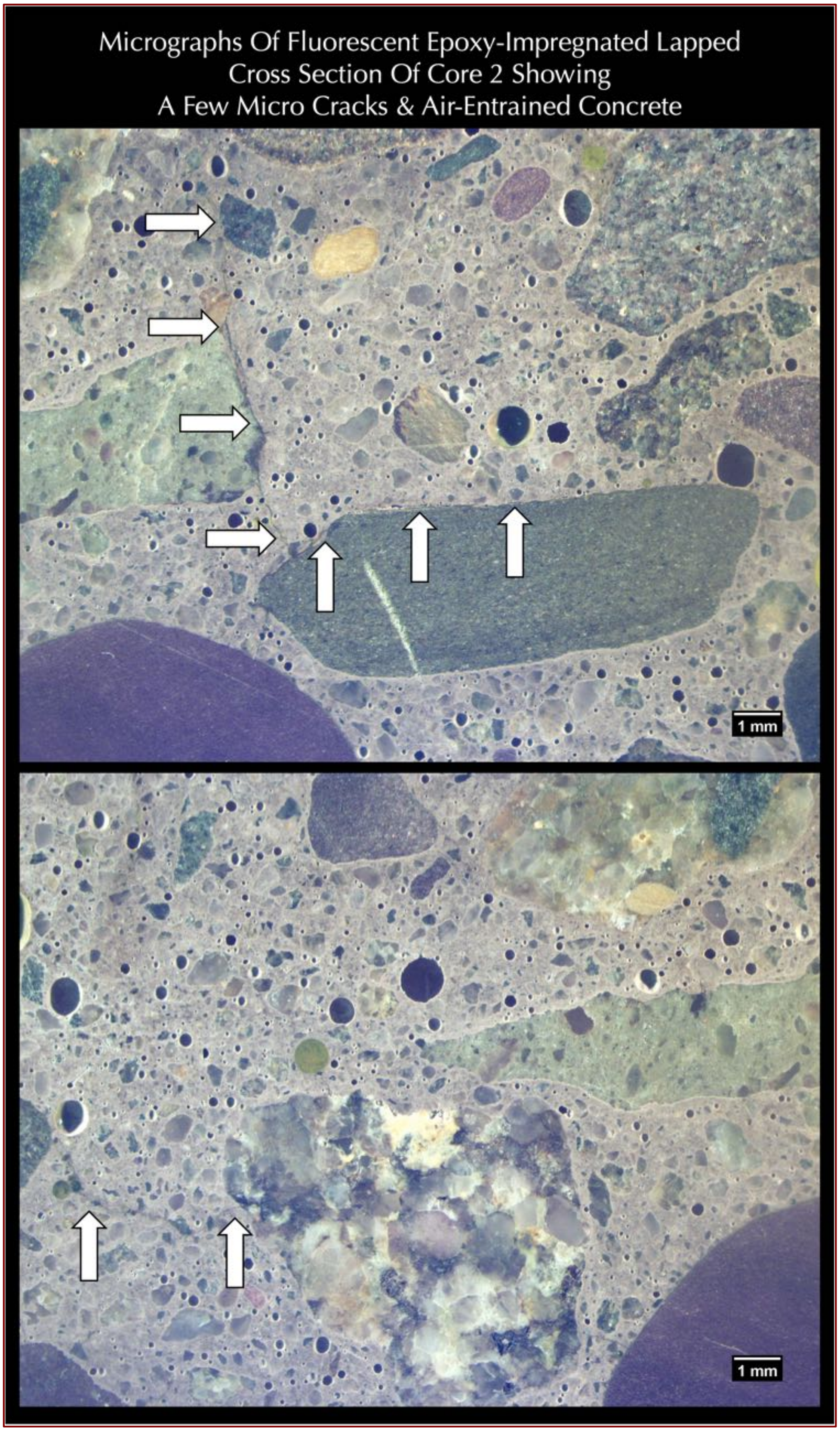

Figure 36: Micrographs of fluorescent epoxy-impregnated lapped cross section of Core 2 from the interior showing:

a. Internal microcracks in concrete marked by white arrows in both photos; and,

b. Air-entrained concrete consisting of numerous fine, discrete spherical and near-spherical entrained voids of sizes 1 mm or less. Air content is estimated to be 6 to 7 percent.

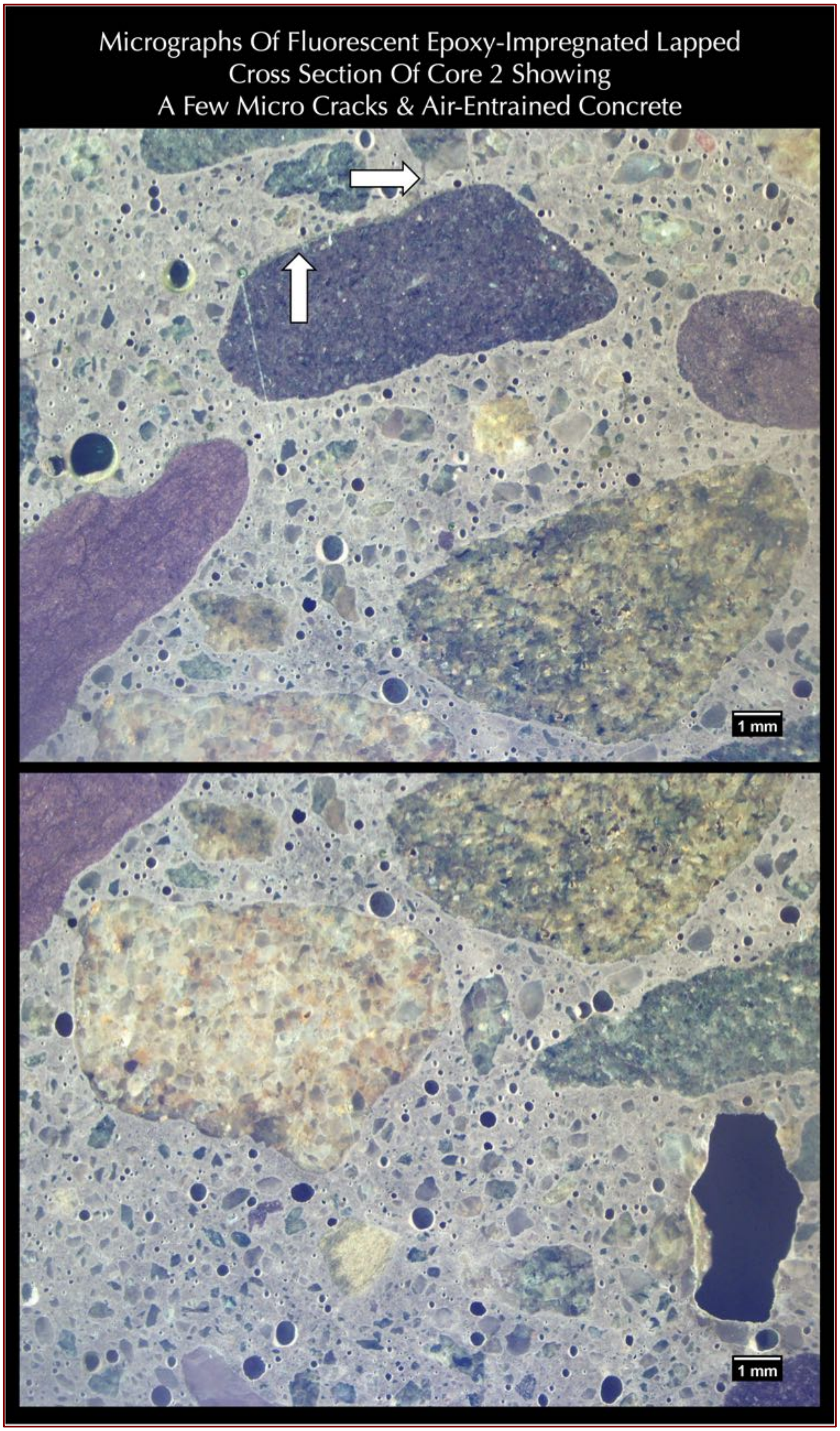

Figure 37: Micrographs of fluorescent epoxy-impregnated lapped cross section of Core 2 from the interior showing:

a. Internal microcracks in concrete marked by white arrows in both photos; and,

b. Air-entrained concrete consisting of numerous fine, discrete spherical and near-spherical entrained voids of sizes 1 mm or less. Air content is estimated to be 6 to 7 percent.

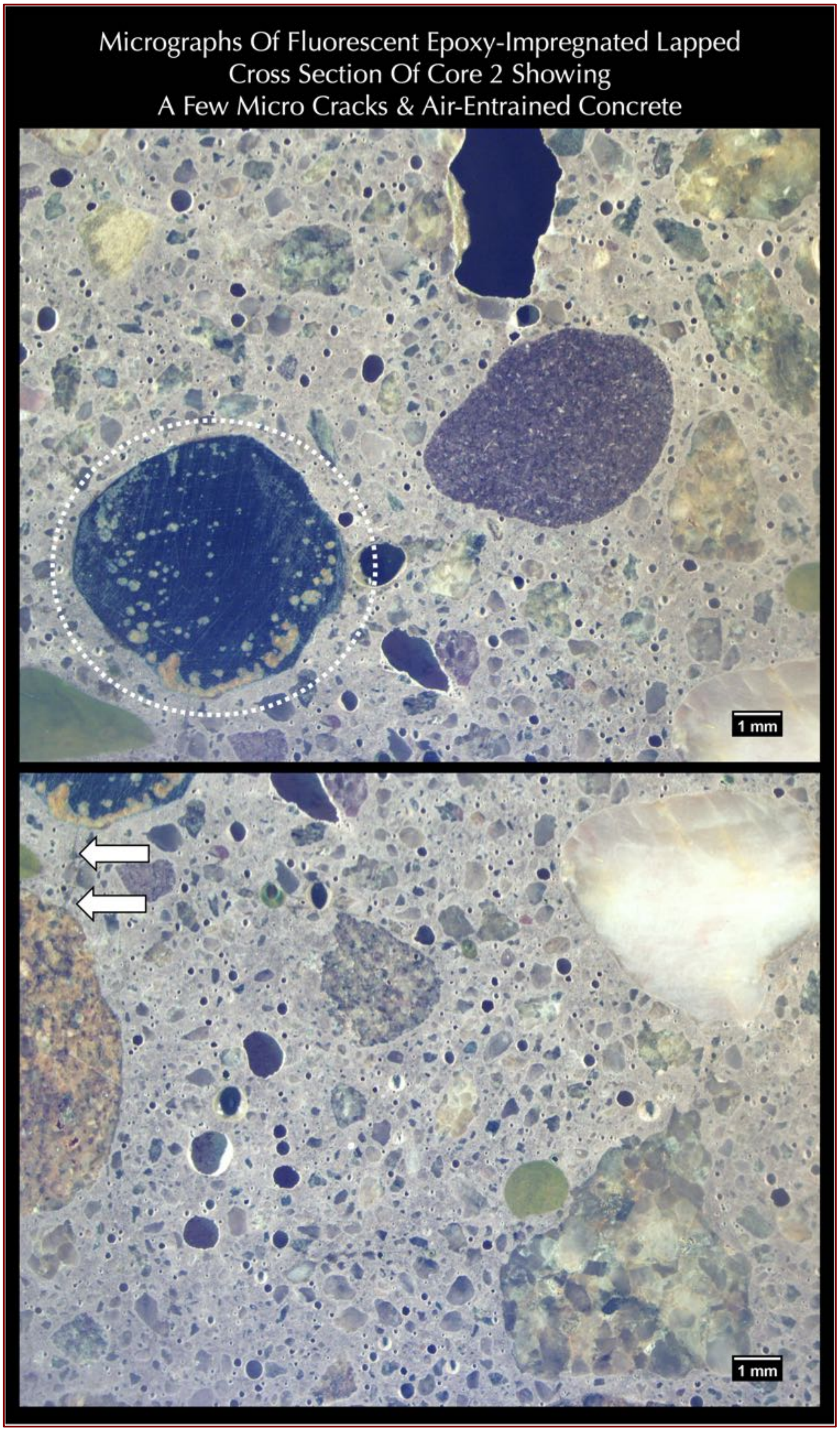

Figure 38: Micrographs of fluorescent epoxy-impregnated lapped cross section of Core 2 from the interior showing:

a. A No. 2 reinforcing steel mesh (circled in the top photo), and a coarse void;

b. A microcrack in the bottom photo marked with white arrows; and,

c. Air-entrained concrete consisting of numerous fine, discrete spherical and near-spherical entrained voids of sizes 1 mm or less. Air content is estimated to be 6 to 7 percent.

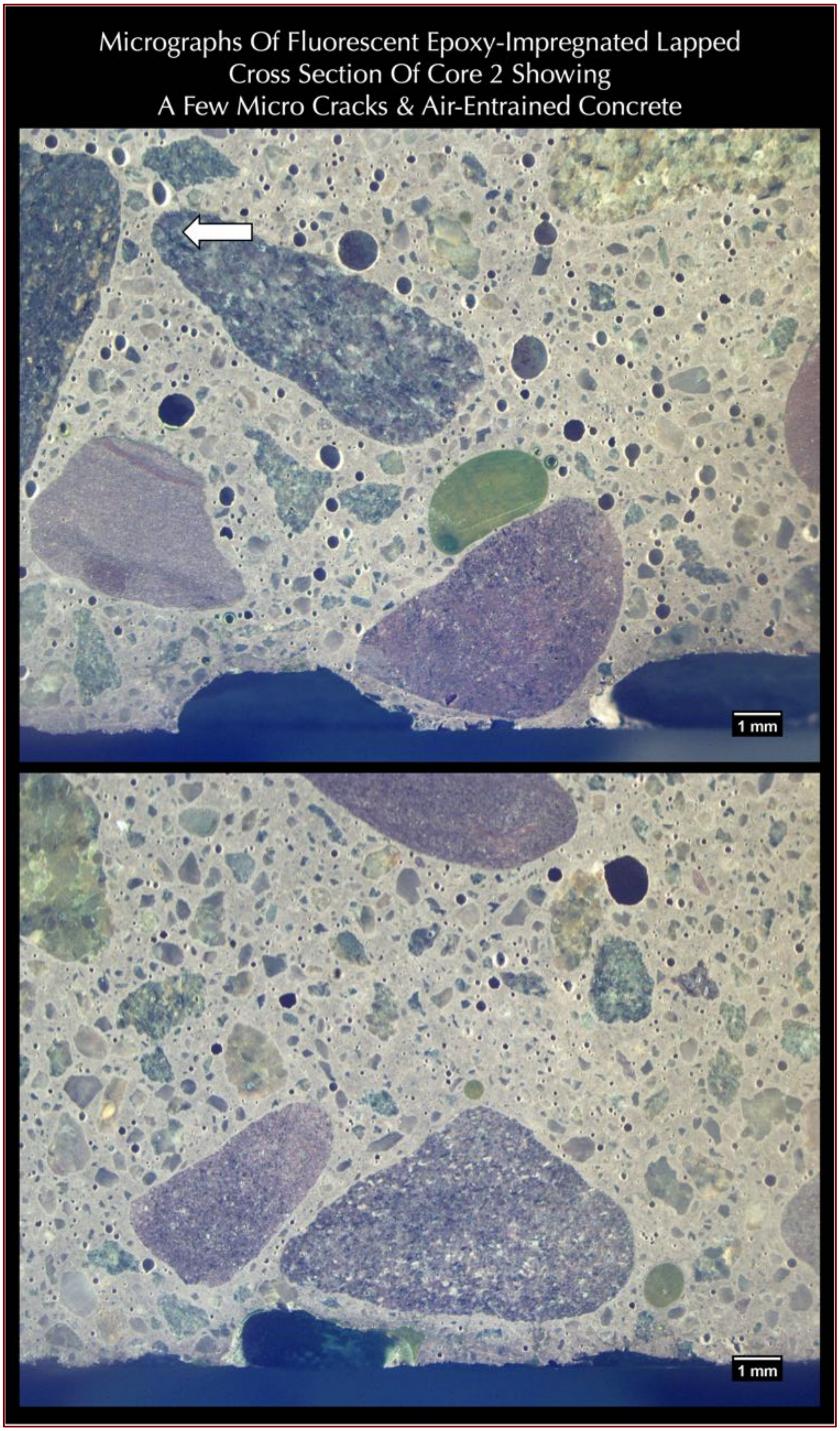

Figure 39: Micrographs of fluorescent epoxy-impregnated lapped cross section of Core 2 from the bottom end showing:

Air-entrained concrete consisting of numerous fine, discrete spherical and near-spherical entrained voids of sizes 1 mm or less. Air content is estimated to be 6 to 7 percent.

THIN SECTIONS

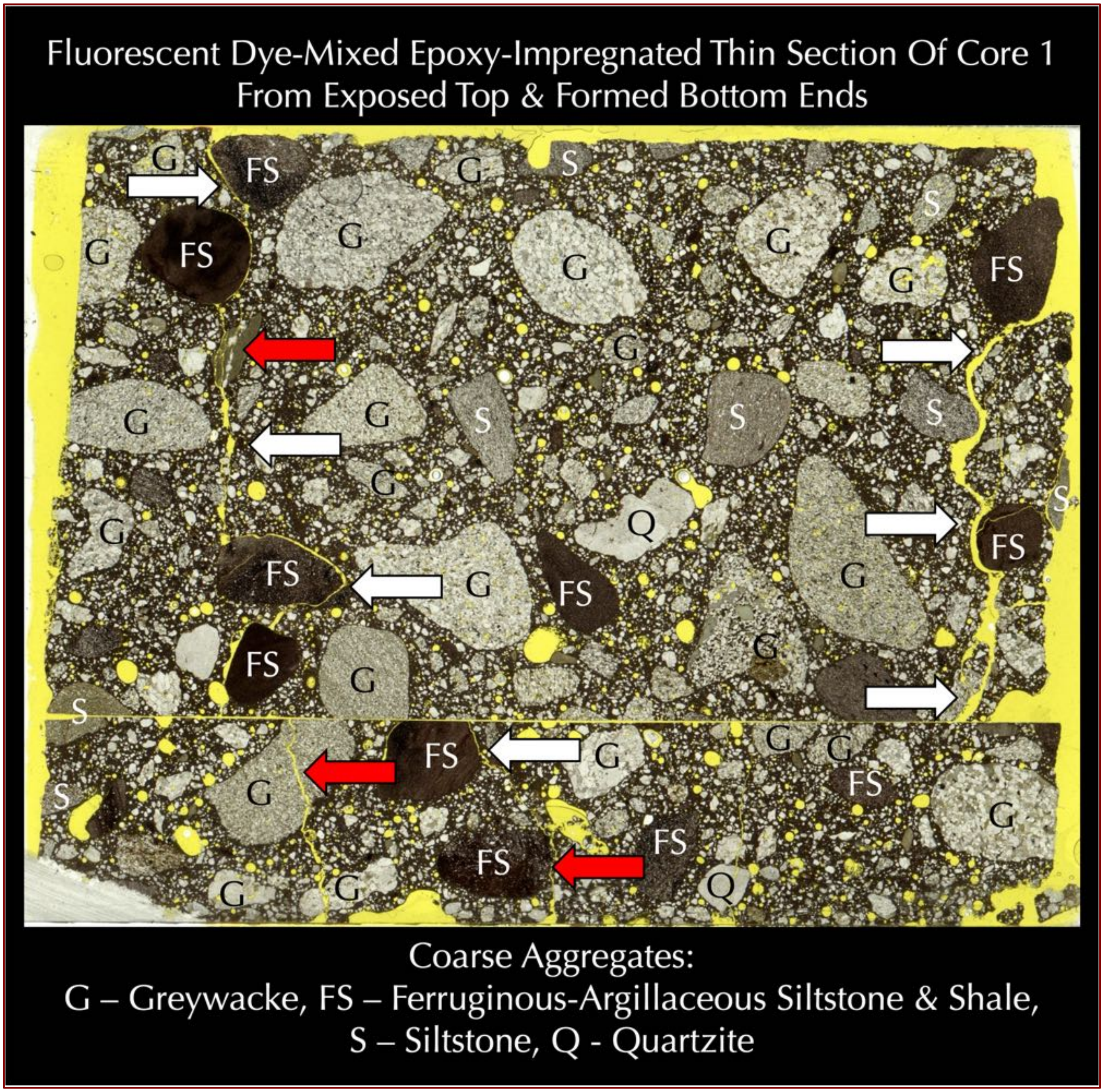

Figure 40: Fluorescent dye-mixed epoxy-impregnated thin section of Core 1 in plane polarized light (PPL) showing: (a) sedimentary pea gravel coarse aggregate particles having nominal maximum size of $^3/_8$ in. (9.5 mm) and consisting of greywacke (marked as 'G,' a type of sandstone containing detrital quartz, and feldspar in an abundant argillaceous or wacke matrix), reddish brown ferruginous and argillaceous siltstone and shale, which contain fine silt to clay-sized quartz and other silicates in an abundant clay and iron-oxide matrix (marked as 'FS'), non-ferruginous shale and siltstone (marked as 'S'), and minor quartzite (marked as 'Q'), where all particles are subrounded to well-rounded, well-graded, and well-distributed; (b) finer natural siliceous-argillaceous-calcareous sand fine aggregate containing many finer (lightly crushed) fractions of gravel coarse aggregate; (c) interstitial Portland cement paste, which has an iron oxide-based pigment; and (d) air entrainment where air voids are highlighted by fluorescent epoxy. Cracks are marked by white arrows (red arrows show internal cracking in aggregates). The section contains a portion from the top 2 inches and a portion from bottom 1 inch of core. The image was formed after scanning the thin section on a film scanner with a polarizing filter.

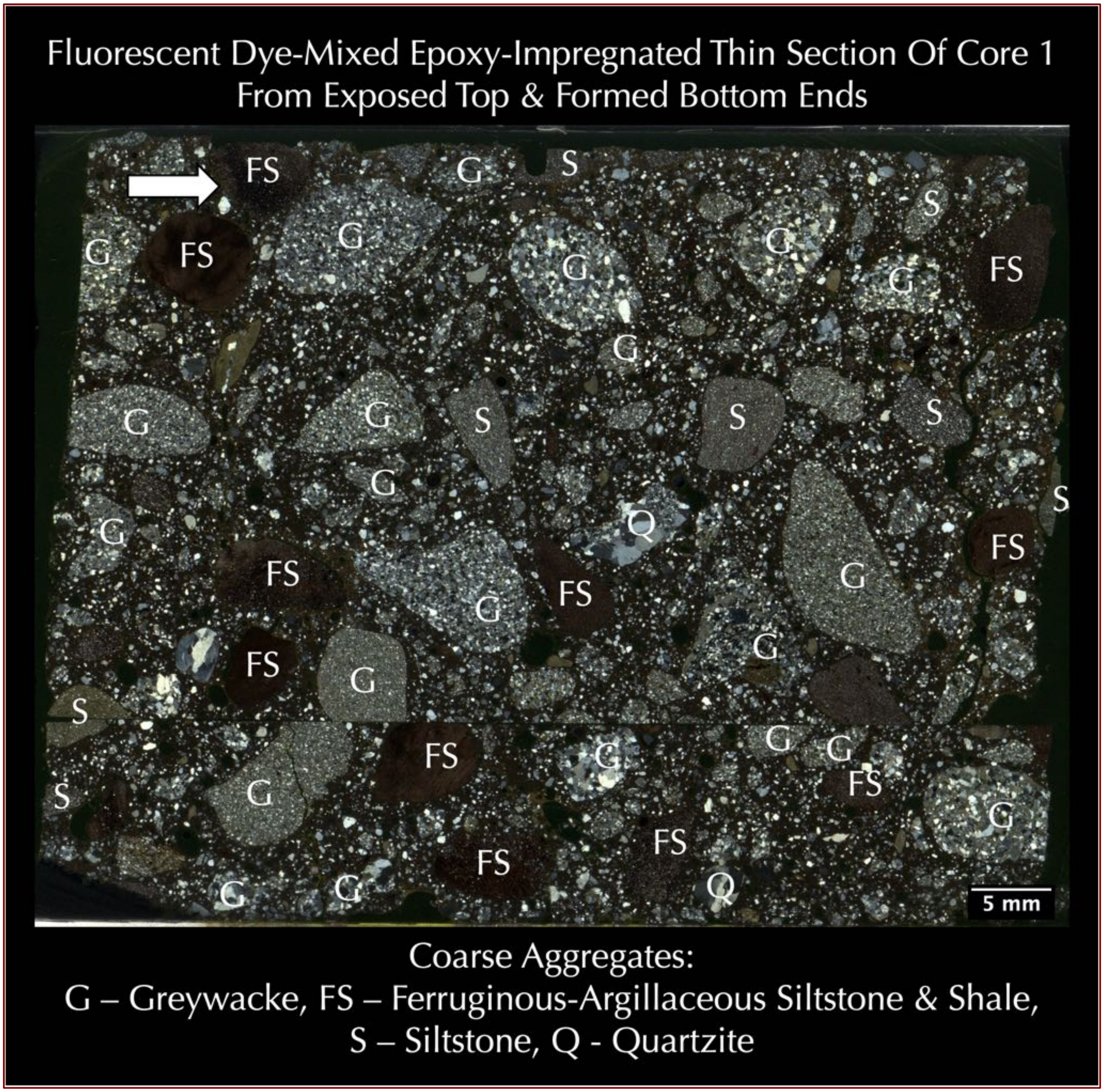

Figure 41: : Fluorescent dye-mixed epoxy-impregnated thin section of Core 1 in cross polarized light (XPL) showing: (a) sedimentary pea gravel coarse aggregate particles having nominal maximum size of $^{3}/_{8}$ in. (9.5 mm) and consisting of greywacke (marked as 'G,' a type of sandstone containing detrital quartz and feldspar in an abundant argillaceous or wacke matrix), reddish brown ferruginous and argillaceous siltstone and shale, which contain fine silt to clay-sized quartz and other silicates in an abundant clay and iron-oxide matrix (marked as 'FS'), non-ferruginous varieties of shale and siltstone (marked as 'S'), and minor quartzite (marked as 'Q'), where all particles are subrounded to well-rounded, well-graded, and well-distributed; (b) finer natural siliceous-argillaceous-calcareous sand fine aggregate containing many finer (lightly crushed) fractions of gravel coarse aggregate; (c) interstitial Portland cement paste, which has an iron oxide-based pigment; and (d) air entrainment where air voids are highlighted by fluorescent epoxy in PPL mode. The section contains a portion from the top 2 inches and a portion from bottom 1 inch of core. The image was formed after scanning the thin section on a film scanner with two perpendicular polarizing filters.

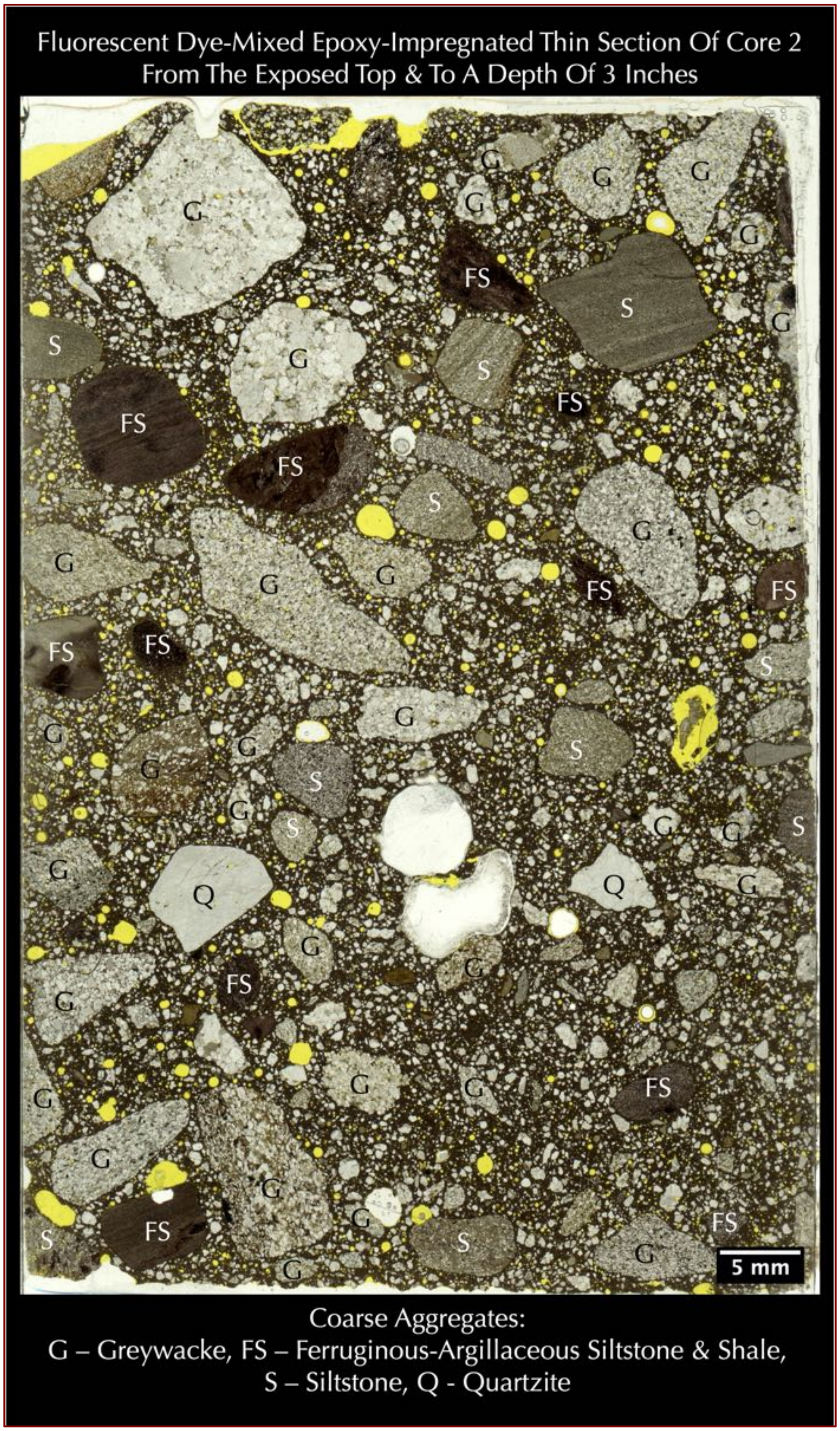

Figure 42: Fluorescent dye-mixed epoxy-impregnated thin section of Core 2 in plane polarized light (PPL) showing:

(a) Sedimentary pea gravel coarse aggregate particles having nominal maximum size of $^3/_8$ in. (9.5 mm) and consisting of greywacke (marked as 'G,' a type of sandstone containing detrital quartz, and feldspar in an abundant argillaceous or wacke matrix), reddish brown ferruginous and argillaceous siltstone and shale, which contain fine silt to clay-sized quartz and other silicates in an abundant clay and iron-oxide matrix (marked as 'FS'), non-ferruginous shale and siltstone (marked as 'S'), and minor quartzite (marked as 'Q'), where all particles are subrounded to well-rounded, well-graded, and well-distributed;

(b) Finer natural siliceous-argillaceous-calcareous sand fine aggregate containing many finer (lightly crushed) fractions of gravel coarse aggregate;

(c) Interstitial Portland cement paste, which has an iron oxide-based pigment; and

(d) Air entrainment where air voids are highlighted by fluorescent epoxy.

The section contains 3 in. portion from the top exposed end of core.

The image was formed after scanning the thin section on a film scanner with a polarizing filter.

Fluorescent Dye-Mixed Epoxy-Impregnated Thin Section Of Core 2
From The Exposed Top & To A Depth Of 3 Inches

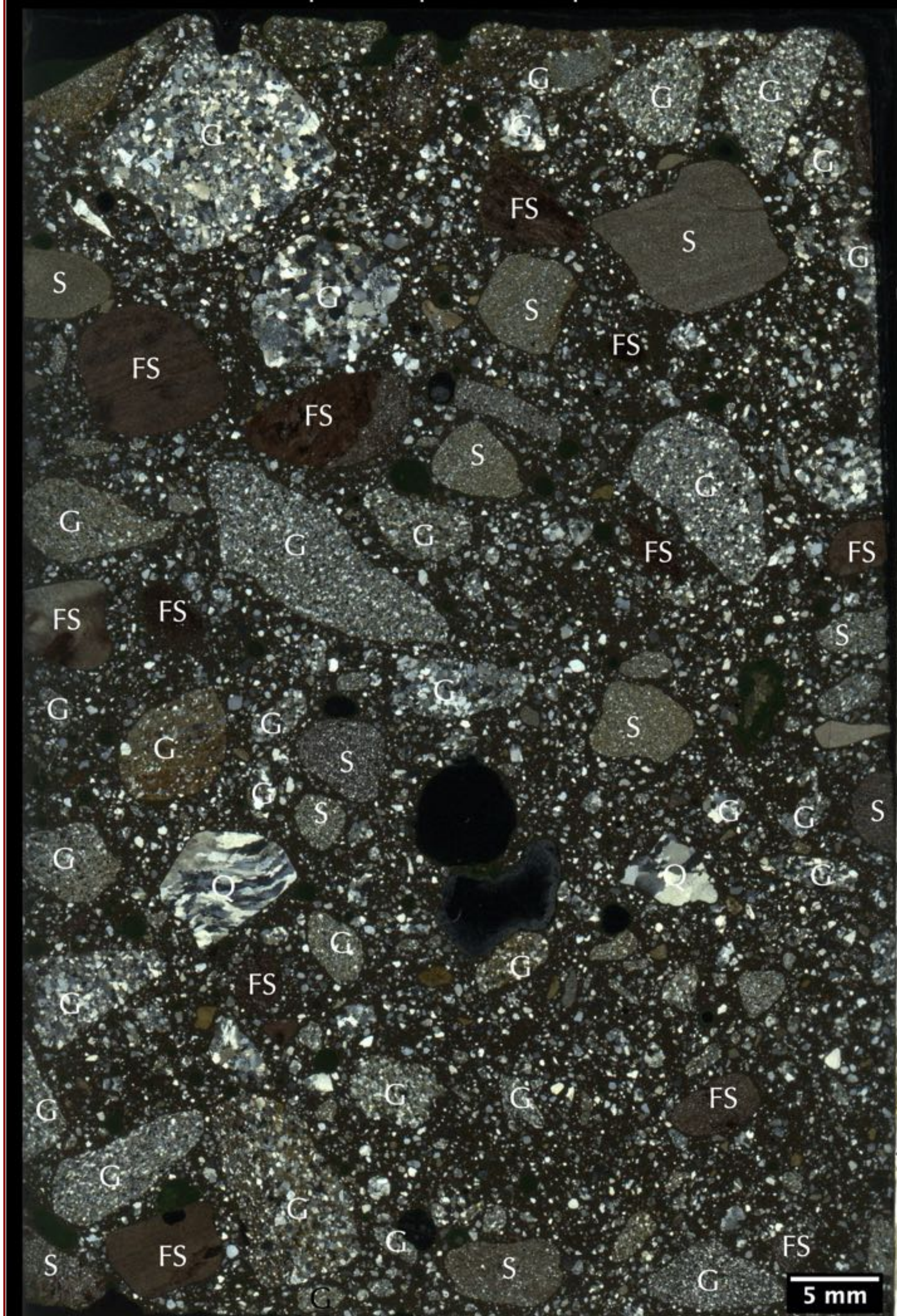

Coarse Aggregates:
G – Greywacke, FS – Ferruginous-Argillaceous Siltstone & Shale,
S – Siltstone, Q - Quartzite

Figure 43: Fluorescent dye-mixed epoxy-impregnated thin section of Core 2 in plane polarized light (PPL) showing:

(a) Sedimentary pea gravel coarse aggregate particles having nominal maximum size of $^3/_8$ in. (9.5 mm) and consisting of greywacke (marked as 'G,' a type of sandstone containing detrital quartz, and feldspar in an abundant argillaceous or wacke matrix), reddish brown ferruginous and argillaceous siltstone and shale, which contain fine silt to clay-sized quartz and other silicates in an abundant clay and iron-oxide matrix (marked as 'FS'), non-ferruginous shale and siltstone (marked as 'S'), and minor quartzite (marked as 'Q'), where all particles are subrounded to well-rounded, well-graded, and well-distributed;

(b) Finer natural siliceous-argillaceous-calcareous sand fine aggregate containing many finer (lightly crushed) fractions of gravel coarse aggregate;

(c) Interstitial Portland cement paste, which has an iron oxide-based pigment; and

(d) Air entrainment where air voids are highlighted by fluorescent epoxy in PPL mode.

The section contains 3 in. portion from the top exposed end of core.

The image was formed after scanning the thin section on a film scanner with two perpendicular polarizing filters.

MICROGRAPHS OF THIN SECTIONS

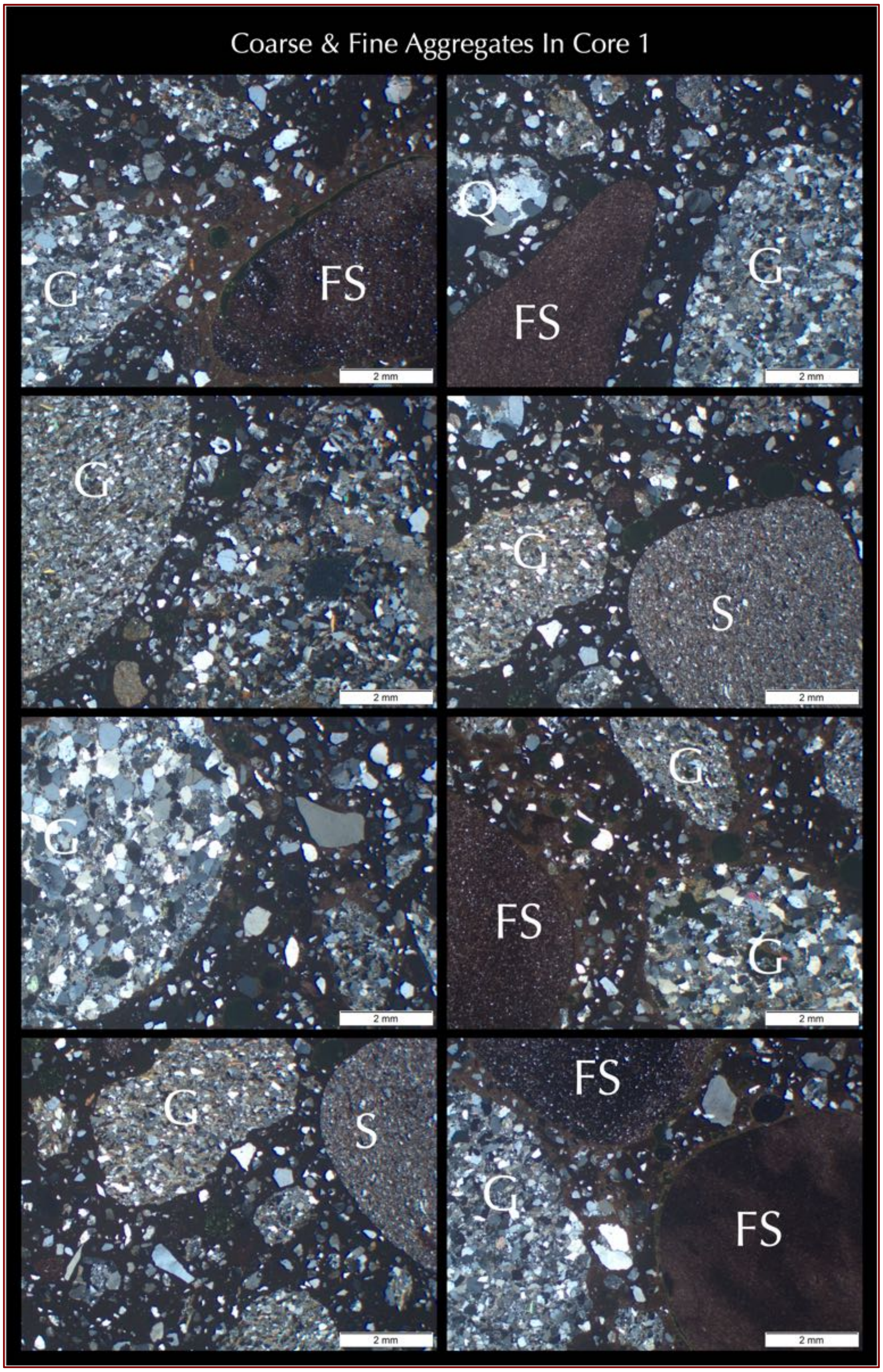

Figure 44: Micrographs of thin section of concrete from Core 1 showing:

(a) Sedimentary pea gravel coarse aggregate particles having nominal maximum size of $^{3}/_{8}$ in. (9.5 mm) and consisting of greywacke (marked as 'G,' a type of sandstone containing detrital quartz, and feldspar in an abundant argillaceous or wacke matrix), reddish brown ferruginous and argillaceous siltstone and shale, which contain fine silt to clay-sized quartz and other silicates in an abundant clay and iron-oxide matrix (marked as 'FS'), non-ferruginous shale and siltstone (marked as 'S'), and minor quartzite (marked as 'Q'), where all particles are subrounded to well-rounded, well-graded, and well-distributed; and,

(b) Finer natural siliceous-argillaceous-calcareous sand fine aggregate containing many finer (lightly crushed) fractions of gravel coarse aggregate.

Micrographs were taken from a transmitted-light stereozoom microscope with polarized-light facilities.

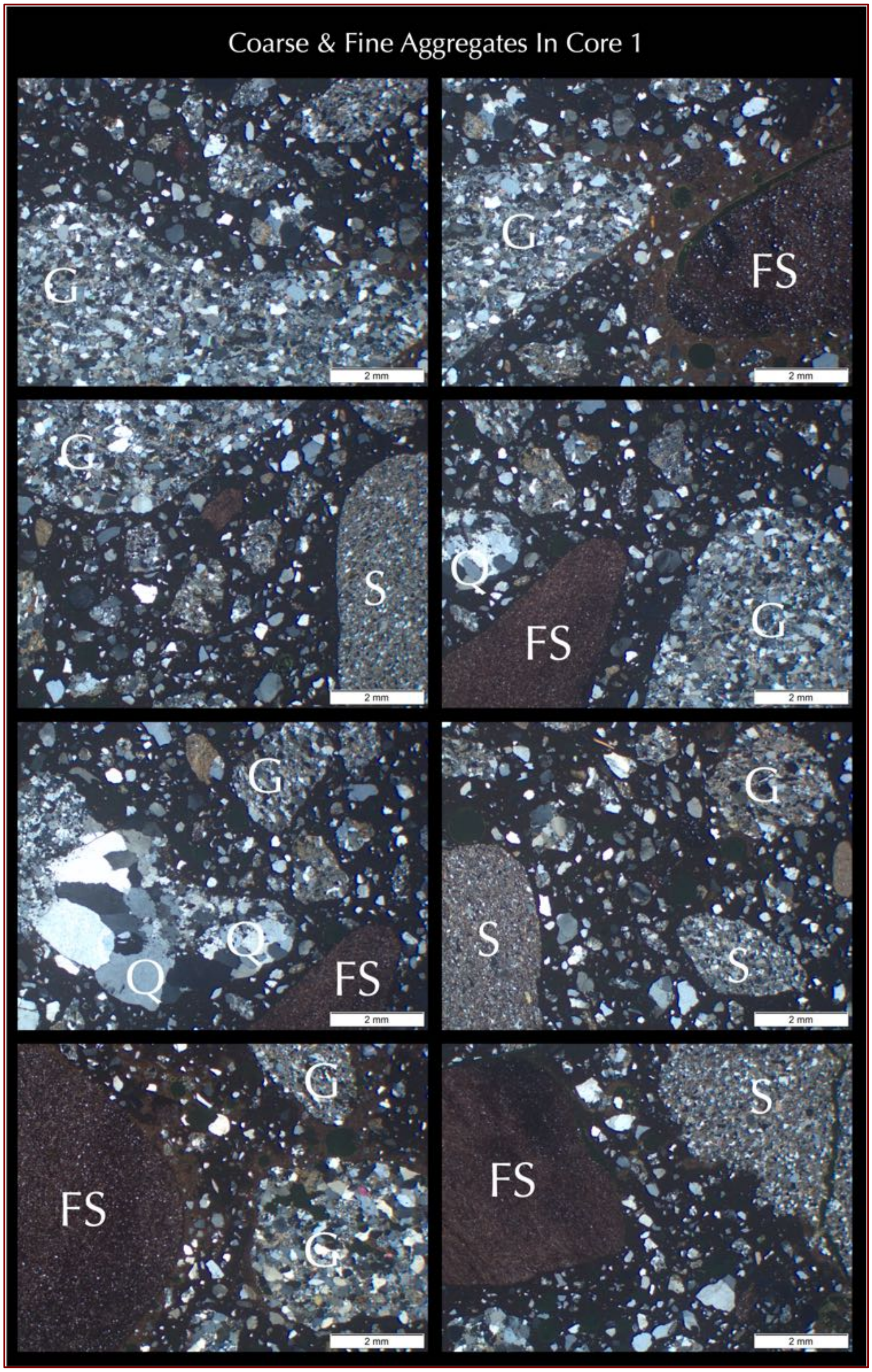

Figure 45: Micrographs of thin section of concrete from Core 1 showing:

(a) Sedimentary pea gravel coarse aggregate particles having nominal maximum size of $^3/_8$ in. (9.5 mm) and consisting of greywacke (marked as 'G,' a type of sandstone containing detrital quartz, and feldspar in an abundant argillaceous or wacke matrix), reddish brown ferruginous and argillaceous siltstone and shale, which contain fine silt to clay-sized quartz and other silicates in an abundant clay and iron-oxide matrix (marked as 'FS'), non-ferruginous shale and siltstone (marked as 'S'), and minor quartzite (marked as 'Q'), where all particles are subrounded to well-rounded, well-graded, and well-distributed; and,

(b) Finer natural siliceous-argillaceous-calcareous sand fine aggregate containing many finer (lightly crushed) fractions of gravel coarse aggregate.

Micrographs were taken from a transmitted-light stereozoom microscope with polarized-light facilities.

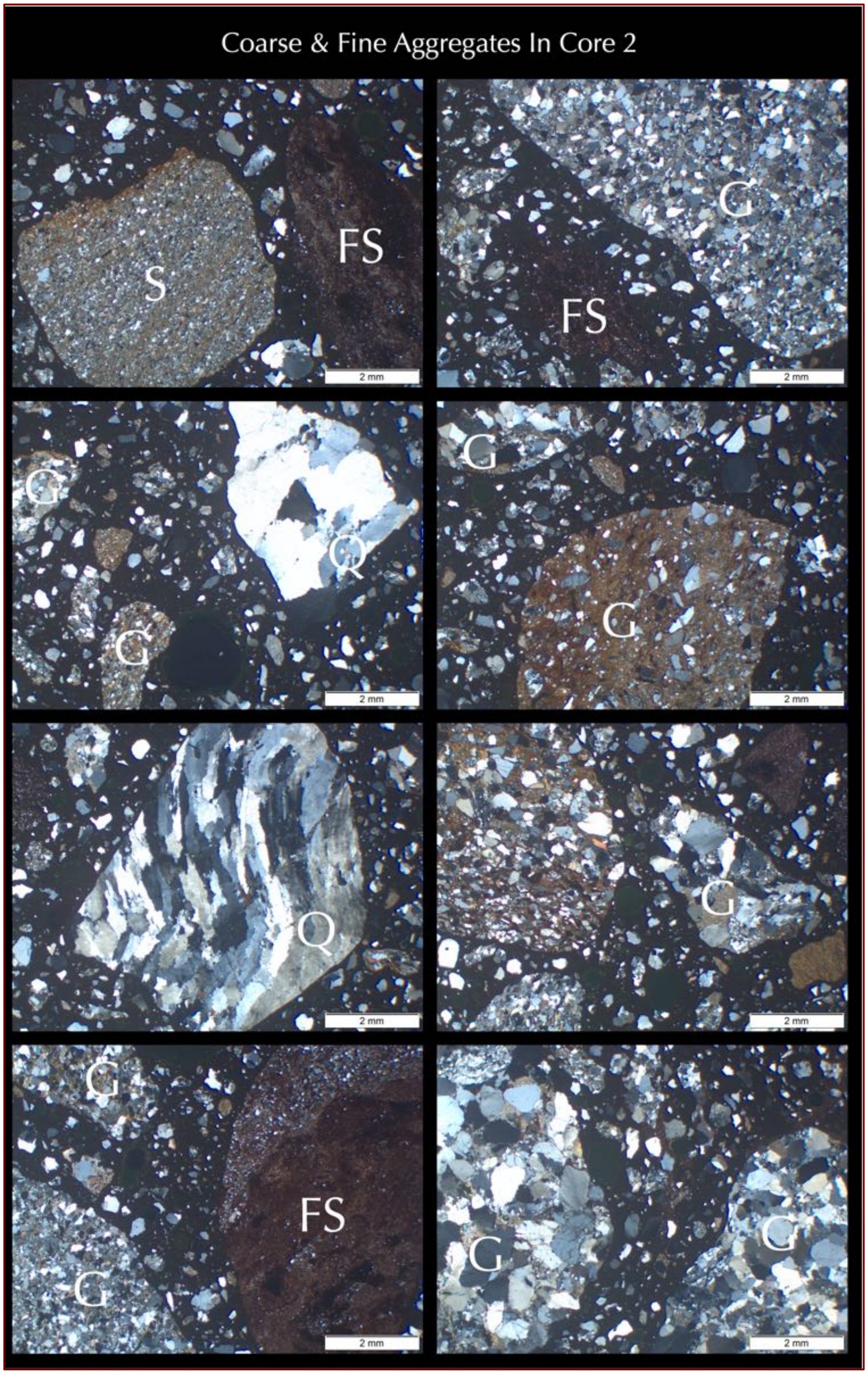

Figure 46: Micrographs of thin section of concrete from Core 2 showing:

(a) Sedimentary pea gravel coarse aggregate particles having nominal maximum size of $^{3}/_{8}$ in. (9.5 mm) and consisting of greywacke (marked as 'G,' a type of sandstone containing detrital quartz, and feldspar in an abundant argillaceous or wacke matrix), reddish brown ferruginous and argillaceous siltstone and shale, which contain fine silt to clay-sized quartz and other silicates in an abundant clay and iron-oxide matrix (marked as 'FS'), non-ferruginous shale and siltstone (marked as 'S'), and minor quartzite (marked as 'Q'), where all particles are subrounded to well-rounded, well-graded, and well-distributed; and,

(b) Finer natural siliceous-argillaceous-calcareous sand fine aggregate containing many finer (lightly crushed) fractions of gravel coarse aggregate.

Micrographs were taken from a transmitted-light stereozoom microscope with polarized-light facilities.

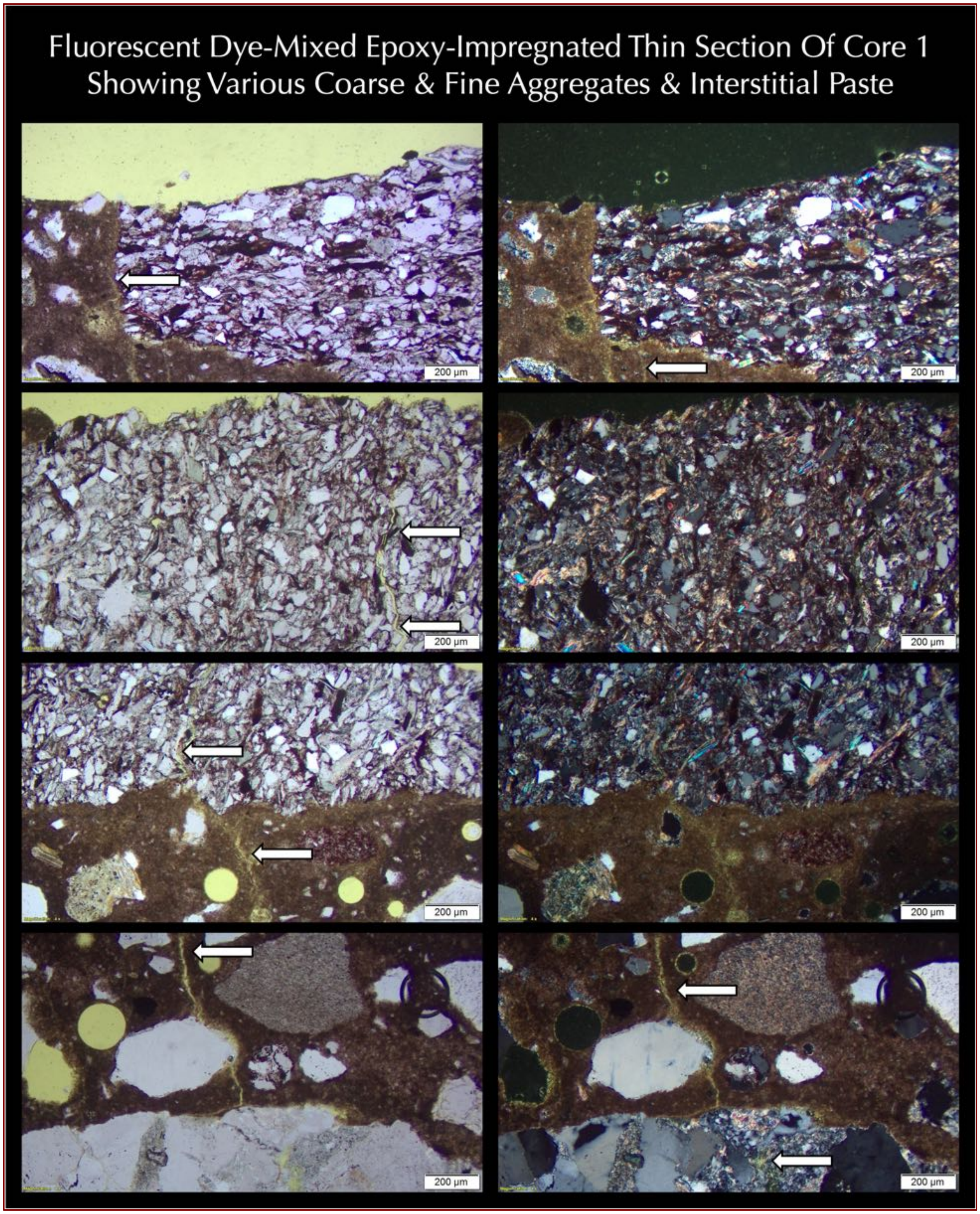

Figure 47: Micrographs of thin section of concrete from Core 1 showing greywacke and ferruginous siltstone paricles in gravel coarse aggregate, many with internal cracking (arrows) often extended into paste, and carbonated paste at the surface region. Micrographs were taken from a petrographic microscope with fluorescent light facilities.

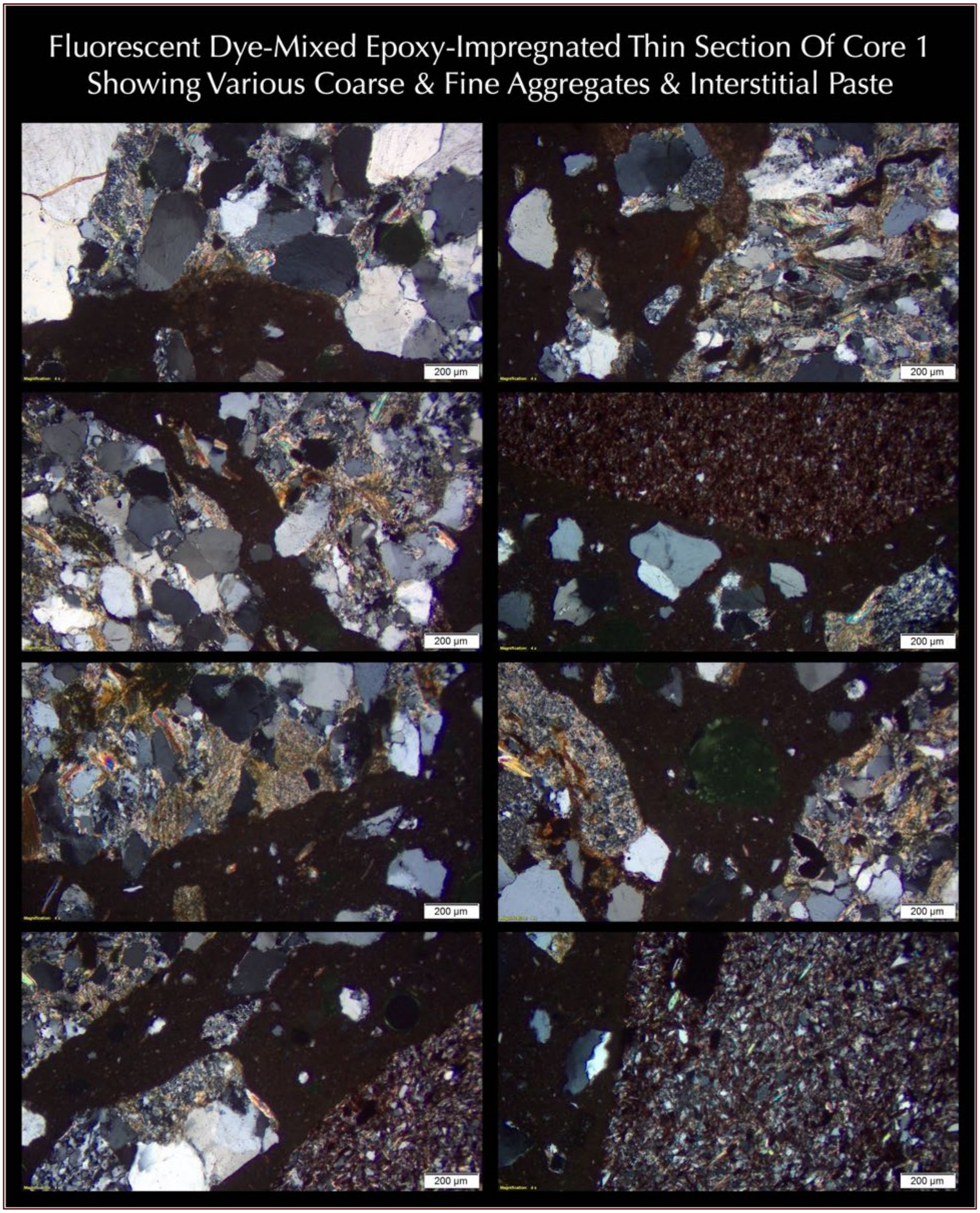

Figure 48: Micrographs of thin section of concrete from Core 1 showing greywacke and ferruginous siltstone paricles in gravel coarse aggregate. Greywacke shows detrital quartz and feldspar in a dominantly argillaceous (wacke) matrix whereas siltstone shows finer silt-size detrital quartz in a dominantly argillaceous and ferruginous (later for reddish brown particles) matrix. Micrographs were taken from a petrographic microscope with fluorescent light facilities.

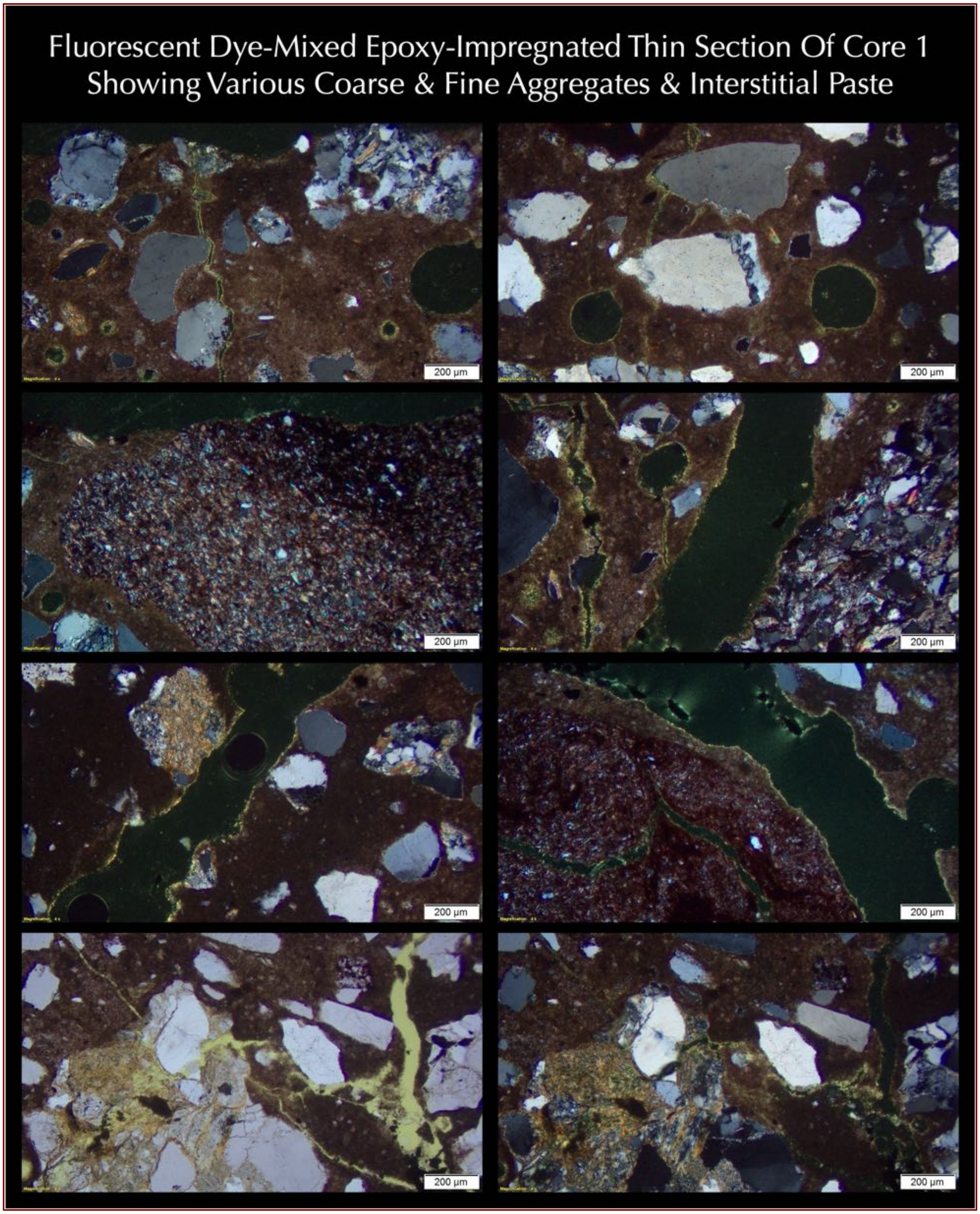

Figure 49: Micrographs of thin section of concrete from Core 1 showing greywacke and ferruginous siltstone paricles in gravel coarse aggregate. Greywacke shows detrital quartz and feldspar in a dominantly argillaceous (wacke) matrix whereas siltstone shows finer silt-size detrital quartz in a dominantly argillaceous and ferruginous (later for reddish brown particles) matrix. Cracks are highlighted by fluorescent epoxy. Micrographs were taken from a petrographic microscope with fluorescent light facilities.

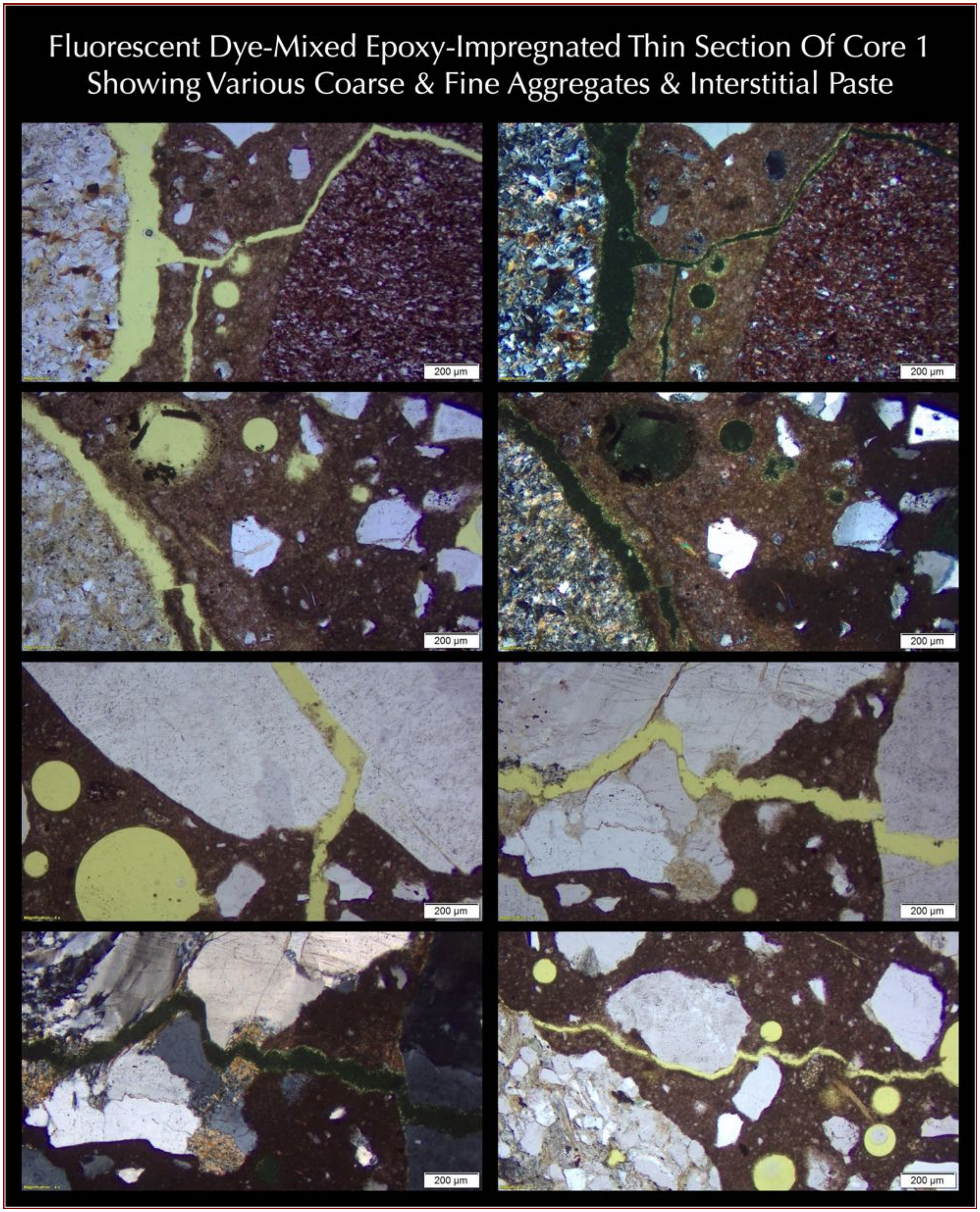

Figure 50: Micrographs of thin section of concrete from Core 1 showing greywacke and ferruginous siltstone paricles in gravel coarse aggregate. Greywacke shows detrital quartz and feldspar in a dominantly argillaceous (wacke) matrix whereas siltstone shows finer silt-size detrital quartz in a dominantly argillaceous and ferruginous (later for reddish brown particles) matrix. Cracks are highlighted by fluorescent epoxy. Micrographs were taken from a petrographic microscope with fluorescent light facilities.

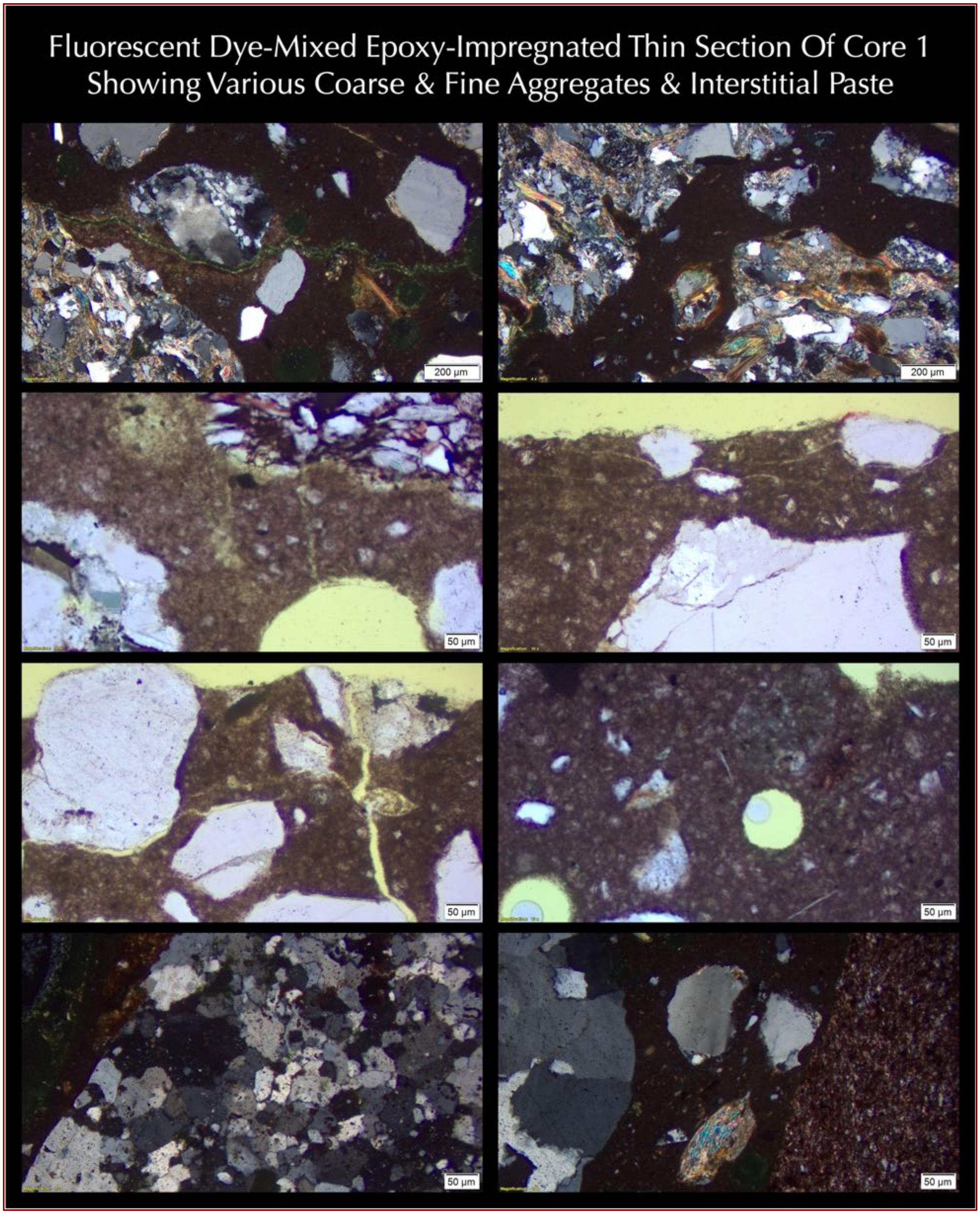

Figure 51: Micrographs of thin section of concrete from Core 1 showing greywacke and ferruginous siltstone paricles in gravel coarse aggregate. Greywacke shows detrital quartz and feldspar in a dominantly argillaceous (wacke) matrix whereas siltstone shows finer silt-size detrital quartz in a dominantly argillaceous and ferruginous (later for reddish brown particles) matrix. Cracks are highlighted by fluorescent epoxy. Paste in 2nd and 3rd rows show pigmented nature with scattered residual Portland cement particles. Micrographs were taken from a petrographic microscope with fluorescent light facilities.

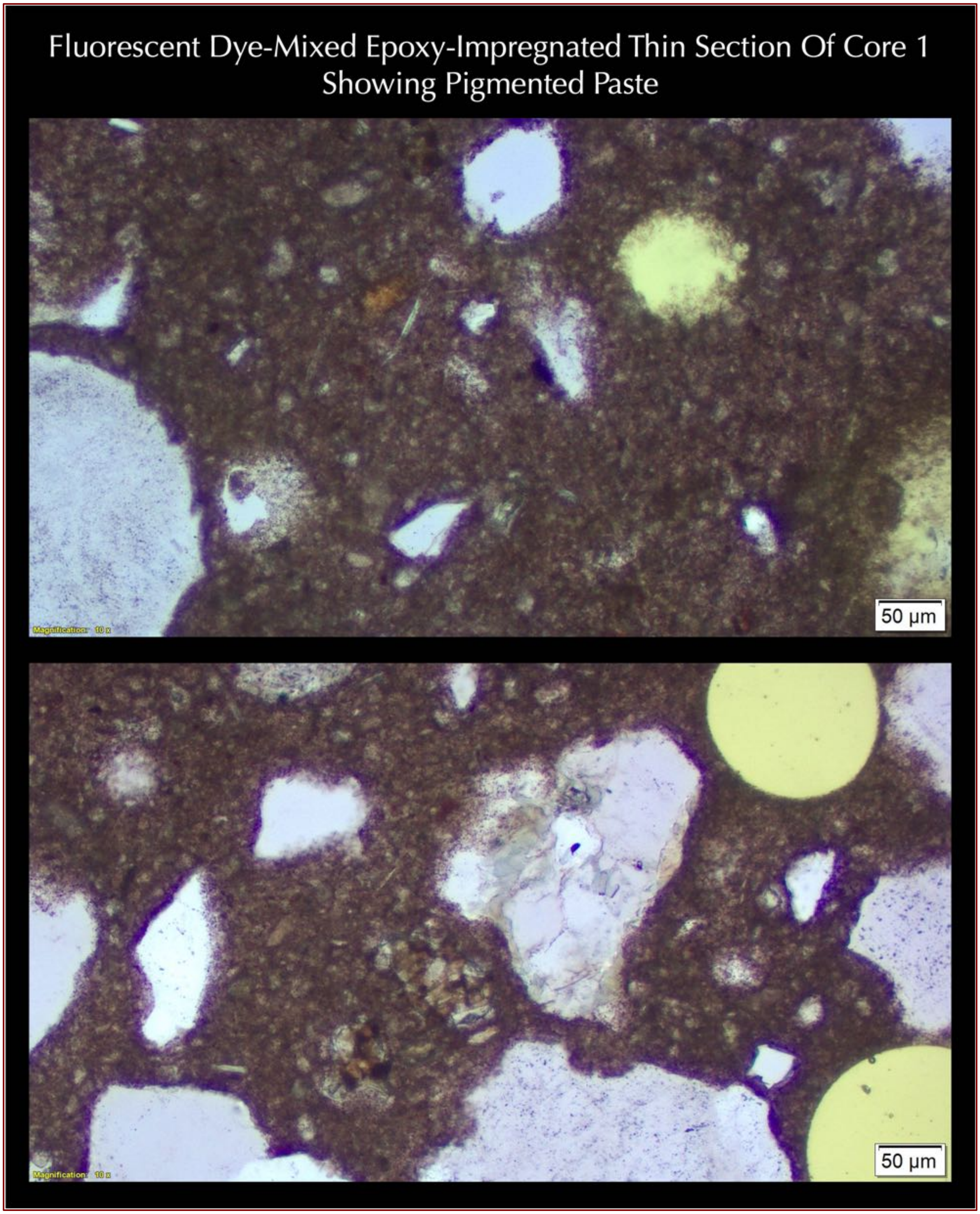

Figure 52: Micrographs of thin section of concrete from Core 1 showing pigmented nature of paste with scattered residual Portland cement particles where pigments are ultrafine-grained iron oxide. Micrographs were taken from a petrographic microscope with fluorescent light facilities.

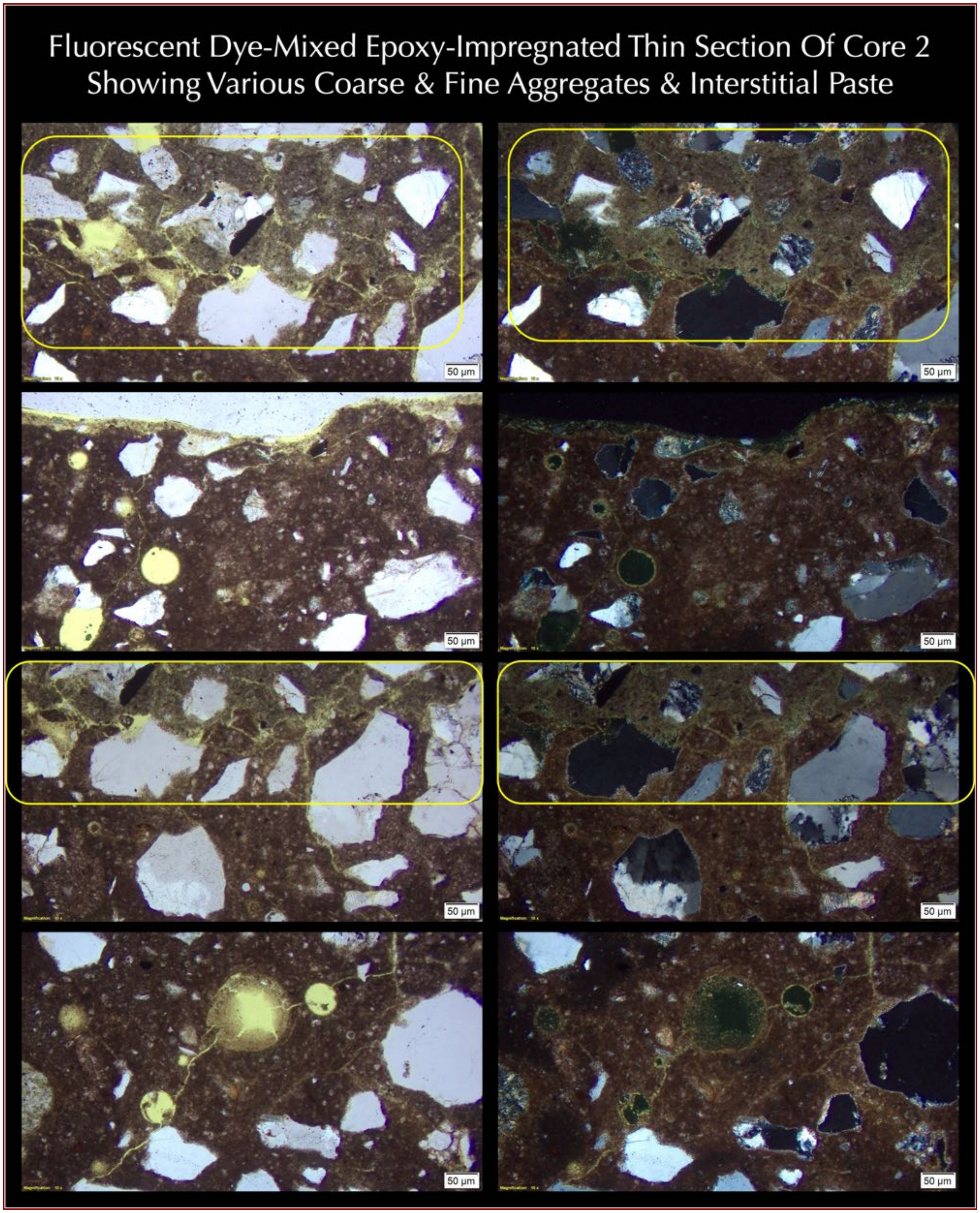

Figure 53: Micrographs of thin section of concrete from Core 2 showing extensive microacking at the surface region that are highlighted by fluorescent epoxy and boxed in 1st and 3rd row photos, and carbonated paste at the surface region. Micrographs were taken from a petrographic microscope with fluorescent light facilities.

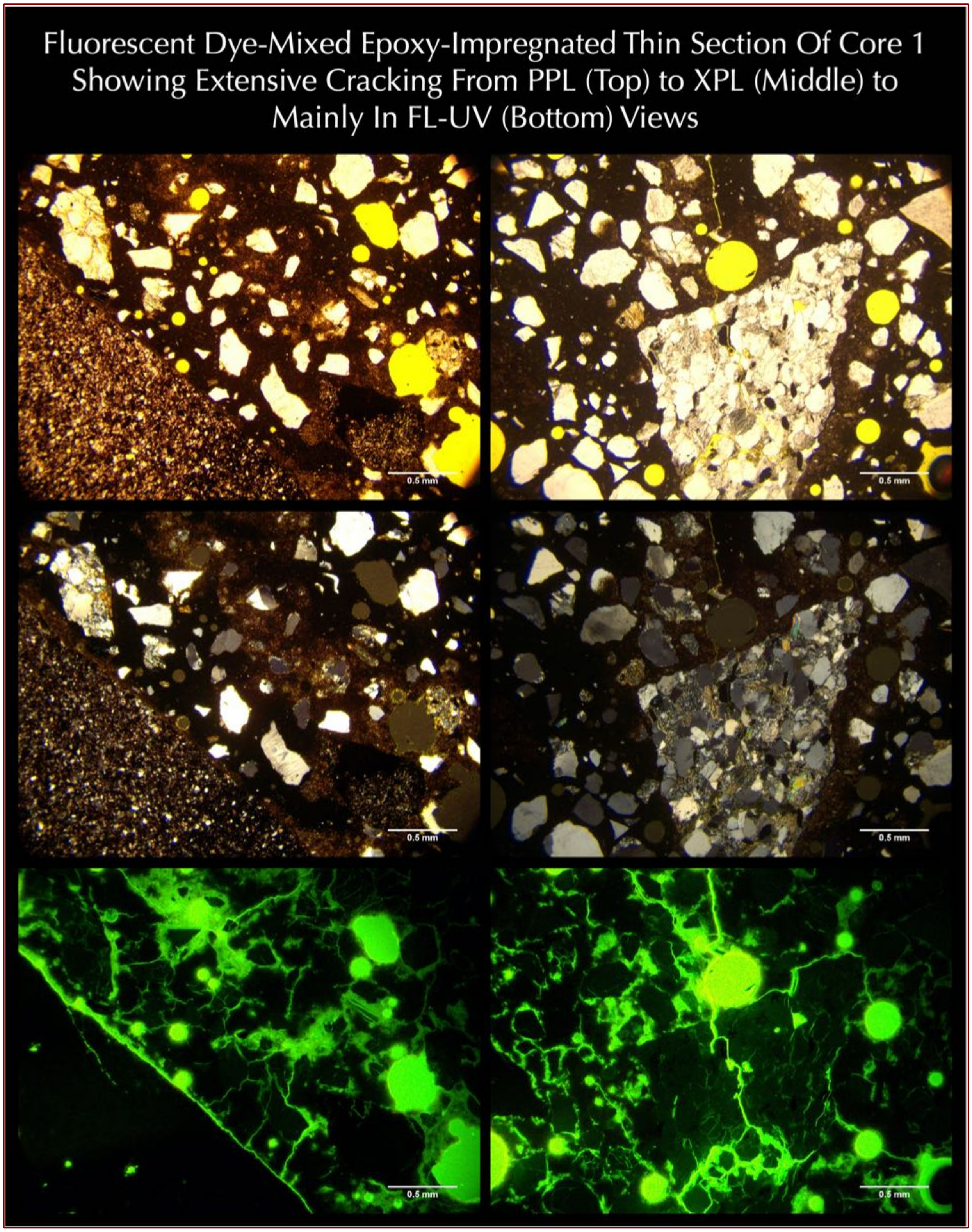

Figure 54: Micrographs of thin section of concrete from Core 1 taken in plane-polarized light (top row), corresponding cross polarized light (middle row), and corresponding fluorescent UV light (bottom row) showing extensive cracking in greywacke and shale-siltsotne gravel particles in coarse aggregate, as well as in interstitial mortar fraction that are best highlighted by fluorescent epoxy when seen in UV light. Micrographs were taken from a petrographic microscope with fluorescent light facilities.

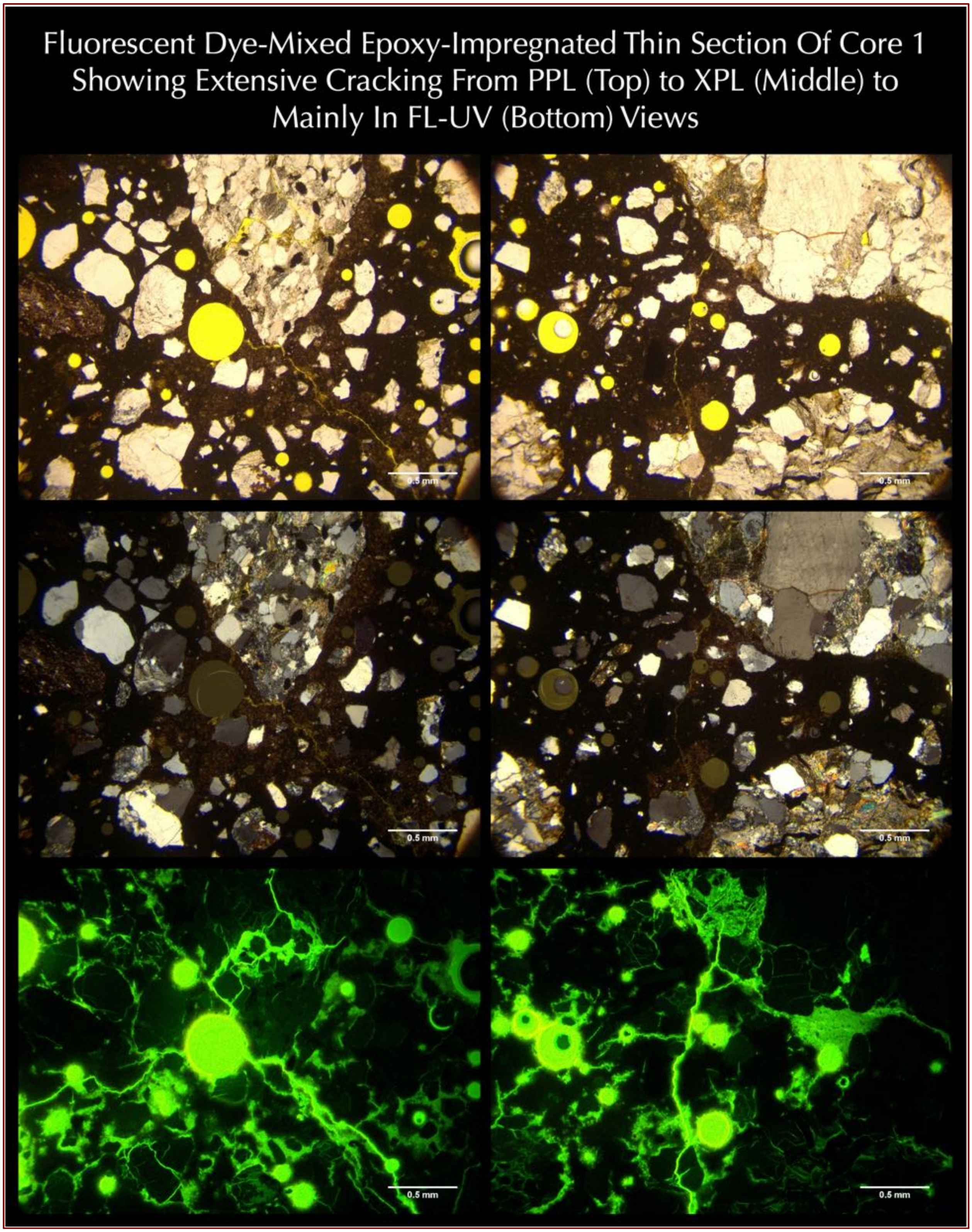

Figure 55: Micrographs of thin section of concrete from Core 1 taken in plane-polarized light (top row), corresponding cross polarized light (middle row), and corresponding fluorescent UV light (bottom row) showing extensive cracking in greywacke and shale-siltsotne gravel particles in coarse aggregate, as well as in interstitial mortar fraction that are best highlighted by fluorescent epoxy when seen in UV light. Micrographs were taken from a petrographic microscope with fluorescent light facilities.

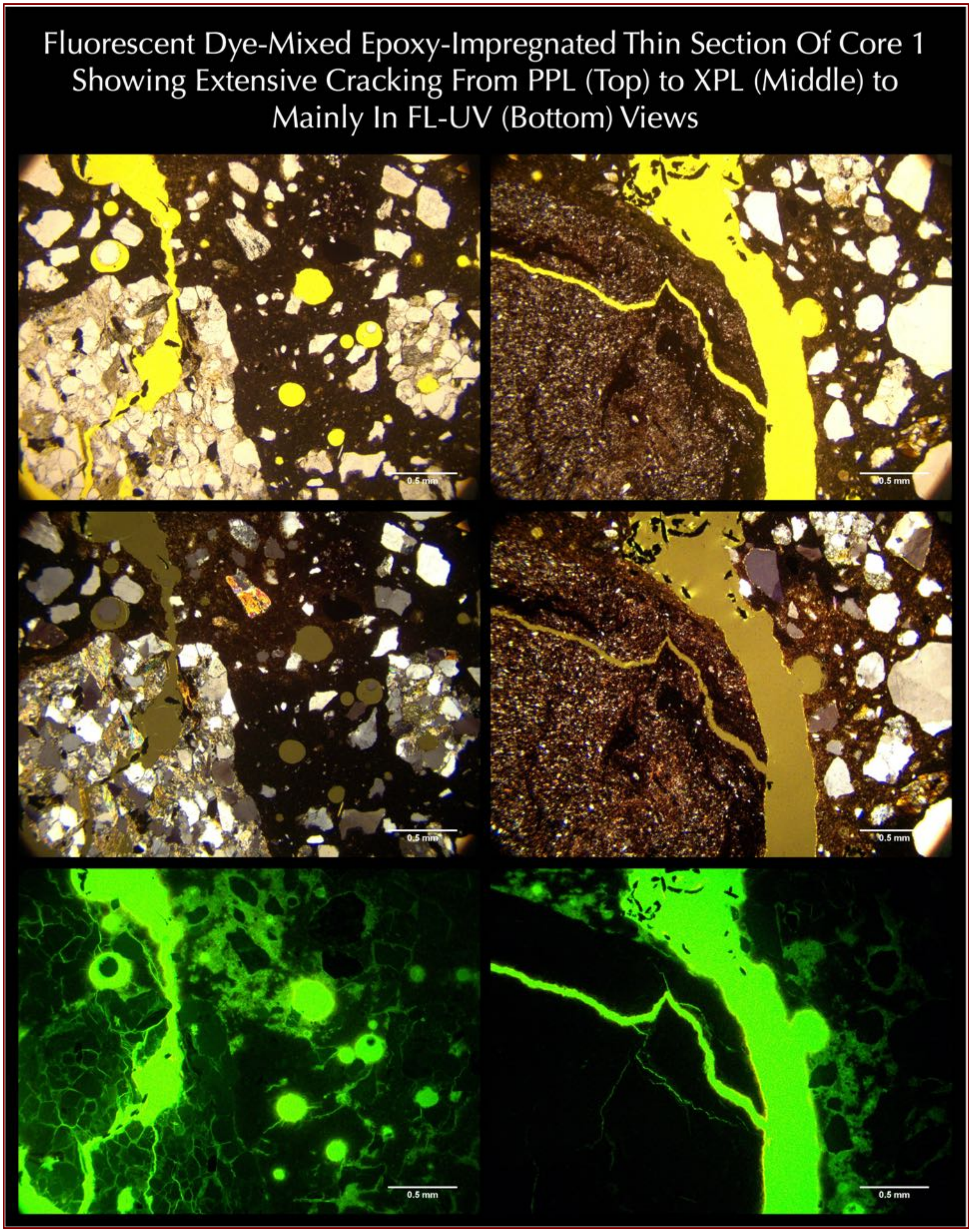

Figure 56: Micrographs of thin section of concrete from Core 1 taken in plane-polarized light (top row), corresponding cross polarized light (middle row), and corresponding fluorescent UV light (bottom row) showing extensive cracking in greywacke and shale-siltsotne gravel particles in coarse aggregate, as well as in interstitial mortar fraction that are best highlighted by fluorescent epoxy when seen in UV light. Micrographs were taken from a petrographic microscope with fluorescent light facilities.

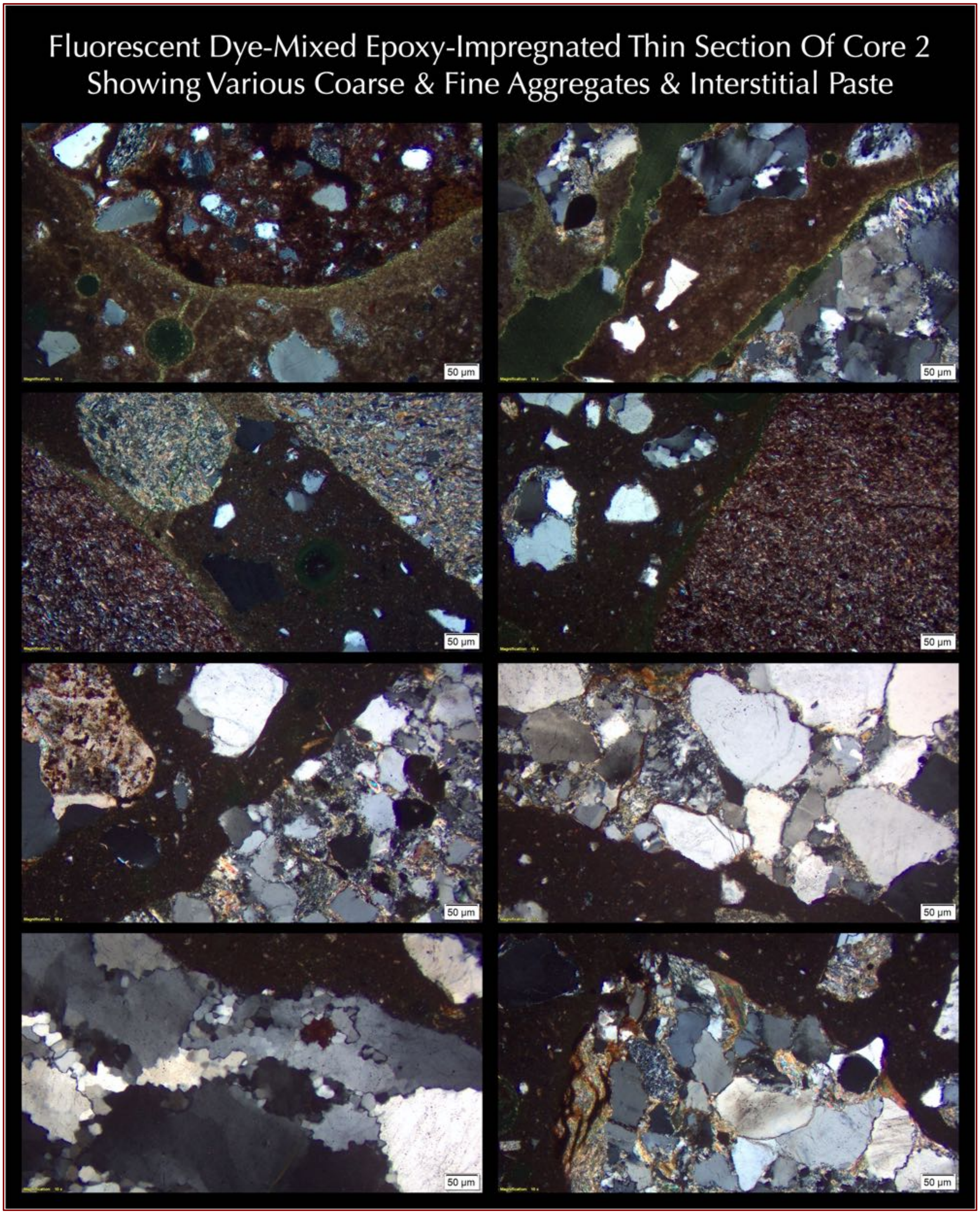

Figure 57: Micrographs of thin section of concrete from Core 2 showing greywacke and ferruginous siltstone paricles in gravel coarse aggregate. Greywacke shows detrital quartz and feldspar in a dominantly argillaceous (wacke) matrix whereas siltstone shows finer silt-size detrital quartz in a dominantly argillaceous and ferruginous (later for reddish brown particles) matrix. Micrographs were taken from a petrographic microscope with fluorescent light facilities.

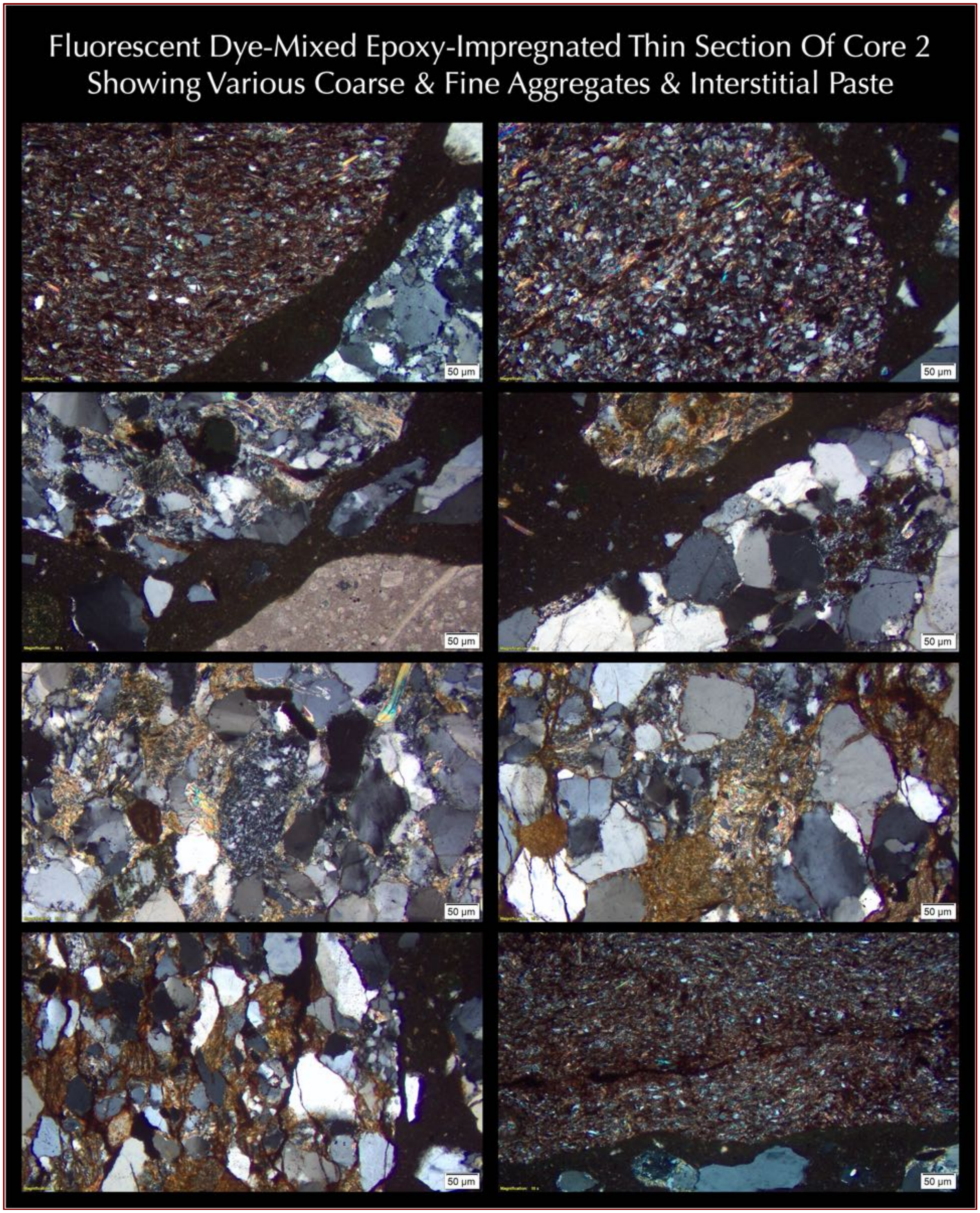

Figure 58: Micrographs of thin section of concrete from Core 2 showing greywacke and ferruginous siltstone paricles in gravel coarse aggregate. Greywacke shows detrital quartz and feldspar in a dominantly argillaceous (wacke) matrix whereas siltstone shows finer silt-size detrital quartz in a dominantly argillaceous and ferruginous (later for reddish brown particles) matrix. Micrographs were taken from a petrographic microscope with fluorescent light facilities.

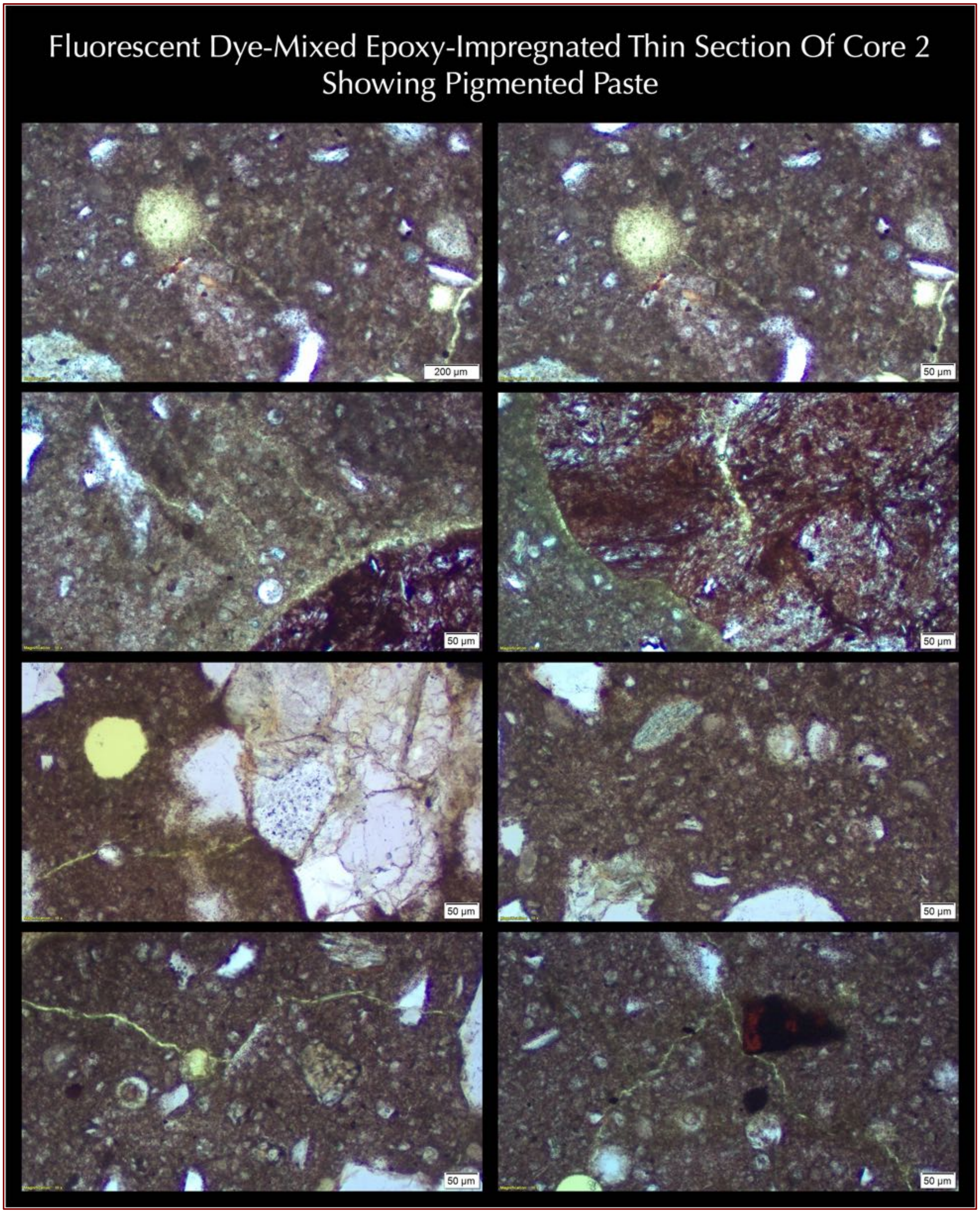

Figure 59: Micrographs of thin section of concrete from Core 2 showing pigmented nature of paste with scattered residual Portland cement particles where pigments are ultrafine-grained iron oxide. Microcracks are highlighted by fluorescent epoxy. Micrographs were taken from a petrographic microscope with fluorescent light facilities.

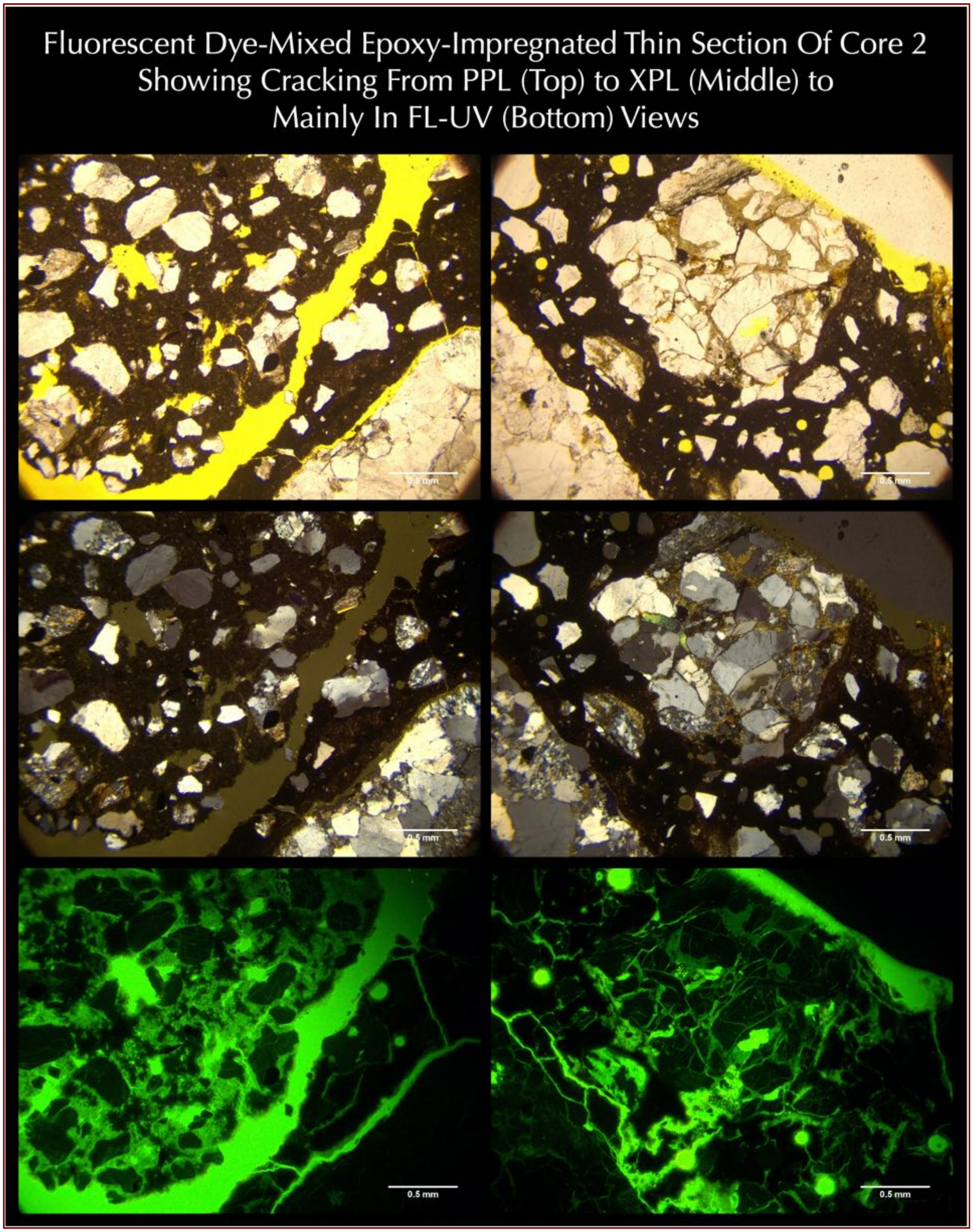

Figure 60: Micrographs of thin section of concrete from Core 2 taken in plane-polarized light (top row), corresponding cross polarized light (middle row), and corresponding fluorescent UV light (bottom row) showing extensive microcracking in greywacke and shale-siltsotne gravel particles in coarse aggregate, as well as in interstitial mortar fraction that are best highlighted by fluorescent epoxy when seen in UV light. Micrographs were taken from a petrographic microscope with fluorescent light facilities.

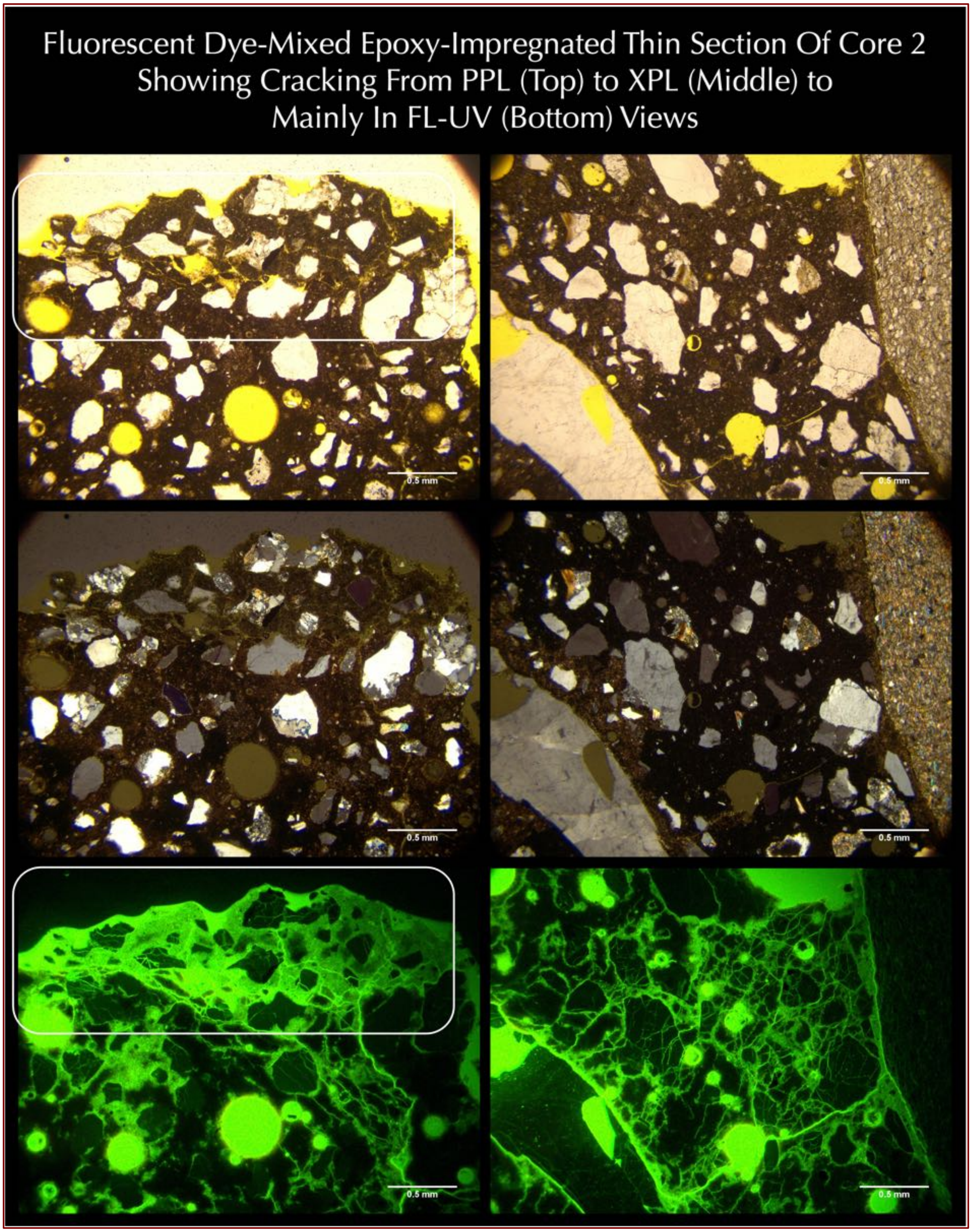

Figure 61: Micrographs of thin section of concrete from Core 2 taken in plane-polarized light (top row), corresponding cross polarized light (middle row), and corresponding fluorescent UV light (bottom row) showing extensive microcracking in the surface region and in greywacke and shale-siltsotne gravel particles in coarse aggregate that are best highlighted by fluorescent epoxy when seen in UV light. Micrographs were taken from a petrographic microscope with fluorescent light facilities.

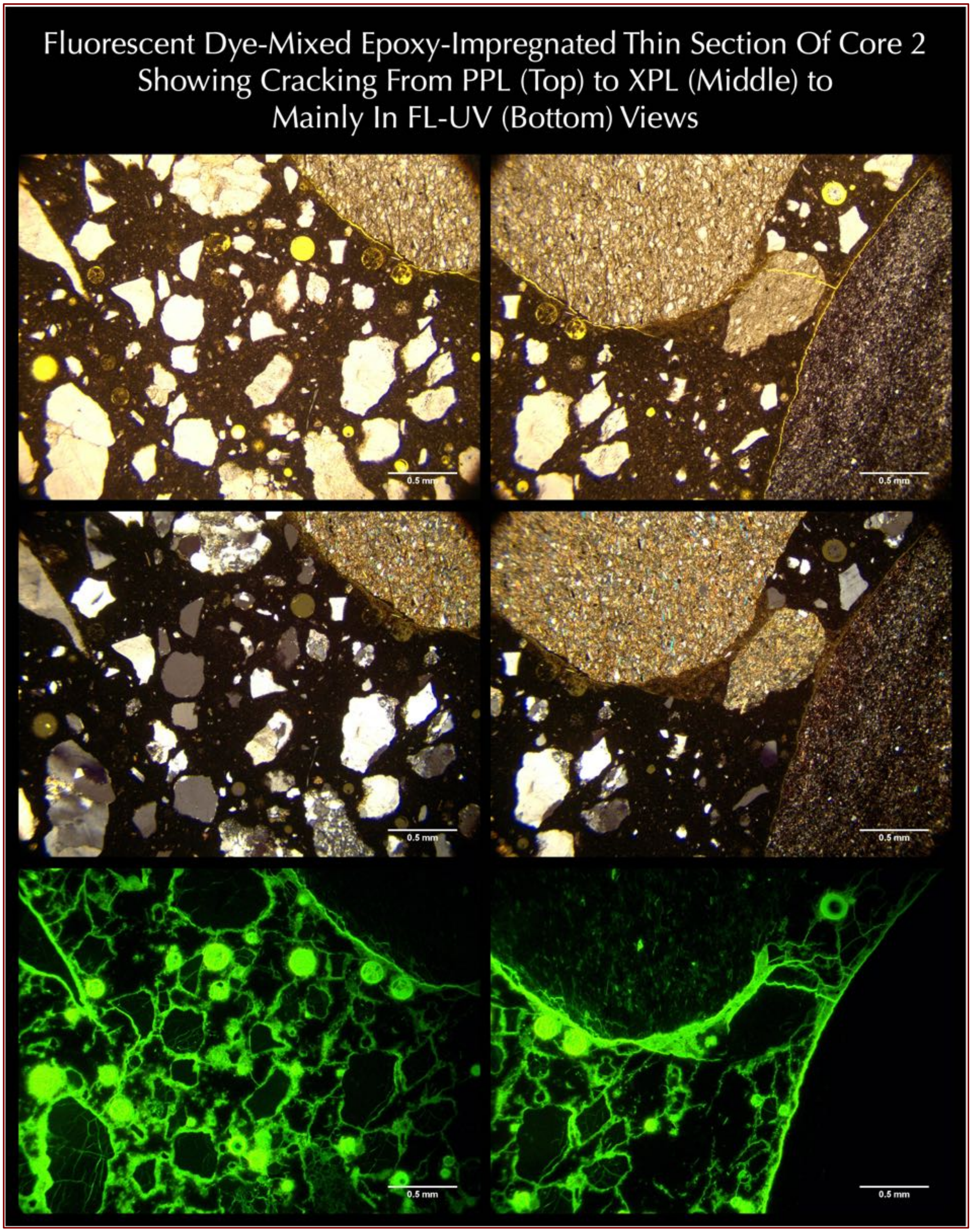

Figure 62: Micrographs of thin section of concrete from Core 2 taken in plane-polarized light (top row), corresponding cross polarized light (middle row), and corresponding fluorescent UV light (bottom row) showing extensive microcracking in greywacke and shale-siltsotne gravel particles in coarse aggregate, as well as in interstitial mortar fraction that are best highlighted by fluorescent epoxy when seen in UV light. Micrographs were taken from a petrographic microscope with fluorescent light facilities.

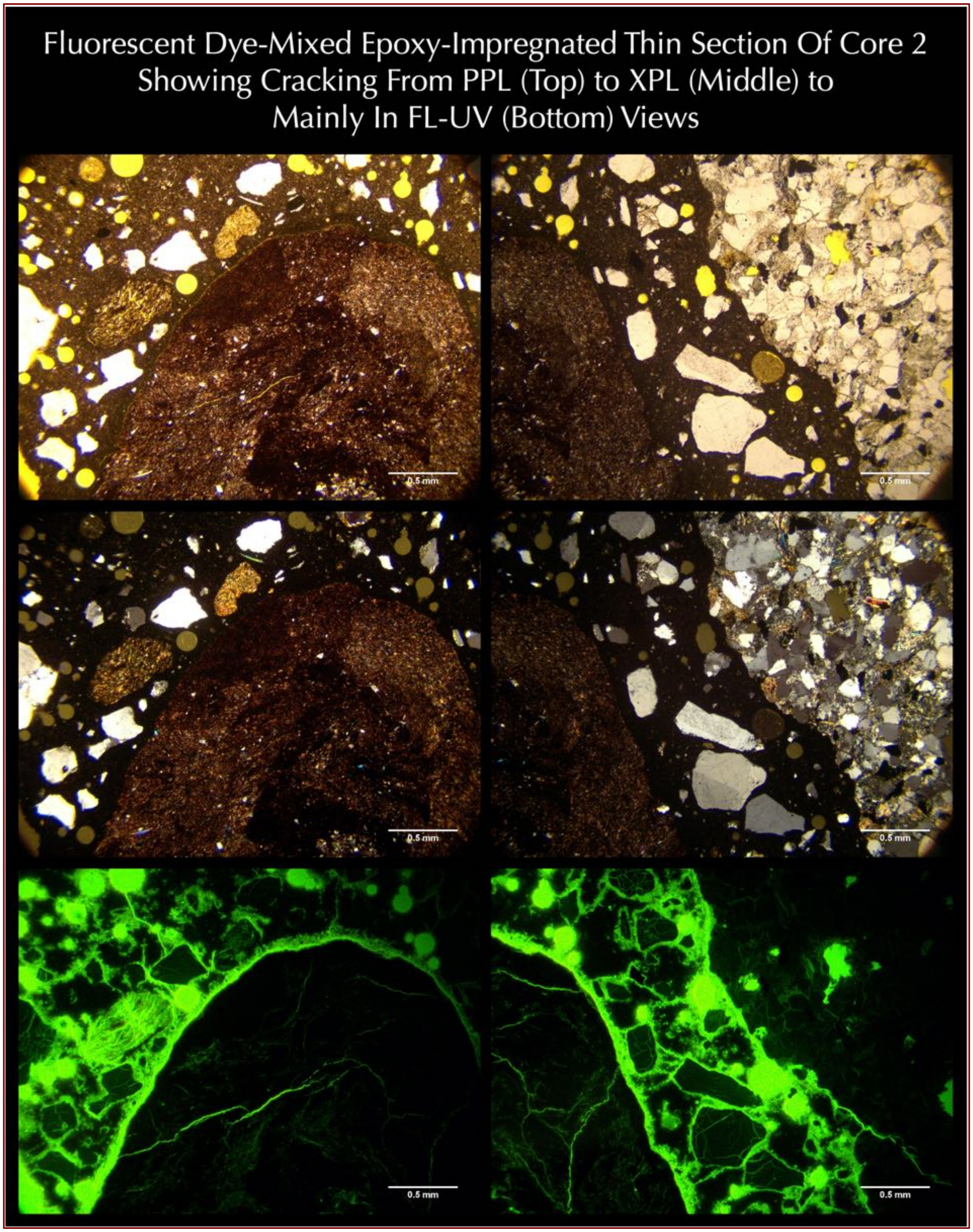

Figure 63: Micrographs of thin section of concrete from Core 2 taken in plane-polarized light (top row), corresponding cross polarized light (middle row), and corresponding fluorescent UV light (bottom row) showing extensive microcracking in greywacke and shale-siltsotne gravel particles in coarse aggregate, as well as in interstitial mortar fraction that are best highlighted by fluorescent epoxy when seen in UV light. Micrographs were taken from a petrographic microscope with fluorescent light facilities.

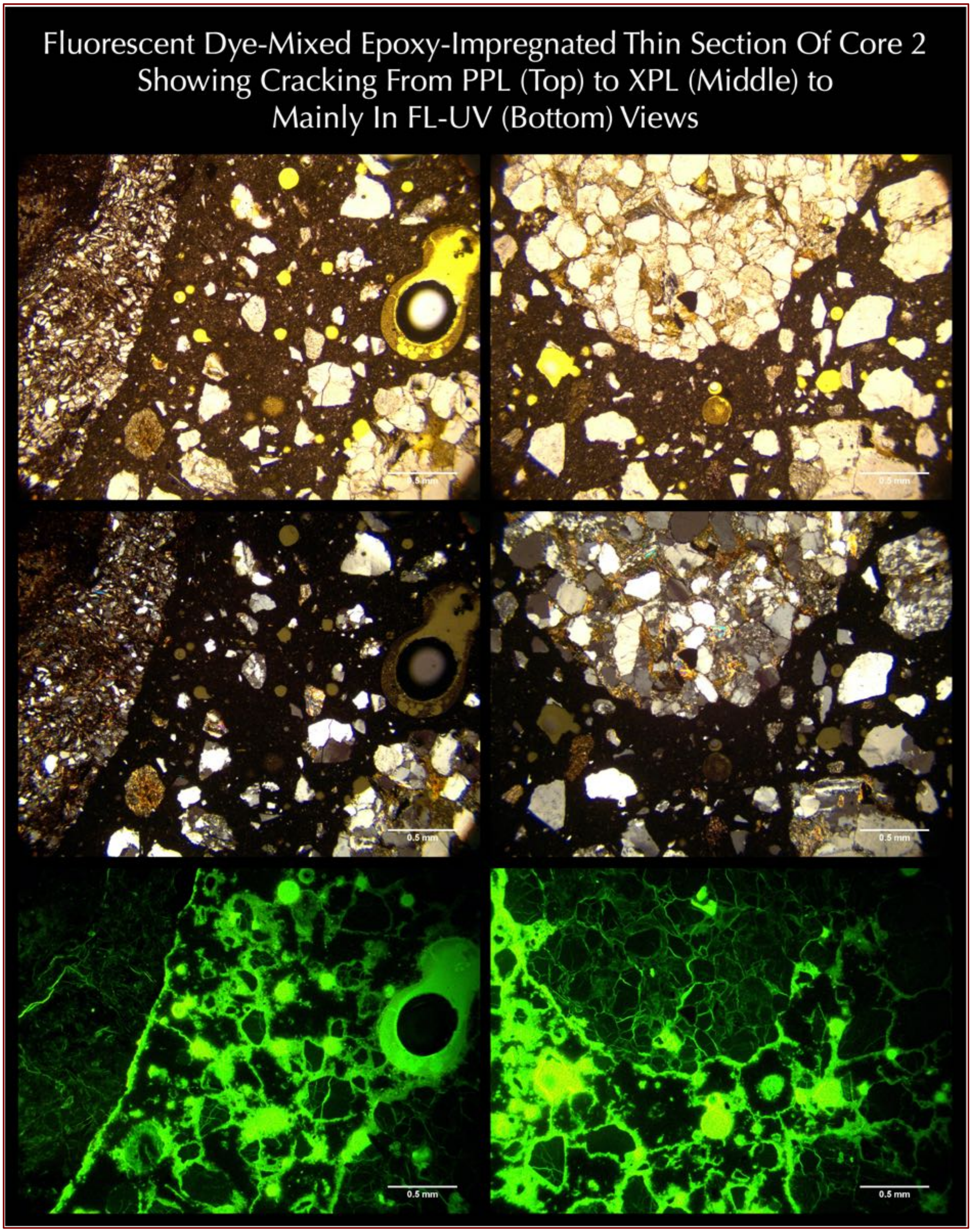

Figure 64: Micrographs of thin section of concrete from Core 2 taken in plane-polarized light (top row), corresponding cross polarized light (middle row), and corresponding fluorescent UV light (bottom row) showing extensive microcracking in greywacke and shale-siltsotne gravel particles in coarse aggregate, as well as in interstitial mortar fraction that are best highlighted by fluorescent epoxy when seen in UV light. Micrographs were taken from a petrographic microscope with fluorescent light facilities.

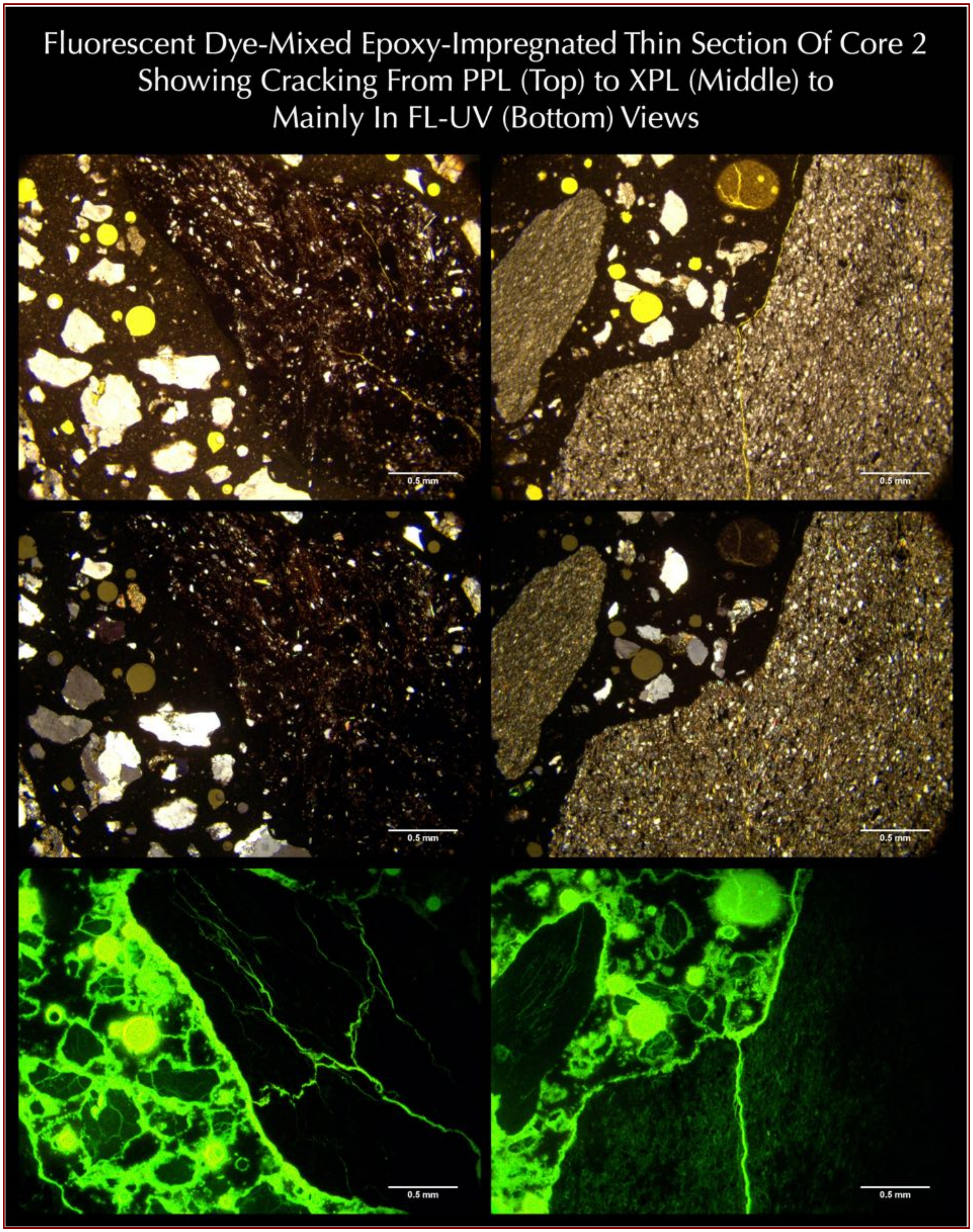

Figure 65: Micrographs of thin section of concrete from Core 2 taken in plane-polarized light (top row), corresponding cross polarized light (middle row), and corresponding fluorescent UV light (bottom row) showing extensive microcracking in greywacke and shale-siltsotne gravel particles in coarse aggregate, as well as in interstitial mortar fraction that are best highlighted by fluorescent epoxy when seen in UV light. Micrographs were taken from a petrographic microscope with fluorescent light facilities.

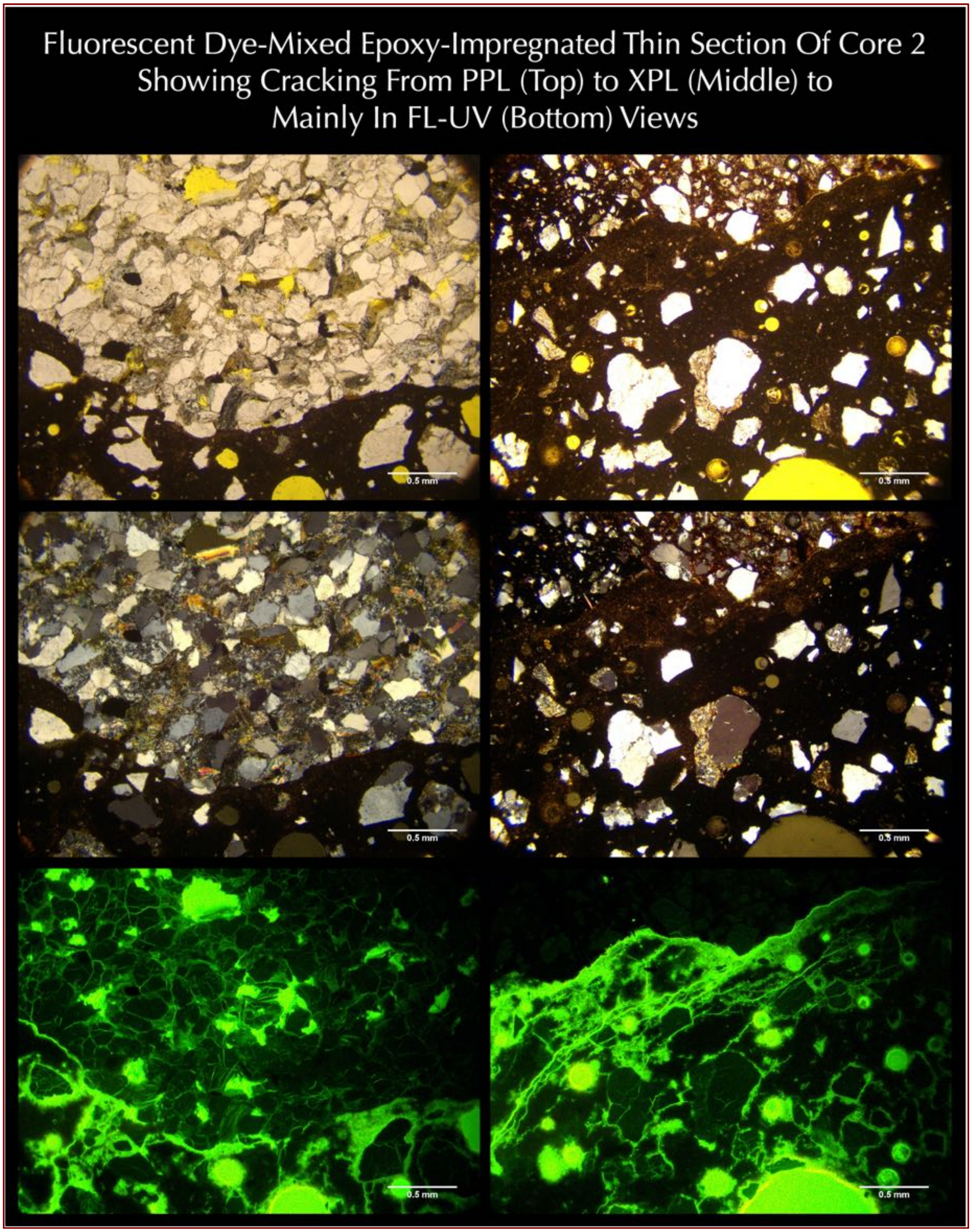

Figure 66: Micrographs of thin section of concrete from Core 2 taken in plane-polarized light (top row), corresponding cross polarized light (middle row), and corresponding fluorescent UV light (bottom row) showing extensive microcracking in greywacke and shale-siltsotne gravel particles in coarse aggregate, as well as in interstitial mortar fraction that are best highlighted by fluorescent epoxy when seen in UV light. Micrographs were taken from a petrographic microscope with fluorescent light facilities.

COARSE AGGREGATES

Coarse aggregates in both cores are compositionally similar sedimentary pea gravels, having nominal maximum sizes of $^3/_8$ in. (9.5 mm) and containing: (a) major amounts of greywacke, which are sandstones having detrital quartz and feldspar in a dominantly argillaceous (wacke) matrix, (b) subordinate amounts of reddish-brown ferruginous and argillaceous siltstone and shale where iron oxide-based ferruginous impurities have imparted the characteristic reddish-brown colors of these particles to be readily identified, (c) subordinate amounts of non-ferruginous but argillaceous shale and siltstone particles where lack of iron oxide impurity has prevented development of reddish brown color tone except having the same fine clay-silt grain size and quartz-feldspar-fine-grained carbonate-clay mineralogies of ferruginous shale-siltstone particles, and (d) minor amounts of quartzite, which are either orthoquartzite or metaquartzite, latter having strained quartz particles. All particles are subrounded to well-rounded, mostly equidimensional, variably hard and porous, well-graded, and well-distributed.

Many greywacke, ferruginous-argillaceous shale-siltstone, and non-ferruginous shale-siltstone particles have shown (i) internal cracking, (ii) many having cracks extended into paste, (iii) many are transected by major visible cracks as well as minor invisible microcracks, (iv) many shown peripheral cracks as well as (v) porous zones of paste along the peripheries – all of which indicate physical unsoundness of these clay-rich argillaceous sedimentary gravels in the presence of moisture during service. When present near the expose face and exposed to moisture during service, as in the case of Core 2 where despite having no visible cracks in the core, a near-surface shale and adjacent greywacke particle in coarse aggregate showed unsoundness as fracturing and popout that had required a repair patch to place over the popout location. Reported widening of cracks in the wall panel is consistent with gross unsoundness of these clay-rich (argillaceous) gravel particles in concrete that have absorbed moisture during service and expanded, followed by repeated volume instabilities during wetting and freezing, and freezing and thawing cycles to cause internal cracking of those particles, eventually leading to development of new cracks in the panel as well as widening of existing cracks.

Apart from physical unsoundness, which appear to be the main reason for observed cracking of the panels, there is no evidence of any potentially deleterious alkali-aggregate reaction of the particles found in the cores. Strained quartz particles in some metaquartzite particles in gravel are potentially alkali-silica reactive. However, there is no evidence of such a rection of those particles found in the concrete, probably for their occurrence only in minor amounts relative to the dominant clay rivals of greywacke-siltstone-shape gravels.

Due to the overwhelming abundance of clay-rich particles in gravels and their wide distribution throughout the entire thickness of the panels, exposure to moisture during service poses threat for continued unsoundness of these particles along with continued development of new cracks, popout of near-surface particles, and widening of pre-existing cracks due to overall volume expansion of concrete when these particles absorb moisture during service.

FINE AGGREGATES

Fine aggregates in both cores are compositionally similar natural siliceous-argillaceous-calcareous sands of nominal maximum sizes $^{1}/_{4}$ in. (6 mm) consisting of: (a) major amount of finer fraction of lightly crushed sedimentary pea gravel particles; (b) major amounts of detrital quartz and feldspar grains; (c) subordinate amount of detrital feldspar, shale, siltstone; and (d) minor amounts of limestone and dolomite as the calcareous component.

Fine aggregate particles are variably colored, subangular to subrounded to well-rounded, variably dense and hard, equidimensional to elongated, unaltered, uncoated, and uncracked.

There is no evidence of alkali-aggregate reactions, or any other potentially deleterious reactions found. Unsoundness of argillaceous particles are mostly seen in the pea gravel and not in their finer sand-size fractions.

The following Table summarizes properties of coarse and fine aggregates in two cores.

Properties and Compositions of Aggregates	Cores 1 and 2
Coarse Aggregate	
Types	Sedimentary pea gravel
Nominal maximum size (in.)	$^{3}/_{8}$ in. (9.5 mm)
Rock Types	(a) Major amounts of greywacke, (b) Subordinate amounts of reddish-brown ferruginous and argillaceous siltstone and shale, (c) Subordinate amounts of non-ferruginous but argillaceous shale and siltstone particles, and (d) Minor amounts of quartzite
Angularity, Density, Hardness, Color, Texture, Sphericity	Variably dense to porous, variably hard, subrounded to well-rounded, mostly equidimensional
Cracking, Alteration, Coating	Unaltered, Uncoated, but many particles are cracked as shown on Figures
Grading & Distribution	Well-graded, well-distributed
Soundness	Chemically sound but physically unsound
Alkali-Aggregate Reactivity	Not seen
Fine Aggregates	
Types	Natural siliceous-argillaceous-calcareous sands
Nominal maximum size (in.)	$^{3}/_{8}$ in. (9.5 mm)
Rock Types	(a) Major amount of finer fraction of lightly crushed sedimentary pea gravel particles; (b) Major amounts of detrital quartz and feldspar grains; (c) Subordinate amount of detrital feldspar, shale, siltstone; and (d) Minor amounts of limestone and dolomite as the calcareous component
Cracking, Alteration, Coating	Variably colored, subangular to rounded, dense, hard, equant to elongated
Grading & Distribution	Well-graded and Well-distributed
Soundness	Sound
Alkali-Aggregate Reactivity	None

Table 2: Properties of coarse and fine aggregates of concretes.

PASTE

Properties and composition of hardened cement pastes in two cores are summarized in Table 3. Paste is compositionally similar dense, and hard in the interior bodies except some patchy discoloration at the minimally carbonated expose surface ends. Freshly fractured surfaces have subtranslucent vitreous lusters and subconchoidal fractures. Residual and relict Portland cement particles are present and estimated to constitute 6 to 8 percent of the paste volumes. Besides residual Portland cement, no other pozzolanic or cementitious materials are found. The entire paste is intermixed with ultrafine iron oxide-based pigment to impart an overall pigmented brown color tone of concrete.

The textural and compositional features of pastes are indicative of Portland cement contents similar in both cores and estimated to be 7 to $7^1/_2$ bags per cubic yard, and water-cement ratios in the bodies similar in both cores and estimated to be 0.40 to 0.45.

Properties and Compositions of Paste	Cores 1 and 2
Color, Hardness, Porosity, Luster	Compositionally similar dense, and hard in the interior bodies except some patchy discoloration at the minimally carbonated expose surface ends. Freshly fractured surfaces have subvitreous lusters and subconchoidal textures
Residual Portland Cement Particles	Normal, 6 to 8 percent by paste volume
Calcium hydroxide from cement hydration	Normal, 10 to 14 percent by paste volume
Pozzolans, Slag, etc.	None
Water-cementitious materials ratio (*w/cm*), estimated	0.40 to 0.45 in the interior bodies
Portland cement content (bags per cubic yard)	7 to $7^1/_2$ bags
Secondary Deposits	None
Depth of Carbonation, mm	Patchy carbonation at exposed ends extended to depths of 5 mm
Microcracking	Extensive microcracking from unsound greywacke-siltstone-shale particles in pea gravel as well as near the exposed surface end found in both cores
Aggregate-paste Bond	Moderately tight to weak in areas where cracks have circumscribed the aggregate particles
Bleeding, Tempering	None
Chemical deterioration	None

Table 3: Proportions and composition of hardened cement paste.

AIR

Concretes in both cores are air-entrained having numerous fine, discrete, spherical and near-spherical voids of sizes 1 mm or less, which are characteristic of entrained air and a few coarse, near-spherical and irregularly-shaped voids greater than 1 mm in size, which are characteristic of entrapped air. Air contents are estimated to be 6 to 7 percent in both cores.

DISCUSSIONS

UNSOUNDNESS OF GREYWACKE AND ARGILLACEOUS SHALE-SILTSTONE PARTICLES IN PEA GRAVEL COARSE AGGREGATE

Petrographic evidence showed gross unsoundness of many greywacke, ferruginous-argillaceous shale-siltstone, and non-ferruginous shale-siltstone particles in pea gravel coarse aggregate as: (i) internal cracking, (ii) internal cracks extended into paste, (iii) gravel transected by major visible cracks as well as minor invisible microcracks, (iv) peripheral cracks, and (v) porous zones of paste along the peripheries. All these textural and microstructural evidence indicate physical unsoundness of these clay-rich argillaceous sedimentary gravels in the presence of moisture during service. All these sedimentary gravel particles have one common compositional feature, which is their clay-rich composition, which makes them susceptible to absorb moisture during service and expand.

POPOUT OF NEAR-SURFACE PEA GRAVEL

Beside cracking, another surface manifestation of unsoundness is popout of many of these particles when present near the exposed face of the panels and exposed to moisture during service. As in the case of Core 2 where despite having no visible cracks in the core, a near-surface shale and adjacent greywacke particle in coarse aggregate showed unsoundness as fracturing and popout that had required a repair patch to place over the popout location.

FAILURE OF SEALER AND WIDENING OF CRACKS DUE TO CONTINUED UNSOUNDNESS OF ARGILLACEOUS GRAVELS DURING EXPOSURE TO MOISTURE

Reported failure of sealer and widening of cracks in the wall panel are consistent with gross unsoundness of these clay-rich (argillaceous) gravel particles in concrete that have absorbed moisture during service and expanded, followed by repeated volume instabilities during wetting and freezing, and freezing and thawing cycles to cause internal cracking of those particles, eventually leading to development of new cracks in the panel as well as widening of existing cracks.

QUESTIONABLE LONG-TERM DURABILITY AND SERVICEABILITY DUE TO OVERWHELMING ABUNDANCE OF UNSOUND ARGILLACEOUS PARTICLES IN GRAVEL

Due to the overwhelming abundance of clay-rich particles in gravels and their wide distribution throughout the entire thickness of the panels, exposure to moisture during service poses threat for continued unsoundness of these particles along with continued development of new cracks, popout of near-surface particles, and widening of pre-existing cracks due to overall volume expansion of concrete when these particles absorb moisture during service. Good air entrainment, use of Portland cement plus iron oxide-based pigment as cementitious and pigment components, respectively in paste, and overall dense and well-consolidated nature of concrete, apparently did not provide the necessary resistance of the panels to combat against potential moisture absorption of the dominant argillaceous gravel coarse aggerate particles that are scattered all throughout the thickness of the panels.

Unfortunately, since past repair attempts with silane sealer did not prevent cracking or widening of existing cracks, replacement of the panels appears to the best option to prevent future cracking. Aggregates to be used in a replaced panel must avoid any clay-rich or other potentially deleterious components since due to their dominance at 60 to 70 percent level by volume, aggregates play a dominant role in future durability and serviceability of concrete. The present case testifies the importance of aggregate in creating a durable and serviceable precast panel, especially exposed to an outdoor moist environment of cyclic freezing and thawing.

REFERENCES

ASTM C 856 "Standard Practice for Petrographic Examination of Hardened Concrete," Vol. 4.02, ASTM International, West Conshohocken, PA, 2017.

Jana, D., "Sample Preparation Techniques in Petrographic Examinations of Construction Materials: A State-of-the-Art Review," *Proceedings of the 28th Conference on Cement Microscopy (ICMA)*, 2006, pp. 23-70.

✪ ✪ ✪ END OF TEXT ✪ ✪ ✪

END OF REPORT[1]

[1] The CMC logo is made using a lapped polished section of a 1930's concrete from an underground tunnel in the U.S. Capitol.